博士論文

PTEN, a phosphatidylinositol 3,4,5-trisphosphate 3-phosphatase, differentially regulates endocytosis, migration, and proliferation in the enteric protozoan parasite *Entamoeba histolytica*

(腸管原虫赤痢アメーバのホスファチジルイノシトール 3 リン酸脱リン酸化酵素(PTEN)はエンドサイトーシス、細胞運動、増殖を多様に制御する)

サミア ヤッサー カドリ

SAMIA YASSER KADRI

PTEN, a phosphatidylinositol 3,4,5-trisphosphate 3-phosphatase, differentially regulates endocytosis, migration, and proliferation in the enteric protozoan parasite *Entamoeba histolytica*

(腸管原虫赤痢アメーバのホスファチジルイノシトール３リン酸脱リン酸化酵素(PTEN)はエンドサイトーシス、細胞運動、増殖を多様に制御する)

The University of Tokyo

Tomoyoshi Nozaki

SAMIA YASSER KADRI

CONTENT

LIST OF ABBREVIATIONS

AGCK : AGC Family Kinase

AKT : RAC-alpha Serine/Threonine-Protein Kinase

BSA : Bovine Serum Albumin

CHO : Chinese Hamster Ovary

CLS : Cytoplasmic Localization Signal

CME : Clathrin-Mediated Endocytosis

CQ1 : Confocal Quantitative Image Cytometer

DNA : Deoxyribonucleic Acid

DSPs : Dual Specificity Protein Phosphatases

E. histolytica : *Entamoeba histolytica*

EhPIPKI : *E. histolytica* Type-I PtdIns Phosphate Kinase

EhPTEN1 : *Entamoeba histolytica* PTEN1

G418 : Geneticin

GS : Gene Silencing

HA : Human Influenza Hemagglutinin

hRBCs : Human Red Blood Cells

HRP : Horseradish Peroxidase

IFA : Indirect Immunofluorescence Assay

IPTG : Isopropyl β-D-Thio Galactopyranoside

NAFLD : Nonalcoholic Fatty Liver Disease

NASH : Nonalcoholic Steato-Hepatitis

N-WASP : Neural-Wiskott-Aldrich Syndrome Protein

PATMK : Phagosome Associated Transmembrane Kinases

PBS : Phosphate Buffered Saline

PBS-T : PBS containing 0.05% Tween 20

PBS-TB : PBS-T containing 1% fat free BSA

PCR : Polymerase Chain Reaction

PHTS : PTEN Hamartoma Tumor Syndrome

PI3K : Phosphatidylinositol 3-Kinase

PMSF : Phenylmethyl Sulfonyl Fluoride

PtdInsPs : Phsophotydylinositol Phosphate

$PtdIns(4,5)P_2$: Phosphatidylinositol (4,5)-Bisphosphate

$PtdIns(3,4,5)P_3$: Phosphatidylinositol (3,4,5)-Trisphosphate

PTPs : Protein Tyrosine Phosphatases

qRT-PCR : Quantitative Real-Time PCR

RNA : Ribonucleic Acid

RT PCR : Reverse Transcriptase Polymerase Chain Reaction

SDS PAGE : Sodium Dodecyl Sulfate-Polyacrylamide Gel Electrophoresis

SNXs : Sorting Nexins

SREHP : Serin-rich *Entamoeba histolytica* Protein

TBS-T : Tris-Buffered Saline and Tween-20

ABSTRACT

PTEN is a lipid phosphatase that is highly conserved protein and is essential in all eukaryotes. Although regulation of phosphatidylinositol (3,4,5)-trisphosphate (PtdIns(3,4,5)P_3) signaling via PTEN in mammalian has been well established, PtdIns(3,4,5)P_3 signaling in parasitic protist *E. histolytica* is still elusive. In this study, I characterized the EhPTEN1, which shows the highest expression at the transcript level in the trophozoite stage among 6 PTEN homologous, to understand the significance of PtdIns(3,4,5)P_3 signaling in *E. histolytica*. Live imaging of GFP-EhPTEN1 expressing amebic trophozoites showed localization mainly in the cytosol with higher concentration to pseudopods and to the leading edge of the trogo-phagocytic cup. Furthermore, using a confocal quantitative image cytometer, I found that EhPTEN1 has an inhibitory role in these biological processes where overexpression of EhPTEN1 caused reduction in trogocytosis and phagocytosis while transcriptional gene silencing of *EhPTEN1* gene caused opposite phenotypes. Conversely, EhPTEN1 acts as a positive regulator for fluid-phase and receptor-mediated endocytosis in *E. histolytica* trophozoites. Moreover, I showed that EhPTEN1 was required for optimal growth and migration of this parasite. However, the phosphatase activity of EhPTEN1 towards PtdIns(3,4,5)P_3 is conserved suggesting that the biological implications of EhPTEN1 are related to its catalytic function. These results are consistent with the premise that EhPTEN1 is differentially involved in signaling in different endocytic pathways. Our study on the PTEN functions in *E. histolytica* provides novel implications of phosphatidylinositol signaling which will expand our understanding of the pathogenesis of this parasite and potentially lead to the design of novel therapeutics against amebiasis.

INTRODUCTION

Phosphatidylinositol phosphates (PtdInsPs) are membrane phospholipids that a play pivotal role in a variety of biological processes such as cytoskeletal reorganization, vesicular trafficking, endocytosis, signal transduction, ion channel activation, and cell migration (Di Paolo and De Camilli, 2006; Balla, 2013). There are seven different species of PtdInsPs in mammalian cells including three phosphatidylinositol monophosphate, three phosphatidylinositol biphosphate, and one phosphatidylinositol triphosphate (Balla, 2013). PtdInsPs kinases and phosphatases regulate the cellular function of PIPs through reversible phosphorylation and de-phosphorylation mechanism (Sasaki et al., 2009). PTEN (phosphatase and tensin homologue) is a lipid phosphatase that dephosphorylates phosphatidylinositol (3,4,5)-trisphosphate (PtdIns(3,4,5)P_3) to phosphatidylinositol (4,5)-bisphosphate (PtdIns(4,5)P_2) thus depleting cellular signaling processes downstream of PtdIns(3,4,5)P_3 (Maehama and Dixon, 1998). PtdIns(3,4,5)P_3 acts as a secondary messenger which activates the proto-oncogenic PI3K–AKT signaling pathway that drive cell survival and cell proliferation by phosphorylating downstream signaling proteins, including B cell lymphoma 2 associated agonist of cell death (BAD), cyclin-dependent kinase inhibitor p27, and negative regulator of mammalian target of rapamycin (mTOR) proline-rich Akt substrate of 40 kDa (PRAS40) (Chalhoub and Baker, 2009; Song et al., 2012). PTEN plays a crucial role in cell proliferation through its cytoplasmic phosphatase activity against the PI3K–AKT cascade (Maehama et al., 2001). Also, PTEN regulates cell polarity and migration via the establishment of a PtdIns(3,4,5)P_3-PtdIns(4,5)P_2 gradient (Martin-Belmonte et al., 2007; Song et al., 2012). PTEN catalysis activity at the apical plasma membrane during epithelial morphogenesis leads to conversion of PtdIns(3,4,5)P_3 to PtdIns(4,5)P_2 which in turn lead to recruitment of Annexin 2 (ANXA2), Cell division control protein 42 homolog (Cdc42), and Atypical protein kinase C

(aPKC) to the apical surface subsequently to promote establishment of polarity (Martin-Belmonte et al., 2007). PTEN has also been implicated in controlling cell migration through its phosphatase activity on PtdIns(3,4,5)P_3 that regulates key downstream effectors such as Rho, Rac1, and Cdc42 which modulate actin cytoskeleton (Song et al., 2012). Many human cancer events are related to PTEN mutations including endometrial tumors, glioblastoma, prostate carcinoma, and melanoma cases and in hereditary cancer predisposition syndromes, such as Cowden disease (Lee et al., 2018; Li et al., 1997). Furthermore, PTEN can modulate immune responses by regulating Fcγ receptor-mediated phagocytosis (Kim et al., 2002; Cao et al., 2004).

Human amebiasis is caused by the infection of the enteric protozoan parasite *Entamoeba histolytica*. World Health Organization estimates 50 million people throughout the world suffer from amebic infections, resulting in around 100,000 deaths annually (Ximenez et al., 2009). Infection by *E. histolytica* usually occurs via ingestion of fecally contaminated food or water with the infective cyst of this parasite (Haque et al, 2003). Destruction of intestinal epithelial tissue by amoebic trophozoites causes colitis and amoebic dysentery while in some patients trophozoites can infect extraintestinal organs where they form abscesses (Stanley, 2003). It is known that major virulence mechanisms of *E. histolytica* are related to actin-mediated processes such as migration, adhesion, and trogo-/phagocytosis as well as vesicular traffic involved in the secretion of proteases (Ralston and Petri, 2011; Ralston et al., 2014; Marie and Petri, 2014; Nakada-Tsukui and Nozaki, 2016). *E. histolytica* conserves an apparently sufficient set of PI-kinases and -phosphatases to generate 7 species of phosphoinositides (Nakada-Tsukui et al., 2019). It has been recently characterized AGC kinases in *E. histolytica* as PtdIns(3,4,5)P_3-binding proteins and revealed their involvement in trogocytosis and phagocytosis (Somlata et al., 2017). In addition, it was previously reported that treatment with wortmannin, inhibitors of PI3K, impaired phagocytosis of several

particles including bacteria, mucin-coated beads, and hRBCs by *E. histolytica* trophozoites (Ghosh and Samuelson, 1997; Powell et al., 2006; Byekova et al., 2010). Thus PtdIns(3,4,5)P_3-mediated signaling is assumed to have a pivotal role in *E. histolytica* virulence. Although a comprehensive analysis of the PTEN functions in higher eukaryotes has been conducted, the role of PTEN in protozoan parasites remained elusive. In the present study, I aimed to characterize the biological roles of EhPTEN1 during different forms of endocytosis and clarify its role in the pathogenesis of *E. histolytica*.

1. Phsophotydylinositol

Phsophotydylinositol phosphate (PtdInsPs) are membrane-bound signaling phospholipids that consist of glycerol backbone, two fatty acid chains, Myo-inositol head group, and phosphate. Seven phosphorylated forms of PtdInsPs result from the interconversion of the phosphorylation states at positions D3, D4, and D5 of the hydroxyl group by PtdInsPs kinases and phosphatases (Balla, 2013). PtdInsPs are localized on different cellular compartments and play a critical role in regulating diverse cellular processes via activation of downstream signaling through interacting with proteins that contain phosphoinositide-binding domains such as FYVE (Fab1, YOTB1, Vac1, early endosomal antigen 1 [EEA1]), phox homology (PX), and pleckstrin homology (PH) domains (Di Paolo and De Camilli, 2006). For example, the predominant subcellular localization of PtdIns(4)P is in Golgi complex but also present at the plasma membrane and a deficiency of this lipid affects Golgi morphology and functions (Balla, 2013). In the other hand, PtdIns(3)P is enriched on early endosomes while PtdIns(3,5)P_2 is concentrated on late endosomes where they play a key role in regulating endocytic trafficking (Schink et al., 2016). It has been well established that in mammalian cells PtdIns(4,5)P_2 is enriched on the plasma membrane while PtdIns(3,4,5)P_3 is transiently increased at the plasma membrane in response to cellular stimuli (Di Paolo and De

Camilli, 2006). PtdIns(3,4,5)P_3 regulates fundamental roles in higher eukaryotes including cell proliferation, survival, and metabolic changes. In addition, PtdIns(4,5)P_2 and PtdIns(3,4,5)P_3 mediate cell shape, motility, chemotaxis, phagocytosis, and macro-pinocytosis through direct interaction with effector proteins like N-WASP or by binding to phosphoinositide-binding domains in the effector proteins such as PH domain in Dynamin, Vav , and Rho GTPase activating proteins (ARHGAP) thus, in turn, regulate the activation and recruitment of a large variety of actin regulatory proteins (Di Paolo and De Camilli, 2006; Balla, 2013). During phagocytosis, a large particle engages specific receptors on the cell surface. The most thoroughly analyzed model is the binding of Fcγ receptors with immunoglobulin G (IgG)-coated particles. Upon clustering of Fcγ receptors, tyrosine kinase Syk will be recruited which in turn recruits and/or phosphorylates effector proteins, such as PI3K, phospholipase C (PLC), and Vav which results in a modest localized increase in PtdIns(4,5)P_2, and a pronounced accumulation of PtdIns(3,4,5)P_3. These changes in lipid content are accompanied by the engagement of Rho-family GTPases that promote actin polymerization. PtdIns(4,5)P_2 is also necessary for endocytosis where almost all the known endocytic clathrin adaptors bind directly to PtdIns(4,5)P_2 (Bohdanowicz and Grinstein, 2013). Thus, PtdIns(4,5)P_2 and PtdIns(3,4,5)P_3 levels on the membrane ruffles are tightly controlled by metabolizing enzymes which ensure the efficiency of endocytic processes (Schink et al., 2016).

2. Phosphatidylinositol 3,4,5-trisphosphate 3-phosphatase (PTEN)

PTEN is a lipid phosphatase that dephosphorylates the D3 position of the inositol ring of PtdIns(3,4,5)P_3 to PtdIns(4,5)P_2 thus depleting cellular signaling processes downstream of PtdIns(3,4,5)P_3 (Maehama and Dixon, 1998). PTEN was initially identified as a tumor suppressor gene located on chromosome 10 where it is the most frequently mutated gene in various human cancers (Li et al., 1997). Additionally, germline mutations in PTEN are associated with the

dominantly inherited Cowden and Bannayan-Zonana syndromes which are characterized by the development of hyperplastic, disorganized cell growth that increase the prevalence of brain, breast, endometrial, and thyroid cancers (Li et al., 1997; Lachlan et al., 2007). Disruption of the mouse PTEN gene results in early embryonic lethality and leads to neoplasia in multiple tissues compatible with Cowden syndrome (Cristofano et al., 1998; Suzuki et al., 1998).

2.1 Domain composition and structural features of the catalytic center

The canonical PTEN contains 403 amino acid; 1–185 residues for N-terminal region which encompass the phosphatase domain follow by 218 amino acid for C-terminal sequence that includes C2 domain, PEST sequence, and PDZ binding motif (Lee et al., 1999; Maehama et al., 2001). The C2 domain is known to be involved in phospholipid membranes binding. While the two PEST sequences at the extreme C-terminal segment of PTEN are known to function as a signal for proteolytic degradation. In addition, PTEN contains PDZ binding motif which may facilitate protein-protein interactions. The active site contains the phosphatase signature motif (HCX_2GX_2R) which is similar to the catalytic site of protein tyrosine phosphatases (PTPs) and dual specificity protein phosphatases (DSPs). However, the phosphatase active site of PTEN is wider and deeper than those of PTPs or DSPs due to the insertion of conserved residues (Valine-166–Threonine-167–Isoleucinee-168) in the TI loop (Figure 4). This larger opening of PTEN pocket would be important in accommodating the large size of the PtdIns(3,4,5)P_3 substrate. In addition, the catalytic site of PTEN is unique as it has two basic residues (Lysine-125 and Lysine-128) in its center. This PTEN motif (H-C-K/R-A-G-K-G-R) is conserved in PTEN homologs from mouse, rat, dog, frog, fruit fly, worm, and yeast as well (Figure 4) (Maehama et al., 2001). Lysine-125 interacts with the phosphate groups at positions D1 of the inositol ring as confirmed by the proximity location between Lysine-125 and position D1 in PTEN crystal structure (Lee et al.,

1999). While Lysine-128 plays a role in the distinct substrate specificity of PTEN as it interacts with the phosphate groups at positions D5 of the inositol ring. PTEN also has PtdIns(4,5)P_2-binding motif encompassing residue 6 to 15 (K/R-x4-K/R-x-K/R-K/R-R, PDM domain) which regulates the recruitment of proteins to cytoskeletal structures or the plasma membrane (Maehama et al., 2001). In vitro and in vivo analysis of PTEN indicates that PtdIns(4,5)P_2 slows down the lateral diffusion and stabilizes the membrane binding of individual PTEN molecules on the lipid bilayer leading to the formation of a positive feedback loop (Yoshioka et al., 2020). The negatively rich sequence between 19 to 25 residues (D-G-F-x-L-D-L) has been shown to mediate cytoplasmic localization where mutations within this cytoplasmic localization signal (CLS) increase nuclear localization (Denning et al., 2007). PTEN also possesses a C2 domain responsible for phospholipid binding and membrane targeting (Lee et al. 1999). However, unlike Ca^{2+}-dependent C2 domains that require cationic Ca^{2+} ions for phospholipid binding, the PTEN C2 domain has lost the residues responsible for cation coordination and in vitro study showed a Ca^{2+}-independent characteristic for lipid binding (Lee et al. 1999, Masson and Roger, 2020). The PTEN C2 domain plays a role in positioning the catalytic phosphatase domain correctly toward its lipid substrates at the membrane (Georgescu et al. 2000). The C terminal segment of PTEN also contains two PEST (proline, glutamine, serine, threonine) sequence (350-375 and 379-396) which acts as a signal peptide for protein degradation (Lee et al., 2018). Furthermore, PDZ-binding motif (PDZ-BM) accommodates the last three amino acids regulating the binding of PTEN to the PDZ domain containing signaling molecules (Maehama et al., 2001, Masson and Roger, 2020).

2.2 Functional role in PtdIns(3,4,5)P_3 signaling, health and diseases

PTEN is predominantly localized to the cytosol, and also dynamically associated with the plasma membrane, where it hydrolyzes PtdIns(3,4,5)P_3 to PtdIns(4,5)P_2 thus antagonizing

PI3K/AKT proliferative pathway (Das et al. 2003; Vazquez et al. 2006). Further evidence showed that cytoplasmic PTEN is required for apoptosis where loss of the cytoplasmic PTEN led to overactivation of PI3K/AKT due to accumulation of PtdIns(3,4,5)P_3 and this contributes to cell survival, proliferation, energy metabolism, and migration (Manning and Cantley, 2007; Chung and Eng, 2005). PTEN has also been implicated in controlling cell migration and polarity which is an essential process in immune response, metastasis, pathogenesis, and angiogenesis. This effect is related to PTEN activity at the plasma membrane on PtdIns(3,4,5)P_3-dependent actin polymerization pathway and the recruitment of PtdIns(3,4,5)P_3 downstream effectors such as Cdc42 and Rac1 (Heit et al., 2008; Liliental et al., 2000). It has also been reported that PTEN regulates cell polarity via establishment of a PtdIns(3,4,5)P_3 – PtdIns(4,5)P_2 gradient to recruit the apical lumen formation machinery proteins (Martin-Belmonte et al., 2007). Regulation of PtdIns(3,4,5)P_3 by PTEN is important for phagocytosis in macrophages (Tamura et al., 1998). PTEN negatively influences phagocytosis where PTEN loss resulted in enhanced clearance of *Candida albicans* and *Pseudomonas aeruginosa* in alveolar macrophages (Serezani et al., 2012, Hubbard et al., 2011). Moreover, several studies revealed numerous metabolic phenotypes induced by PTEN loss which emphasize the role of PTEN as a metabolic regulator (Lee et al., 2018). In this regard, PTEN influences a plethora of metabolic processes through its inhibitory effect on the PI3K–AKT pathway. PtdIns(3,4,5)P_3 is generated by PI3K in response to growth factor stimulation which in turn causes recruitment and activation of AKT to the plasma membrane through interaction of PtdIns(3,4,5)P_3 with AKT PH domain. Activated AKT will then enhances glucose uptake and promotes insulin hypersensitivity by increasing the translocation of glucose transporter type-4 (GLUT4) to the plasma membrane through the inhibition of TBC1 domain family member 4 (TBC1D4). In addition, PI3K–AKT signaling inhibits gluconeogenesis by blocking the activities

of forkhead box protein O1 (FOXO1) and peroxisome proliferator-activated receptor- γ (PPARγ) co-activator 1α (PGC1α), while augments lipid biosynthesis by activation of the key lipogenic transcription factor sterol regulatory element-binding proteins (SREBPs) through the inhibition of glycogen synthase kinase-3 (GSK-3). Thus, PTEN regulates the cellular metabolic pathway through opposing PI3K function through its lipid phosphatase activity leading to inactivation of AKT signaling. PTEN hamartoma tumor syndrome (PHTS), benign tumor-like malformation due to mutations of the PTEN gene, in Cowden patients heterozygous for PTEN mutations showed an increased risk of obesity while decreasing the risk of type-2 diabetes due to augmentation of insulin sensitivity through overactivation of the PI3K-AKT pathway caused by loss-of-function mutations in PTEN (Pal et al., 2012). Another study reported the critical role of PTEN as a negative regulator of insulin-induced glucose uptake in vitro and in vivo through heterozygous inactivation of PTEN in mice (Wong et al., 2007). Also, PTEN plays a key role in lipogenesis in the liver as hepatic-specific PTEN-null mice showed pronounced hepatomegaly, steatohepatitis, triglyceride accumulation, insulin hypersensitivity, and increased tumorigenesis which led to the development of nonalcoholic fatty liver disease (NAFLD) and nonalcoholic steato-hepatitis (NASH) (Stiles et al., 2004; Peyrou et al., 2013; Horie et al., 2004; Galicia et al., 2010). In addition, PTEN loss and AKT activation enhance ATP hydrolysis leading to a compensatory increase in aerobic glycolysis; a phenomenon termed ‘the Warburg effect’ which supports the proliferation and growth of cancer cells (Fang et al., 2010). While systemic PTEN elevation induces healthy metabolism opposing Warburg state, characterized by increased energy expenditure and protected metabolic pathologies by reducing body fat accumulation (Ortega-Molina et al., 2012; Garcia-Cao et al., 2012).

2.3 PTEN in various organisms, plant, nematode, fish, and social amoeba

PTEN homolog in the moss *Physcomitrella patens* suppress the development of both rhizoid and gametophore as triple and quadruple *pten* knockout mutants exhibited higher division rate but lower cells size and number with up-regulation of S-Phase cell cycle genes PpPCNA, PpMCM, and PpRNR compared to wild-type (Saavedra et al., 2015). While AtPTEN1, a homolog of PTEN in *Arabidopsis thaliana*, is crucial for pollen development and endomembrane trafficking of autophagic bodies (Gupta et al., 2002; Zhang et al., 2011). AtPTEN2a protein was detected in young plant organs while AtPTEN2b protein accumulated in seedlings which supports the role of AtPTEN2 in plant development (Pribat et al., 2012). Daf-18 is the only PTEN homolog in Caenorhabditis elegans and functions non-autonomously in the somatic gonad to regulate the developmental quiescence in dauer larvae and mains germline mitotic arrest (Ogg and Ruvkun, 1998; Tenen and Greenwald, 2019). Loss of the DAF-18 causes post-dauer adults' infertility and inappropriate germline growth (Fukuyama et al., 2006; Suzuki and Han, 2006). DAF-18 also functions as a negative regulator of the insulin/IGF-like pathway in which promotes cells longevity (Mihaylova et al., 1999; Gil et al., 1999; Masse et al., 2005). The zebrafish has two PTEN genes, PTENa and PTENb, which display favorable phosphatase activity toward PtdIns(3,4,5)P_3, like human PTEN (Stumpf et al., 2015; Faucherre et al., 2008). PTEN mutant zebrafish induces abnormal angiogenesis and embryogenesis which make them more prone to cancer (Choorapoikayil e al., 2012; Stumpf et al., 2015). The social amoeba *Dictyostelium discoideum* encode *ptenA* gene which is a homolog of the human PTEN gene and reserve its activity toward PtdIns(3,4,5)P_3 (Iijima et al., 2004). PtenA in *D. discoideum* plays a fundamental role in lateral pseudopod formation, motility, chemotaxis, and natural aggregation (Lusche et al., 2014; Wessels et al., 2007).

3. Intestinal protozoan parasite *Entamoeba histolytica*

Entamoeba histolytica is an intestinal protozoan parasite that causes amebiasis, a major cause of morbidity and mortality in developing countries. It remains to be a worldwide health problem affecting 50 million patients and causing 100,000 deaths annually (Ximenez et al., 2009). Disease transmission occurs via ingestion of the infectious cyst through fecally-contaminated food or water. Excystation of the cyst after ingestion produces the trophozoites which invade the intestinal epithelium (Haque et al, 2003). The parasite exploits virulence-related mechanisms which enable the invasion of intestinal epithelial tissue and extraintestinal tissue Symptoms can vary ranging from diarrhea, colitis, and dysentery to liver abscess (Stanley, 2003).

3.1 Pathogenesis and virulence factors of *E. histolytica*

Pathogenesis in amoebiasis is related to virulence-associated biological processes in *E. histolytica*, including adhesion, motility, and phago-/trogo-cytosis as well as vesicular traffic involved in secretion of proteases. *E. histolytica* trophozoites attach to the epithelial cells through several novel molecules, such as GAL/GalNAc lectin, phagosome associated transmembrane kinases (PATMK), and serin-rich *Entamoeba histolytica* protein (SREHP). Adherence of *E. histolytica* to the cell surface then will initiate signaling cascade including Ca^{2+} and phosphoinositide which subsequently triggers the recruitments of other molecules involved in actin remodeling to activate phagocytosis (Marie and Petri, 2014). Motility of trophozoites is necessary for invasion of intestinal tissue and reaching blood circulation to infect extraintestinal organs (Faust and Guillen, 2012). In addition to ingesting of the whole foreign cells by phagocytosis, *E. histolytica* also inherited capacity of bite off or nibble to ingest distinct host cell fragments by trogocytosis (Ralston et al., 2014). The signaling pathways that differentiates between these processes are incompletely understood. AGC kinase 1, a PtdIns(3,4,5)P_3 binding protein, was

identified as a factor that could differentiates the two processes where it is exclusively involved in trogocytosis, but not phagocytosis in *E. histolytica* (Somlata et al., 2017).

3.2 Phosphoinositides and its regulators in *E. histolytica*

Even though several PtdInsPs have been reported in *E. histolytica*, enzymes that metabolize the interconversion of these PtdInsPs are poorly studied. During phagocytosis of *E. histolytica*, phosphatidylinositol 3-phosphate (PtdIns(3)P) and PtdIns(3,4,5)P_3 are involved in the phagocytic cup formation (Powell et al., 2006; Nakada-Tsukui et al., 2009; Byekovs et al., 2010). In addition, PtdIns(4,5)P_2 is shown to localize on the plasma membrane of *E. histolytica* while PtdIns(3)P was found on the membrane of internal vesicles (Koushik et al., 2013; Nakada-Tsukui et al., 2009). Furthermore, extended pseudopodia exhibited rich concentration of PtdIns(3,4,5)P_3 where may regulate parasite motility (Byekovs et al., 2010). *E. histolytica* type-I PtdIns phosphate kinase (EhPIPKI) has been recently characterized biochemically as active PtdIns(4)P kinase and plasma membrane localized protein. EhPIPKI was found to be recruited to the phagocytic cup and pseudopods during phagocytosis and motility (Sharma et al., 2019). Additionally, recent studies showed the involvement of EhRoh1 in motility and phagocytosis through modulation PI3K pathway. Activated EhRho1 interacts with EhProfilin1 which the latter might bind to PtdIns(4,5)P_2 rich region and activate PI3K that lead to increase the level of PtdIns(3,4,5)P_3 at the plasma membrane which supports the membrane flexibility to form a phagocytic cup (Bharadwaj et al., 2017; Bharadwaj et al., 2018). These suggest involvement of EhPIPKI in regulation of actin dynamics through modulating of PtdInsPs levels. Furthermore, sorting nexins (SNXs) were identified as PtdIns(3)P_3-binding protein and showed involvement in trogocytosis of *E. histolytica* (Watanabe et al., 2020). The parasite performs their function through complex vesicle trafficking which highlights the importance of lipid signaling in virulence.

3.3 PTEN of *E. histolytica*

In silico analysis using human PTEN as a query for BLAST search showed that *E. histolytica,* has six PTEN homologs (Nakada-Tsukui et al., 2019). Prosite Scan for domain structure were used to confirm the conservation of phosphatase domain in the candidate's homologs. The presence of multiple orthologs in amoeba species may reinforce the significance of PTEN for parasitic proliferation and pathogenesis. The genetic expression levels of PTEN homolog (EHI_197010, EhPTEN1) in *E. histolytica* trophozoites is ten times higher than other isoforms. Additionally, this homolog possesses all conserved domains in mammalian PTEN including PtdIns(4,5)P_2-binding motif, phosphatase domain, C2 domain, and CLS. Besides, EhPTEN1were detected by proteomic studies of purified phagosome using a FYVE domain green fluorescent-labeled protein (Watanabe et al., 2020). These results may propose that this isoform act as a canonical PTEN in *E. histolytica*. Thus, I aimed to clarify the role of EhPTEN1 during trogo- phagocytosis, endocytosis, as well as migration to elucidate its role in pathogenic mechanisms in the protozoan parasites *E. histolytica*.

MATERIALS AND METHODS

1. Identification and comparison of PTEN protein sequences

To search for *E. histolytica* homologues of PTEN, BLAST search was conducted using human PTEN (P60484) protein as query. Amino acid sequences of PTEN protein from *E. histolytica* and other organisms were gained from AmoebaDB (http://amoebadb.org/amoeba/) and NCBI (https://www.ncbi.nlm.nih.gov) respectively and aligned using Clustal W program (http://clustalw.ddbj.nig.ac.jp/) to examine the domain configuration and the sequences surrounding the key residues for phosphatase activity (Thompson et al., 1994).

2. Organisms, cultivation, and reagents

Trophozoites of *E. histolytica* clonal strains HM-1:IMSS cl6 (Diamond et al., 1972) and G3 strain (Bracha et al., 2006) were cultured axenically in 6 ml screw-capped Pyrex glass tubes in Diamond's BI-S-33 (BIS) medium (Diamond et al., 1978) at 35.5°C as described previously. Chinese hamster ovary (CHO) cells were grown at 37°C in F12 medium (Invitrogen-Gibco, New York, USA) supplemented with 10% heat-inactivated fetal bovine serum (Sigma Aldrich, Missouri, USA) on a 10-cm-diameter tissue culture dish (IWAKI, Shizuoka, Japan). *Escherichia coli* BL21 (DE3) strain was purchased from Invitrogen (California, USA). Ni2+-NTA His-bind slurry was obtained from Novagen (Darmstadt, Germany). Rhodamine B isothiocyanate-Dextran (RITC-Dextran) and anti-GFP antibody were purchased from Sigma-Aldrich (Missouri, USA). The anti-HA 16B12 monoclonal mouse antibody was purchased from Biolegend (San Diego, USA). Anti-His antibody was purchased from Cell Signaling Technology (Massachusetts, USA). Lipofectamine, PLUS reagent, and geneticin (G418) were purchased from Invitrogen. CellTracker Green, Orange, and Blue were purchased from Thermo Fisher Scientific (Massachusetts, USA). Restriction enzymes and DNA modifying enzymes were purchased from New England Biolabs

(Massachusetts, USA) unless otherwise mentioned. Luria-Bertani (LB) medium was purchased from BD Difco (New Jersey, USA). Other common reagents were purchased from Wako Pure Chemical (Tokyo, Japan), unless otherwise stated.

3. Establishment of *E. histolytica* transformants

To construct a plasmid to express EhPTEN1 (EHI_197010) fused with HA or GFP tag at the amino terminus, a DNA fragment corresponding to cDNA encoding EhPTEN1 was amplified by polymerase chain reaction (PCR) from *E. histolytica* cDNA using the following primers: 5'-CCGCCCGGGATGAAAGAACTAAATAATTTA-3' and 5'-CCGCTCGAGTTAAGCTTTCGGATCTTTAAC-3' where the restriction enzymes sites are underlined. The PCR-amplified fragments were digested with XmaI and XhoI and cloned into pEhEx-HA and pEhEx-GFP vectors (Nakada-Tsukui et al., 2009; Somlata et al., 2017) that had been predigested with XmaI and XhoI, to produce pEhExHA-EhPTEN1 and pEhExGFP-EhPTEN1. For antisense small RNA-mediated transcriptional silencing of *EhPTEN1* gene, a 420 bp fragment of the protein coding region of *EhPTEN1* gene, corresponding to the amino terminus of the protein, was amplified by PCR from cDNA with the following sense and antisense oligonucleotides containing StuI and SacI restriction sites: 5'-GGGAGGCCTATGAAAGAACTAAATAATTTA-3' and 5'-GGGGAGCTCACAATGAAGTGCAATAACATT-3' where restriction enzyme sites are underlined. The amplified product was digested with StuI and SacI and ligated into the compatible sites of the double digested psAP2-Gunma plasmid (Mi-ichi et al., 2011) to synthesize a gene silencing plasmid designated as psAP2-EhPTEN1. Two plasmids, pEhExHA-EhPTEN1 and pEhExGFP-EhPTEN1, were introduced into the trophozoites of *E. histolytica* HM-1:IMSS cl6 strain, whereas psAP2-EhPTEN1 was introduced into G3 strain by lipofection as described

previously (Nozaki et al., 1999). Transformants were initially selected in the presence of 1 μg/ml G418 until the drug concentration was gradually increased to 10 μg/ml for the *EhPTEN1* gene silenced stain and 20 μg/ml for the GFP- and HA-EhPTEN1 overexpressing stains. Finally, all transformants were maintained at 10 or 20 μg/ml G418 in BIS medium.

4. Reverse transcriptase polymerase chain reaction (RT-PCR)

Reverse transcriptase PCR was performed to check mRNA levels of EhPTEN1 in *EhPTEN1* gene silenced and control strains. Total RNA was extracted from trophozoites of *EhPTEN1* gene silenced and control strains that were cultivated in the logarithmic phase using TRIZOL reagent (Life Technologies, California, USA). Approximately one μg of DNase treated total RNA was used for cDNA synthesis using Superscript III First -Strand Synthesis System (Thermo Fisher Scientific, Massachusetts, USA) with reverse transcriptase and oligo (dT) primer according to the manufacture's protocol. ExTaq PCR system was used to amplify DNA from the cDNA template using the following primer set: EhPTEN1 (forward) 5'-AGCTAGACATGGAGTTGGAG-3' and (reverse) 5'-TTAAGCTTTCGGATCTTTAACACTTGGTTT-3'; RNA polymerase II forward 5'-GATCCAACATATCCTAAAACAACA-3' and RNA polymerase II reverse 5'-TCAATTATTTTCTGACCCGTCCTTC-3'. The PCR conditions were as follow: initial denaturation at 98°C for 10 sec; then 25 cycles at 98°C for 10 sec, 55°C for 30 sec, and 72°C for 20 sec; and a final extension at 72°C for 7 min. The PCR products obtained were resolved by agarose gel electrophoresis.

5. Immunoblot analysis

Trophozoites of amoeba transformants expressing HA-EhPTEN1 or GFP-EhPTEN1 grown in the exponential growth phase were harvested and washed three times with phosphate

buffer saline (PBS). After resuspension in lysis buffer (50 mM Tris-HCl, pH 7.5, 150 mM NaCl, 0.1% Triton-X 100, 0.5 mg/ml E-64, and 1x cOmplete Mini protease inhibitor cocktail (EDTA free; (Roche, Mannheim, Germany), the trophozoites were kept on ice for 30 min, followed by centrifugation at 500 × g for 5 min. Approximately 20 µg of the total cell lysates were separated on 10% SDS-PAGE and subsequently electrotransferred onto nitrocellulose membranes. The membranes were incubated in 5% non-fat dried milk in Tris-Buffered Saline and Tween-20 (TBST; 50 mM Tris-HCl, pH 8.0, 150 mM NaCl, and 0.05% Tween-20) for 1 hr at room temperature to block non-specific proteins. The blots were reacted with one of the following primary antibodies diluted as indicated: anti-HA 16B12 monoclonal mouse antibody at a dilution of 1:1,000, anti-GFP mouse monoclonal antibody (1:100), and anti-CS1 rabbit polyclonal antisera (Nozaki et al., 1998) (1:1,000) at 4°C overnight. The membranes were washed with TBST and further reacted with horseradish peroxidase-conjugated (HRP) anti-mouse or anti-rabbit IgG antisera (1:10,000) at room temperature for 1 hr. After washings with TBST, the specific proteins were visualized with a chemiluminescence HRP Substrate system (Millipore, Massachusetts, USA) using LAS 4000 (Fujifilm Life Science, Cambridge, USA) according to the manufacture's protocol.

6. Live cell imaging

Approximately 5×10^5 trophozoites of the transformant strain expressing GFP-EhPTEN1 were cultured on a 35 mm (in diameter) collagen-coated glass-bottom dish (MatTek Corporation, Massachusetts, USA) in 3 ml of BIS medium under anaerobic conditions. CHO cells were stained with BIS medium containing 10 µM CellTracker Orange for 40 min followed by washing three times with PBS. Approximately 2×10^4 pre-stained CHO cells 200 µl BIS were gently overlayed to trophozoites grown on the glass-bottom dish as prepared above. The central part of the dish was

then carefully covered with a 1 cm square coverslip and the edge of the coverslip was sealed with nail polish. Live imaging was performed, images were captured on LSM780 confocal microscope using 40x objective, and analyzed by ZEN software (Carl-Zeiss, Oberkochen, Germany).

7. Indirect immunofluorescence assay (IFA)

Approximately 5×10^3 trophozoites in 50 µl BIS were transferred to a 8 mm round well on a slide glass (Matsunami Glass Ind, Osaka, Japan). After 30 min incubation in an anaerobic chamber at 35.5°C, 5×10^4 CHO cells that had been pre-stained with 10 µM CellTracker Blue in 50 µl BIS were added to the well and the mixture was incubated for 15 min. After removing the medium, cells were fixed with PBS containing 3.7 % paraformaldehyde at room temperature for 10 min, and subsequently permeabilized with PBS containing 0.2% Triton 100-X and 1 % bovine serum albumin (BSA) for 10 min each at room temperature. The cells were then reacted with anti-HA mouse monoclonal antibody (1:1000) for 1 hr at room temperature. Then the sample was reacted with Alexa Flouor-488 conjugated anti-mouse IgG (1:1000) antibody (Thermo Fisher, Massachusetts, USA). The images were then captured using LSM 780 confocal microscope and analyzed by ZEN software (Carl-Zeiss, Oberkochen, Germany).

8. Trogocytosis and phagocytosis assay using CQ1

Trophozoites of *E. histolytica* were incubated in BIS containing 10 µM CellTracker Blue at 35.5°C for 1 hr. After staining, ameba trophozoites were washed 3 times with PBS and resuspended in OPTI-MEM medium (Thermo Fisher Scientific, Massachusetts, USA) containing 15% heat-inactivated adult bovine serum (Sigma-Aldrich, Missouri, USA). Approximately 2×10^4 ameba trophozoites were seeded into a well on a 96-well glass bottom plate (IWAKI, Shizuoka, Japan) and incubated in anaerobic chamber for 40 min. After incubation, about 1×10^5 live CHO cells or 1×10^5 heat killed, treated at 55˚C for 15 min, CHO cells that have been stained with 10

μM CellTracker Orange were added to the well containing amebae. The images were taken on a Confocal Quantitative image cytometer CQ1 (Yokogawa Electric Corporation, Tokyo, Japan) using 20× objective every 10 min for 1 hr. The images were analyzed using CellPathfinder software (Yokogawa Electric Corporation, Tokyo, Japan) according to the manufacture's protocol. The multiple parameters were measured to evaluate the efficiency of trogocytosis and phagocytosis: the average number of internalized CHO cells per amoeba, the combined volume of internalized CHO cells per amoeba, and the percentage of amebic trophozoites that ingested the target cells (CHO) in the whole population.

9. Measurement of fluid-phase and receptor-mediated endocytosis

Approximately 2.5×10^5 amebic transformants were incubated in BIS medium containing 2 mg/ml fluorescent fluid-phase marker RITC-dextran at 35 °C for indicated time points. The cells were collected, washed three times with PBS, and resuspended in 250 μl of lysis buffer (50 mM Tris-HCl, pH 7.5, 150 mM NaCl, and 0.1% Triton-X 100). Fluorescence intensity was measured using a plate reader (SpectraMax Paradigm Multi-Mode, MOLECULAR DEVICES, California,USA) at an excitation wavelength of 570 nm and an emission wavelength of 610 nm. Protein amount was measured using Lowry method by Biorad DC protein Assay (Biorad, California, USA). The fluorescence of incorporated RITC-dextran was normalized to the protein concentration in total cell lysate.

Approximately 2×10^4 amebic transformants were incubated in BIS containing 20 μM CellTracker Blue at 35.5°C for 1 hr. After staining, amebic transformants were resuspended in 100 μl of BIS medium and transferred to a well on a 96-well glass-bottom plate. After incubation at 35.5°C in an anaerobic chamber for 40 min, 0.5 mg/ml of transferrin conjugate with Alexa Fluor 568 was added to the well and images were acquired by CQ1 and analyzed as above.

10. Migration (motility) assay

Amoebic trophozoites grown in the logarithmic growth phase were harvested and labelled with 20 μM CellTracker Green for 1 hr at 35.5°C. After washing 3 times with PBS, cells were transferred to a well on a 96-well glass-bottom plate and time lapse images were captured on CQ1 (Yokogawa Electric Corporation, Tokyo, Japan). The motility of the cells was measured using CellPathfinder software (Yokogawa Electric Corporation, Tokyo, Japan).

11. Quantitative real-time (qRT) PCR

The relative levels of mRNA of *EhPTEN1* gene and *RNA polymerase II* gene, as an internal standard, were measured by qRT-PCR. PCR reaction was prepared using Fast SYBR Master Mix (Applied Biosystems, California, USA) with cDNA and the following primer set: EhPTEN1 (forward) 5'-AGCTAGACATGGAGTTGGAG-3' and (reverse) 5'-TTAAGCTTTCGGATCTTTAACACTTGGTTT-3'; RNA polymerase II forward 5'-GATCCAACATATCCTAAAACAACA-3' and RNA polymerase II reverse 5'-TCAATTATTTTCTGACCCGTCCTTC-3'. PCR was conducted using the StepOne Plus Real-Time PCR system (Applied Biosystems, California, USA) with the following cycling conditions: an initial step of denaturation at 95°C for 20 sec, followed by 40 cycles of denaturation at 95°C for 3 sec, annealing and extension at 60°C for 30 sec. The mRNA expression level of *EhPTEN1* gene in the transformants was expressed as relative to that in the control transfected with psAP2.

12. Growth assay of *E. histolytica* trophozoites

Approximately 10^4 trophozoites of *E. histolytica* G3 strain transformed with psAP2-EhPTEN1 and psAP2 (control), grown in the logarithmic phase, were inoculated into 6 ml of fresh BIS medium containing 10 μg/mL G418, and the parasites were counted every 24 hr on a hemocytometer.

13. Production of EhPTEN1 recombinant protein

To construct the plasmid for the production of recombinant EhPTEN1 containing a histidine-tag at the amino terminus, the full-length protein coding sequence of *EhPTEN1* gene was amplified by PCR using the following oligonucleotide primers: 5'-GGGGGATCCATGAAAGAACTAAATAATTTA and GGGGTCGACTTAAGCTTTCGGATCTTTAAC where the restriction enzyme sites are underlined. PCR was performed with PrimeSTAR Max DNA polymerase (Takara Bio Inc, Shiga, Japan) with the following parameters: initial incubation at 95°C for 1 min; followed by 30 cycles of denaturation at 98°C for 10 sec; annealing at 55°C for 5 sec; and elongation at 72°C for 15 sec; and a final extension at 72°C for 30 sec. The PCR fragment was digested with BamHI and SalI and ligated into BamHI and SalI double digested pCOLD-1 vector (Takara Bio Inc, Shiga, Japan) to produce pCOLD1-EhPTEN1 plasmid. The pCOLD-1-EhPTEN1 was introduced into *E. coli* BL21 (DE3) cells by heat shock at 42°C for 45 sec. *E. coli* BL21 (DE3) strain harboring pCOLD-1-EhPTEN1 was grown at 37°C in 50 ml of LB medium (BD Difco, New Jersey, USA) in the presence of 100 µg/ml ampicillin. The 50 ml of overnight culture was used to inoculate 500 ml of fresh medium, and the culture was further continued at 37°C with shaking at 220 rpm for approximately 2 hr. When A_{600} absorbance reached 0.6, the culture was incubated at 15 °C without shaking for 30 min, then 1mM of IPTG was added, and cultivation was continued for another 24 hr at 15°C. The *E. coli* cells from the induced culture were harvested by centrifugation at 75,000 rpm for 20 min at 4°C. The cell pellet was washed three times with PBS, re-suspended in 30 ml of the lysis buffer (50 mM Tris–HCl, pH 8.0, 300 mM NaCl, and 0.1% Triton X-100) containing 100 µg/ml lysozyme, and 1 mM PMSF, and incubated at room temperature for 30 min. After incubation, the mixture was sonicated on ice and centrifuged at 13,000 rpm for 20 min at 4°C. The supernatant

was mixed with 1 ml of 50% Ni2+-NTA His-bind resin (Qiagen, Hilden, Germany), incubated for 1 hr at 4°C with mild rotatory shaking. The resin that recombinant His-EhPTEN1 bound was washed in a disposal column three times with 5 ml of lysis buffer containing 10-30 mM of imidazole. Bound proteins were eluted with 3 ml each of lysis buffer containing 100-300 mM imidazole to obtain recombinant EhPTEN1. The integrity and the purity of the recombinant protein were confirmed with 10% SDS-PAGE analysis, followed by Coomassie Brilliant Blue staining. Then the protein was concentrated, and the buffer was replaced with 50 mM Tris-HCl, 150 mM NaCl, pH 8.0 using Amicon Ultra 50K centrifugal device (Millipore, Massachusetts, USA). The protein was stored at -30 °C with 50% glycerol in small aliquots until further use.

14. Lipid phosphatase assay

EhPTEN1 enzymatic activity was determined by the method previously described (Mak and Woscholski, 2015). Di-C8 phosphatidylinositol phosphate(s) (PIPs) (Echelon Bioscience, Salt Laken City, USA) were dissolved in 100 mM MOPS, pH 6.0, solution, flash frozen in liquid nitrogen, and stored at -20°C between uses. For determination of pH optimum, the following buffers were used, 100 mM acetate buffer (pH 4.0, pH 4.5, pH 5.0, pH 5,5), 100 mM MOPS buffer (pH 6.0, pH 6.5, pH 7.0), and 100 mM Tris-HCl (pH 7.5, pH 8.0, pH 8.5, pH 9.0). For determination of substrate specificity, a reaction mixture was composed of 25 µl of 100 mM MOPS pH 6.0 containing 5 µg of recombinant EhPTEN1 and 100 µM PIPs. The reaction was carried out at 37°C for 40 min and terminated by the addition of 100 µl of Malachite Green Reagent (Cell Signaling technology, Massachusetts, USA). After incubation for 15 min at room temperature, the absorbance was measured at a wavelength of 630 nm. The Lineweaver Burk Plot was used to calculate the kinetic parameters of EhPTEN1.

15. Lipid membrane overlay assay

Approximately 6×10^6 trophozoites of GFP-EhPTEN1 expressing strain were harvested, washed with PBS, and concentrated by centrifugation. Approximately 100 μl of lysis buffer (50 mM Tris-HCl, pH 7.5, 150 mM NaCl, and 0.1 % Triton X-100, 1× cOmplete Mini, and 0.5 mg/ml E64) was added to the cell pellet. The mixture was incubated on ice for 30 min and centrifuged at 13000 rpm for 5 min. The supernatant was collected and used as the total lysate. GFP-EhPTEN1 was immunoprecipitated using GFP-Trap Agarose Kit (ChromoTek, Planegg, Germany) according to the manufacturer's instruction and confirmed by immunoblot. Lipid membranes on which a panel of phospholipids were immobilized (PIP strips: P-6001 Echelon Bioscience, Salt Laken City, USA) were blocked with PBS-TB for 1 hr at room temperature. The membranes were then incubated with 2 ml of lipid binding solution [PBS-TB, 1x cOmplete Mini protease inhibitor cocktail (EDTA free; Roche, Mannheim, Germany), 0.05 mg/ml E64, 20 μl of eluted lysate] for 3 hr at 4°C. After the membrane were washed twice with PBS-T at 4ºC, they were reacted with anti-GFP at 1:100 dilution with PBS-TB in for 3 hr at 4°C. After incubation with the first antibody, the membranes were further reacted with HRP conjugated anti-mouse IgG antiserum at 1:10,000 dilution with PBS-TB in at 4°C for 1 hr. The membranes were washed three times with PBS-T at 4ºC and the specific proteins were visualized with a chemiluminescence HRP substrate system (Millipore, Massachusetts, USA) using LAS 4000 (Fujifilm Life Science, Cambridge, USA) according to the manufactures' protocol. Recombinant EhPTEN1 protein was also used except that 1 μg/ml of recombinant protein were incubated on the membrane over night at 4°C and anti-His antibody was used as the first antibody with a dilution of 1:1,000.

RESULTS

1. Identification and features of *PTEN* gene in *E. histolytica*

A genome-wide survey of PTEN in the genome of *E. histolytica* HM-1:IMSS reference strain (AmoebaDB, http://amoebadb.org) by BLASTP analysis using human PTEN (P60484) as a query, revealed that *E. histolytica* possesses 6 possible PTEN or PTEN-like proteins that contain PTEN phosphatase domain, and show different domain configuration (Figure 1) (Nakada-Tsukui et al., 2019). I tentatively designated them firstly in an ascending order of the number of recognizable domains and secondly in a descending order of the overall length (EhPTEN1-6) (EhPTEN1, EHI_197010; EhPTEN2, EHI_098450; EhPTEN3, EHI_131070; EhPTEN4, EHI_054460; EhPTEN5, EHI_041900; EhPTEN6, EHI_010360). Our previous transcriptome data (Penuliar et al., 2015; Nakada-Tsukui et al., 2012; Furukawa et al., 2012) verified that one protein (EhPTEN1, EHI_197010) is highly expressed in the trophozoite stage in both *E. histolytica* HM-1: IMSS cl6 and G3 strains, while the 5 other PTENs are expressed at relatively low levels (Figure 2). EhPTEN1 shows 39% mutual identity to human PTEN at the amino acid level (Table 1). Multiple sequence alignment by Clustal W program (http://clustalw.ddbj.nig.ac.jp) shows that the key catalytic residues in the phosphatase domain (H-C-K/R-A-G-K-G-R) needed for lipid and protein phosphatase activity (Maehama and Dixon, 1998; Lee et al., 1999) are well conserved in EhPTEN1 (Figure 3). In addition, the PtdI(4,5)P_2-binding motif (K/R-x4-K/R-x-K/R-K/R-R, PDM domain), which is predicted to regulate the recruitment of protein to the plasma membrane, located at the amino terminus, is also conserved in EhPTEN1 (Maehama et al., 2001; Yoshioka et al., 2020). The cytosolic localization signal (D-G-F-x-L-D-L, CLS) where mutation of phenylalanine residue induces nuclear localization, as well as threonine and isoleucine residues responsible for TI loop formation in an extension of the active site pocket are also conserved

(Figure 3) (Lee et al., 1999; Denning et al., 2007). EhPTEN1 also had C2 domain which has an affinity for phospholipid membranes and helps PTEN to associate with the cell membrane (Lee et al. 1999). InterPro domain search annotates the region of a.a. 550 to 680 of EhPTEN1 as a domain of unknown function (DUF457). The two PEST sequences, that are rich in proline, glutamic acid, serine, and threonine residues at the C terminus of human PTEN, are not conserved in EhPTEN1. Although PEST sequences are known to enhance proteolytic sensitivity, the regulation of EhPTEN1 functions may differ from the human PTEN (Georgescu et al., 2000). EhPTEN1 also lacks PDZ-binding motif (T/S-x-V) located at the C-terminal end in human PTEN and facilitates the protein-protein interactions (Maehama et al., 2001, Masson and Roger, 2020). PTEN has been shown to interact with several PDZ domain-containing proteins, such as membrane-associated guanylate kinase inverted (MAGI) and Na^+/H^+ exchanger regulatory factor (NHERF) in a PDZ-dependent manner (Song et al., 2012; Lee et al., 2018). Interaction of MAGI to the PTEN C-terminal PDZ domain facilitates targeting of PTEN to the plasma membrane, thereby activating its activity (Lee et al., 2018). While NHERF regulates the activation of the PI3K–AKT pathway by binding and recruitment of PTEN to platelet-derived growth factor receptor (PDGFR) (Song et al., 2012). The ~400 a.a. carboxyl-terminal extension which is absent in human ortholog and rich in charged amino acids could be involved in regulating its protein-protein interactions.

2. Cellular localization and dynamics of EhPTEN1 in the motile *E. histoltyica* trophozoite

To examine the cellular localization of EhPTEN1 in trophozoites, I established a transformant line expressing EhPTEN1 with the GFP-tag at the amino terminus (GFP-EhPTEN1). The expression of GFP-EhPTEN1 and GFP (control) in transformant trophozoites was verified by immunoblot analysis using anti-GFP antibodies. A single band corresponding to non-truncated

GFP fusion protein with an expected molecular mass of GFP-EhPTEN1 (90 kDa plus 26 kDa for the GFP tag) was observed in the GFP-EhPTEN1-expressing transformant (Figure 5). Live imaging analysis revealed that GFP-EhPTEN1 was localized throughout the cytosol with higher intensity on pseudopods or protrusions (Figure 6 A). This is analogous to the localization of mammalian PTEN, which predominantly shows cytosolic localization that is responsible for conversion of PtdIns(3,4,5)P_3 to PtdIns(4,5)P_2 through dynamic interaction with the inner face of the plasma membrane (Das et al., 2003; Vazquez et al., 2006). While the localization of *D. discoideum* PTEN changes in response to chemoattractant where PTEN is uniformly associated with the plasma membrane in resting cells but under chemoattractant stimulation, PTEN transiently dissociates from the membrane and diffuses into the cytosol with higher accumulation at the rear of the chemotaxis cells (Iijima et al., 2004). The line intensity plots across transfects of the GFP-PTEN1 overexpressing trophozoites further demonstrated the enrichment of GFP-PTEN1 along the extended pseudopod of the motile trophozoite (Figure 6 B). The normalized average fluorescence intensities at the leading regions of pseudopods were nearly 1.5-fold higher in GFP-EhPTEN1 overexpressing trophozoites compared to mock transformants (Figure 7). Furthermore, the intensity line plot of GFP-expressing control strain showed no accumulation of GFP signal on pseudopods (Figure 8). These findings confirm the enrichment of GFP-EhPTEN1 in the pseudopod-like protrusive structures. For further confirmation, I established a transformant line expressing EhPTEN1 with the HA-tag at the amino terminus (HA-EhPTEN1). The expression of HA-EhPTEN1 in transformant trophozoites was verified by immunoblot analysis using anti-HA antibodies (Figure 9). Similarly, immunofluorescence imaging of HA-EhPTEN1 overexpressing trophozoites using anti-HA antibody revealed that HA-EhPTEN1 was localized mostly in the cytoplasm in steady-state and enriched in the pseudopods (Figure 10). The migration (motility) of

the GFP-EhPTEN1 overexpressing trophozoites using the montage of time-lapse imaging was 0.54±0.09 μm/sec (mean±S.D.), which was significantly greater than that of control GFP expressing transformant (0.27±0.08 μm/sec) (Figure 11). I also investigated the effect of repression of *EhPTEN1* gene expression and found that *EhPTEN1* gene silencing reduced migration (see below).

3. Localization of EhPTEN1 during trogocytosis and phagocytosis

The fact that EhPTEN1 was previously identified as a PtdIns(3)P-binding effector and suggested to be involved in the phagosome biogenesis (Watanabe et al., 2020) promoted further characterization of the role of EhPTEN1 in host cell internalization. Also, it has been recently identified AGC kinases as PtdIns(3,4,5)P_3-binding proteins and revealed their involvement in trogocytosis and phagocytosis in *E. histolytica* (Somlata et al., 2017). To examine the role of EhPTEN1 in ingestion of mammalian cells, I first examined trogocytosis (i.e., nibbling or chewing of a part of a live cell) of CHO cells in GFP-EhPTEN1 or GFP expressing transformant lines. I co-cultured trophozoites of the two transformant lines with live CHO cells that had been stained with CellTracker Orange. Time-lapse imaging of trogocytosis of CHO cells by the amoebae revealed that GFP-EhPTEN1 was accumulated in the region that covers, but not always in close proximity to, the tunnel-like structure, which is the extended neck (or tube)-like structure connecting the unenclosed (or being enclosed) trogosome and the remaining portion of the target cell that is partially ingested (Figure 12 A - 12 D). Upon completion of trogocytosis by closure of the trogosome, GFP-EhPTEN1 was dissociated from the trogosomes and the tunnel-like structure (Figure 12 E). The quantification of the fluorescence intensity in a cross section of the cell confirmed the dynamism of GFP-EhPETN1 during trogocytosis. In contrast, at the very early phase of trogocytosis, GFP-EhPTEN1 was not concentrated on the newly formed trogocytic cup

(Figure 12 B - 12 E). The dynamics of GFP-EhPTEN1 in a course of phagocytosis (i.e., internalization with a single bite) of dead CHO cells was also examined. The live imaging of GFP-EhPTEN1 expressing trophozoites co-cultured with pre-killed CHO cells showed an enrichment of GFP-EhPTEN1 at the tip of the leading edge of the phagocytic cup during the internalization of dead host phagosome closure (Figure 13 A and 13 B). Soon after closure of the phagosome, GFP-EhPTEN1 was concentrated on the closing side of the phagosome (Figure 13 A - 13 C), and rapidly disappeared soon after (Figure 13 D). The fluorescence intensity line plot of a cross section (as indicated by arrows) of the cell also reinforced the observation (Figure 13 A-13 D). As control, GFP-expressing mock strain showed no observable concentration of GFP signal in a course of CHO ingestion (Figure 14).

4. Effect of overexpression of EhPTEN1 on trogocytosis and phagocytosis

The dynamism of GFP-EhPTEN1, as revealed by live imaging, suggests that EhPTEN1 plays a role in the early stage of trogo- and phagocytosis. I examined the effect of GFP-EhPTEN1 overexpression on the efficiency (i.e., speed and volume of internalization of prey) of trogocytosis and phagocytosis. GFP-EhPTEN1 expressing and mock transformant strains were incubated with either live or pre-killed CHO cells that had been stained with CellTracker Orange to allow trogocytosis or phagocytosis, respectively. Internalization of CHO cells by the amoebae were measured by CQ1 confocal quantitative image cytometer. Three parameters were measured and compared between GFP-EhPTEN1 expressing and mock transformant strains: the number of CHO cell-containing trogosomes or phagosomes per ameba, the volume of all CHO cell-containing trogosomes or phagosomes per ameba, and the percentage of the amebae that ingested CHO cells. GFP-EhPTEN1 overexpression caused a reduction in all three parameters above in both trogocytosis (Figure 15) and phagocytosis (Figure 16).

5. Gene silencing of *EhPTEN1* enhances trogocytosis and phagocytosis in *E. histolytica*

Conversely, I attempted to verify if repression of *EhPTEN1* gene expression by antisense small RNA-mediated transcriptional gene silencing (Mirelman et al., 2008) causes reverse phenotypes: enhancement of trogocytosis and phagocytosis on image cytometer CQ1. The silencing of the *EhPTEN1* gene expression was confirmed by RT-PCR and the level of silencing was estimated to be approximately 77.0±9.2% compared to the mock control (G3 transfected with the empty psAP2-Gunma vector) by qRT-PCR assessment (Figure 17). Non-specific off-target gene silencing of other PTEN genes (*EhPTEN2-6*) was ruled out, except for *EhPTEN2*, which showed a slight reduction in *EhPTN1* gene silenced strain, validating gene-specific silencing (Figure 18). The *RNA pol II* transcript level was also unaffected. *EhPTEN1* gene silenced and mock transformants were cultivated with live or dead CHO cells and images were captured every 10 min for 1 hr. As expected, *EhPTEN1* gene silenced strain showed an enhancement of trogocytosis (Figure 19) and phagocytosis (Figure 20). All three parameters to evaluate trogocytosis and phagocytosis, as above, i.e., the number of CHO cell-containing trogosomes or phagosomes per ameba, the volume of all CHO cell-containing trogosomes or phagosomes per ameba, and the percentage of the amebae that ingested CHO cells was significantly increased in *EhPTEN1* gene silenced strain compared to the mock control stain. For instance, the volume of trogosomes and phagosomes increased by around 1.4 fold for trogocytosis and 2 fold for phagocytosis, respectively, in *EhPTEN1* gene silenced strain at later time points of coincubation(at 40-60 mins). Together with the results of EhPTEN1 overexpression, these data indicate that EhPTEN1 serves as a negative regulator of trogocytosis and phagocytosis.

6. EhPTEN1 is a positive regulator for fluid-phase and receptor-mediated endocytosis in *E. histolytica*

Endocytosis encompasses several distinct internalization processes, including uptake of large particles by phagocytosis, internalization of extracellular fluids and solutes by pinocytosis, and clathrin-mediated receptor endocytosis. To investigate the role of EhPTEN1 in other forms endocytosis, I examined the internalization of RITC-dextran and transferrin. Pinocytosis was analyzed by measuring the fluorescence intensity of fluid-phase marker, RITC-dextran, which was internalized after incubation of amoebic transformants with RITC-dextran at 35°C for up to 1 hr. Overexpression of GFP-EhPTEN1 cause approximately 30% increase in pinocytosis in comparison to mock control (53±5.3 or 28±13% at time 30 or 60 min, respectively; $p<0.05$, Figure 21 A). Conversely, *EhPTEN1* gene silenced strain showed an approximately 30% decrease in pinocytosis at 30-60 min, as compared to mock control cells (30±8.2 or 25±5.1% decrease at time 30 or 60 min, respectively, $p<0.05$, Fig 21 B). I next examined internalization of transferrin conjugated with AlexaFluor 568 by CQ1 where transferrin is presumed to be internalized via receptor-mediated endocytosis. The volume of endosomes that contained transferin-AlexaFluor 568 increased by 30-50% in GFP-EhPTEN1 overexpressing trophozoites compared to mock control at all time points up to 1 hr ($p<0.05$, Figure 22 A). Conversely, transferrin endocytosis decreased by 30%-40% in *EhPTEN1* gene silenced strain compared to the mock strain at 40-60 mins ($p<0.05$, Figure 22 B). These data indicate that EhPTEN1 positively regulates pinocytosis of the fluid-phase maker and receptor-mediated endocytosis in *E. histolytica*.

7. EhPTEN1 is essential for optimum growth and migration *E. histolytica*

The biological role of EhPTEN1 in trogo-, phagocytosis, and endocytosis was clearly demonstrated as above. To investigate other physiological roles of EhPTEN1 in *E. histolytica,* the

growth kinetic was monitored in *EhPTEN1* gene silenced and control strains. *EhPTEN1* gene silencing caused significant growth defect: the population doubling time of *EhPTEN1* gene silenced and control strains was 28.1±0.41 and 19.1±0.52 hr, respectively ($P<0.05$; Figure 23 A). I next examined the migration of the trophozoites of *EhPTEN1* gene silenced and control strains using time lapse imaging by CQ1. The velocity of motility was around >60% reduced in *EhPTEN1* gene silenced strain (0.16±0.07 µm /min) compared to the mock control (0.44±0.08 µm /min) (Figure 23 B).

8. Demonstration of phosphatase activity and substrate specificity of EhPTEN1

To see if EhPTEN1 possesses lipid phosphatase activity, bacterial recombinant EhPTEN1 with the histidine tag at the amino terminus was produced using the pCOLD I *E. coli* expression system. SDS-PAGE analysis followed by Coomassie Brilliant Blue staining showed that the purified recombinant EhPTEN1 was apparently homogenous with the predicted molecular mass of 96 kDa including the histidine tag (Figure 24 A). Immunoblot analysis of the purified recombinant protein using His-Tag antibody confirmed the absence of truncation (Figure 24 B). I first examined the enzymatic activities of recombinant EhPTEN1 using a variety of phosphoinositides (PIs) as substrates. EhPTEN1 revealed reasonable activity in a broad pH range with maximum activity obtained at pH 6.0 when the reaction was performed with 50 µM of PtdIns(3,4,5)P_3 at 37°C with for 40 min (Figure 25). I then determined the substrate specificity of EhPTEN1, using a panel of di-C8 PIs. EhPTEN1 showed highest activity with PtdIns(3,4,5)P_3 with the apparent specific activity of 8.18±0.78 nmol/min/mg (Figure 26). EhPTEN1 also catalyzed dephosphorylation of PtdIns(3,4)P_2 and PtdIns(3,5)P_2 with 6 or 3-fold lower specific activities, respectively, compared to that toward PtdIns(3,4,5)P_3. The activities against PI monophosphates and PtdIns(4,5)P_2 were relatively low. All these characteristics are similar to

those of human PTEN (Pagliarini et al., 2004; Taylor and Dixon, 2003). A comparison of kinetic parameters of EhPTEN1 reveals a higher affinity towards PtdIns(3,4,5)P_3 (Km=92.5 ± 4.72 µM) as compared to PtdIns(3,4)P_2 (Km=292 ± 18.8 µM) and PtdIns(3,5)P_2 (Km=160 ± 20.1 µM) demonstrating that in vitro is as well the preferred substrate (Table 2).

9. Demonstration of phospholipid binding of EhPTEN1

The lipid overlay assay using amebic lysates from GFP-EhPTEN1 expressing and mock transformants showed that EhPTEN1 preferentially bound to PtdIns(3)P, PtdIns(4)P, PtdIns(5)P, PtdIns(3,5)P_2, and PtdIns(4,5)P_2 (Figure 27). Furthermore, recombinant EhPTEN1 also revealed a similar binding affinity toward a panel of PIs on the membrane, which is similar to the data given for recombinant human PTEN (Naguib et al., 2015).

Discussion

PTEN regulates fundamental roles in higher eukaryotes including cell survival, metabolic changes, cell polarity, and migration (Lee et al., 2018). In this study, I have characterized the pivotal functions of EhPTEN1 in different forms of endocytosis, migration, and cellular proliferation in *E. histolytica* using GFP tag overexpressing and gene silencing strains. Although the transformant line that has been used for analysis is expressing EhPTEN1 with the GFP-tag at the amino terminus, a linker has been used between the target protein and GFP tag to eliminate the possibility of GFP interference with the target protein. Also, immunofluorescence imaging of HA-EhPTEN1 overexpressing trophozoites revealed similar localization to GFP-EhPTEN1 which suggests that EhPTEN1 behaves similarly regardless of the inserted tag. Furthermore, reliable control with GFP empty vector expressing transformants was used as well as gene silencing of EhPTEN1 showed the opposite effect. The overall data suggests the robustness of the methodology, although further experiments with GFP tag at carboxyl terminus is required for further confirmation. Furthermore, the off-target gene silencing of other PTEN genes (EhPTEN2-6) was ruled out by RT-PCR using a specific primer for each *E. histolytica* PTEN isoforms as shown in Figure 18. While the off-target effect in GFP-EhPTEN1-expressing transformant strains is less likely to occur as the major role of PTEN is regulating PtdIns(3,4,5)P_3 level. Also, EhPTEN1 conserves the catalytic domain that is needed for lipid phosphatases activity, and the enzymatic activity of the recombinant EhPTEN1 demonstrated that PtdIns(3,4,5)P_3 is the preferred substrate. However, transcriptome analysis is required for further confirmation.

1. Role of EhPTEN1 in trogocytosis and phagocytosis

Confocal live imaging demonstrated the involvement of EhPTEN1 in the initial and intermediate stages of trogocytosis and phagocytosis events. In trogocytosis of a live mammalian

cell, EhPTEN1 was enriched in the region where the trogocytic tunnel. Similarly, EhPTEN1 was accumulated on the cell periphery close to the leading edge of the phagocytic cup during the internalization of a dead host cells. The recruitment of EhPTEN1 was transient as it gradually became dissociated from the region after the completion of ingestion of CHO cells. These results are in line with the previous study that showed PTEN localization was associated with forming IgG conjugated zymosan containing phagosomes but disappeared once particle ingestion was complete (Allen et al., 2005). One main concern about cell condition on localization experiment, I performed this experiment with 2 independent transformants and obtained the same result (data not shown). The biochemical analysis showed that GFP-EhPTEN1 overexpression caused a reduction in trogocytosis and phagocytosis. In good agreement with these results, knockdown of *EhPTEN1* caused remarkable enhancement in phagocytosis of dead CHO cells while trogocytosis toward live CHO cells was slightly increased. These results match those observed in earlier studies where PTEN deficient macrophages displayed enhanced phagocytic ability both in vitro and in vivo, while overexpression of PTEN significantly inhibited phagocytosis in macrophages (Cao et al., 2004; Schabbauer et al., 2010; Mondal et al., 2011). It was previously demonstrated that PTEN can down-regulates phagocytosis through dephosphorylation of PtdIns(3,4,5)P_3 which subsequently will affect the downstream events such as the activation of Rac through the pleckstrin homology domain-containing guanine-nucleotide exchange factor, Vav1 (Cao et al., 2004). The depletion of PTEN in macrophages resulted in elevated PtdIns(3,4,5)P_3 levels, leading to activation of Vav1 and subsequent activation of Rac1 GTPase, the latter of which induces F-actin polymerization, which in turn enhances the engulfment of targeted cells (Li et al., 2011). While PtdIns(4,5)P_2 regulates pseudopods extensions on the forming phagocytic cups through activation of the Rho GTPases that stimulate actin polymerization (Schink et al., 2016). Furthermore, it has

been shown that PTEN negatively regulates Fcγ receptor-mediated phagocytosis by repressing the downstream conversion of guanosine diphosphate–Rac (GDP-Rac) to guanosine triphosphate–Rac (GTP-Rac) (Kim et al., 2002). While PtdInsPs mediated signaling and downstream effector in *E. histolytica* is not yet well understood, it has been recently reported that two AGC kinase family from *E. histolytica* have the ability to bind PtdIns(3,4,5)P_3 and are involved in a panel of endocytic events including trogo-, phago-, and pinocytosis (Somlata et al., 2017). In addition, it has also been shown that PtdIns(4,5)P_2 is localized on the plasma membrane of *E. histolytica* whereas PtdIns(3,4,5)P_3 is localized on the phagocytic cup and the extended pseudopodia in *E. histolytica* trophozoites (Byekova et al., 2010; Koushik et al., 2013). These observations suggest that the control of PtdIns(3,4,5)P_3 synthesis and decomposition are important for the regulation of endocytic events in *E. histolytica*. We have clearly demonstrated phosphatase activity and preferred substrate specificity toward PtdIns(3,4,5)P_3 of EhPTEN1. Hence, it is highly conceivable that EhPTEN1 can regulate the local concentrations of PtdIns(4,5)P_2 and PtdIns(3,4,5)P_3 at those target sites during trogo- and phagocytic processes. It seems conceivable that EhPTEN1 negatively regulates trogo- and phagocytosis by reducing the local PtdIns(3,4,5)P_3 concentration, leading to the suppression of actin-dependent cytoskeletal reorganization needed for trogo- and phagocytosis, but further investigation is needed to explore EhPTEN1 roles at the molecular level during trogo- and phagocytosis. Indeed, the concentration of EhPTEN1 is swiftly reduced on and close to trogo- and phagocytic cups (not-yet-enclosed) and trogosomes and phagosomes (enclosed) soon after the completion of ingestion.

2. EhPTEN1 involved in fluid-phase and receptor-mediated endocytosis

I have shown that EhPTEN1 is involved in receptor-mediated endocytosis and macropinocytosis of the fluid-phase marker in an opposite fashion as in trogo- and phagocytosis.

GFP-EhPTEN1 overexpression enhanced transferrin uptake while *EhPTEN1* gene silencing decreased it. It was shown that at least two concentration-dependent mechanisms for transferrin endocytosis exist in *E. histolytica* (Reyes-López et al., 2015): Receptor-mediated endocytosis active at low transferrin concentrations (Reyes-López et al., 2011) and receptor-independent internalization at high transferrin concentrations (Welter et al., 2006). As previously demonstrated, receptor-mediated endocytosis of transferrin in *E. histolytica* is indeed clathrin-mediated [clathrin-mediated endocytosis (CME)] (López-Soto et al., 2009), and receptor-mediated endocytosis is in general clathrin-mediated and actin independent (Bohdanowicz and Grinstein, 2013). Unlike trogo- and phagocytosis, CME is also distinct in that it depends on PtdIns(4,5)P_2 and does not require PtdIns(3,4,5)P_3 (Bohdanowicz and Grinstein, 2013; Schink et al., 2016). PtdIns(4,5)P_2 binds and recruits several proteins associated with CME formation to the membrane including cargo-recognizing adaptor AP2, clathrin nucleator FCHO, the clathrin-regulatory protein AP180, the cargo adaptor Epsin, Dynamin, Amphiphysin, and Snx9 (Di Paolo and De Camilli, 2006; Bohdanowicz and Grinstein, 2013; Schink et al., 2016). Accordingly, depleting cells of PtdIns(4,5)P_2 prevents AP2 recruitment, and CME formation is reduced as the forming endosomes lack the linkage between cargo and clathrin. Taken together, EhPTEN1 possibly facilitates the transferrin internalization through augmentation of PtdIns(4,5)P_2 synthesis. Furthermore, EhPTEN1showed similar phenotypes toward pinocytosis of the fluid-phase marker. As stated above, transferrin, when present at high concentrations, is internalized by receptor independent fashion in *E. histolytica* (Welter et al., 2006). Thus, it is consistent with previous observation that *E. histolytica* internalization of the fluid-phase marker and transferrin by actin-dependent macropinocytosis (S7 and S8 Movies), also as previously shown (Das et al., 2021). Also, it has previously shown that EhAGCK2, which preferentially binds PtdIns(3,4,5)P_3 over PtdIns(4,5)P_2,

is involved in pinocytosis of the fluid-phase marker (Somlata et al., 2017). However, it was shown that the local production of PtdIns(4,5)P_2 in the early stages of macropinocytosis is essential for the formation of ruffles and is partly responsible for the remodeling of the actin cytoskeleton (Fujii et al., 2013). Altogether, EhPTEN1 may accelerate transient synthesis PtdIns(4,5)P_2 on the plasma membrane which facilitates the formation of actin-containing pinocytic cup. Although phagocytosis and macropinocytosis both construct a cup in an actin-dependent manner, phagocytosis is a receptor-guided zipper-like model that conforms to particle geometry while macropinocytosis is self-organized with little or no guidance from receptors and can form in the absence of particles (Swanson, 2008). Moreover, a number of previous studies have shown that macropinocytosis and phagocytosis are distinct. For instance, RacC or Rap1 overexpressing cells or profilin-null cells displayed a higher phagocytosis rate but macropinocytosis was significantly reduced (Temesvari et al., 2000; Seastone et al., 1998; Seastone et al., 1999). Regarding the PtdInsPs metabolism, PtdIns(4,5)P_2 and PtdIns(3,4,5)P_3 levels are tightly controlled during phagocytosis and macropinocytosis to ensure the efficiency of internalization (Schink et al., 2016, Bohdanowicz and Grinstein, 2013). However, the signaling mechanism regulating phagocytosis and macropinocytosis is very complicated and the exact mechanism that differentiates them is still debated. It has been reported previously that deletion of PTEN in *D. discoideum* caused a reduction in fluid uptake (Veltman et al., 2016). Nevertheless, the lipid rafts in the plasma membrane of *E. histolytica* is highly enriched with PtdIns(4,5)P_2 (Koushik et al., 2013) and disruption of lipid rafts with cholesterol-binding agents significantly inhibited fluid-phase pinocytosis of *E. histolytica* (Laughlin et al., 2004). Altogether, we assume that EhPTEN1 accelerates transient synthesis of PtdIns(4,5)P_2 on the plasma membrane which in turn facilitates the formation of actin-associated macropinocytic cup. Another possible role of EhPTEN1 in regulating endocytic processes is

related to its direct or indirect effect on the downstream molecules such as extracellular signal-regulated kinase (ERK), AKT, Rab7, and cofilin-1. PTEN showed an antagonizing effect of PI3K on ERK activation via Ras and Rab1 that facilitates the endocytosis of tropomyosin receptor kinase A (TrkA) (York et al., 2000). In addition, Epidermal Growth Factor Receptor (EGFR) and PTEN preferentially localize to short-lived Clathrin-coated pits (CCPs) where the phosphatase activity of PTEN influence the AKT signaling that corresponds with induction of clathrin-dependent Epidermal Growth Factor signaling pathway (Rosselli-Murai et al., 2018). Furthermore, PTEN has protein phosphatase activity toward multiple substrates such as focal adhesion kinase (FAK), cAMP-responsive element-binding protein (CREB), Rab7, and Coflin-1 (Song et al., 2012). It has been shown that PTEN regulates endosome maturation through dephosphorylation of inactive Rab7 in the cytosol which facilitates its interaction with GDP dissociation inhibitor (GDI) leading to activation and recruitment of Rab7 at the endosomal membrane and subsequent endosomal maturation (Shinde and Maddika, 2016). Moreover, Cofilin-1 activation in *Candida albicans* was mediated by PTEN protein phosphatase activity which in turn decreases F-actin assembly and causes reduction of *C. albicans* phagocytosis (Serezani et al., 2012). It was previously reported that *E. histolytica* contains actin-binding protein of the ADF/cofilin family (Coactosin) as well as multiple Rab7 isotypes that are involved in actin dynamics, phagocytosis, and trogocytosis (Saito-Nakano et al., 2021; Kumar et al., 2014). However, further analysis is needed to investigate the specific downstream signaling of EhPTEN1 that could be involved in endocytic events.

3. EhPTEN1 regulates pseudopods formation and migration

I have shown that EhPTEN1, in two forms of tagged/fusion proteins, GFP-EhPTEN1 and HA-EhPTEN1, enhances cell migration while repression of *EhPTEN1* gene expression causes inhibition of motility. These observations agree well with the fact that EhPTEN1 was transiently

concentrated in newly formed pseudopods. The GFP-EhPTEN1 distribution in *E. histolytica* is similar to the localization of mammalian PTEN, which predominantly shows cytosolic localization and mediates conversion of PtdIns(3,4,5)P_3 to PtdIns(4,5)P_2 through dynamic interaction with the inner face of the plasma membrane (Das et al., 2003; Vazquez et al., 2006). It was also shown that in *D. discoideum* the localization of PTEN changed in response to the chemoattractant stimulation via increase in extracellular cAMP. In resting cells, PTEN is uniformly associated with the plasma membrane, but upon chemoattractant stimulation, PTEN transiently dissociates from the membrane and diffuses into the cytosol with accumulation at the rear of the chemotaxis cells (Iijima et al., 2004). These data suggest that EhPTEN1 is involved in pseudopods formation and motility. In *D. discoideum*, PTEN was also implicated in cell migration as a positive regulator of motility, because an ameba strain lacking PTEN showed a reduction in migration speed and defect in chemotactic efficiency due to disruption of PtdIns(3,4,5)P_3 / PtdIns(4,5)P_2 concentration gradient throughout the cell (Wessels et al., 2007; Iijima and Devreotes, 2002; Arai et al., 2010). In contrast, in mammalian cell types including B cells, glioma cells, and fibroblasts, PTEN was shown to inhibit migration (Leslie et al., 2008; Song et al., 2012). The behavioral analysis of *D. discoideum* showed that loss of PTEN caused a reduction in cell motility due to their inability to repress the formation of lateral pseudopodia that misdirect them, compared with wild-type cells, which produce only one large pseudopod at a time (Wessels et al., 2007; Iijima and Devreotes, 2002). In addition, loss of PTEN also resulted in dysregulation of myosin II assembly at the cell cortex, where PTEN prevents the formation of lateral pseudopodia and promotes cell body contraction and posterior retraction in *D. discoideum* (Wessels et al., 2007; Kölsch et al., 2008). PtdIns(4,5)P_2, produced by PTEN, can recruit and activate a wide variety of actin regulatory proteins at the plasma membrane, thereby controlling motility (Di Paolo and De Camilli, 2006;

Schink et al., 2016). For example, PtdIns(4,5)P_2 activates N-WASP directly or indirectly through interaction with IQGAP1 which result in promoting actin polymerization by activation of N-WASP–Arp2/3 complex (Di Paolo and De Camilli, 2006; Schink et al., 2016; Tsujita and Itoh, 2015). Among them, myosin II and Arp2/3 complex are conserved in *E. histolytica*, where myosin II plays a critical role in movement (Arhets et al., 1998; Labruyère and Guillén, 2006) and Arp2/3 complex is involved in actin nucleation (Manich et al., 2018). Thus, it is conceivable that EhPTEN1 mediates signaling for pseudopod formation and migration through regulation of PtdIns(3,4,5)P_3 metabolism.

4. PIPs specificity of EhPTEN1

Furthermore, EhPTEN1 reserves its activity toward PtdIns(3,4,5)P_3 and showed a wide binding spectrum toward PtdInsPs similar to human PTEN. Determination of human PTEN substrate specificity reveals that PTEN activity is approximately 2 fold greater toward PtdIns(3,4,5)P_3 than with either PtdIns(3,4)P_2 or PtdIns(3,5)P_2 (Pagliarini et al., 2004; Taylor and Dixon, 2003). In addition, a recent study detected the binding of human PTEN with PI monophosphates on the lipid membranes with immobilized phospholipids and identified the binding of PtdIns(3)P with C2 domain of PTEN target its localization to endosomal membranes (Naguib et al., 2015). Interestingly, differential proteomic analysis has detected EhPTEN1 as PtdIns(3)P-binding effector in *E. histolytica* trophozoites which may suggest the evolutionary function of EhPTEN1 in endocytosis (Watanabe et al., 2020). However, the role of PTEN binding with broad spectrum of lipids has not been studied. This may indicate that various roles of EhPTEN1 needed to be elucidated with further studies. In addition, EhPTEN1 has a carboxyl-terminal extension that is unique and conserved among other *Entamoeba* species (data not shown).

The effect of this unique carboxyl-terminal extension is not yet known and further studies are needed to address this interesting issue in future research.

5. EhPTEN1 plays an important role in proliferation of *E. histolytica*

We have shown that repression of gene expression of *EhPTEN1* caused significant growth defect. This phenotype can be possibly explained by reduced ability in nutrient uptake. Furthermore, it was previously demonstrated that the growth defect in *E. histolytica* in low iron medium was rescued by the addition of iron-loaded holo-transferrin, and that holo-transferrin was recognized by an amoebic transferrin receptor and endocytosed via clathrin-coated vesicles (Reyes-López et al.,2011; Reyes-López et al., 2020). These data, taken together, underscore the importance of endocytosis of transferrin for the proliferation of amoebae. Macropinocytosis was previously identified as a mechanism by which malignant cells satisfy their unique metabolic needs and hence support cancer progression (Commisso et al., 2013). In the amoebae, macropinocytosis is the primary and widely used method for feeding (Hacker et al., 1997). On the other hand, the downstream signaling molecules that correspond to mammalian PTEN and are related to cellular proliferation, such as B cell lymphoma 2 associated agonist of cell death (BAD) and cyclin-dependent kinase inhibitor p27 (Chalhoub and Baker, 2009; Song et al., 2012), have not yet been identified in *E. histolytica*. Instead, *E. histolytica* possesses two genes encoding TOR-like proteins by biocomputational approach (Muñoz-Muñoz et al., 2021). These data may suggest that regulation of amoebic growth by PTEN is distinct in *E. histolytica*. On the other hand, it was previously shown that loss of PTEN significantly lowered growth in *D. discoideum*, possibly attributable to mislocalization of myosin II during cytokinesis (Janetopoulos et al., 2005; Pramanik et al., 2009). Similarly, myosin II mutants caused reduction in growth and multinucleation in *E. histolytica* (Arhets et al., 1998). These observations likely support the premise that EhPTEN1

regulates amoebic cell proliferation by regulation of cytokinesis and/or nutrient uptake by macropinocytosis. Furthermore, the requirement of EhPTEN1 for optimum proliferation indicates that *E. histolytica* apparently does not possess compensatory mechanisms for the PIPs dysregulation caused by the loss of EhPTEN1, and thus have posed it as rational drug target.

This study identifies the roles of EhPTEN1 in the actin-related virulence process including different forms of endocytosis and migration which may facilitate the degradation of intestinal epithelial cells and invasion of extraintestinal organs by *E. histolytica* trophozoites. Additionally, EhPTEN1 is essential for cell viability which highlights the crucial impact of EhPTEN1 on the pathogenicity of *E. histolytica*. It has been known that phagocytosis and migration are conserved in *E. histolytica* and are considered to be important factors for invasion of intestinal tissue and reaching blood circulation to infect extraintestinal organs (Faust and Guillen, 2012). Similar to cancer cells, *E. histolytica* also inherited the capacity of macropinocytosis as a primary feeding mechanism (Song et al., 2021; Somlata et al., 2017). This research expands our knowledge on PTEN biology and function in general, which will eventually contribute to molecular drug targeting against amebiasis.

In conclusion, I have shown the biological significance of EhPTEN1 on different forms of endocytosis including trogocytosis, phagocytosis, pinocytosis, and clathrin-mediated endocytosis. The present study also demonstrated the essentiality of EhPTEN1 in pseudopod formation, motility, and optimal growth of *E. histolytica*. Though it is most likely that phenotypic changes in EhPTEN1 overexpressing and gene silencing strains in *E. histolytica* are caused by affecting PtdIns(3,4,5)P_3 signaling, further investigation is needed to study the effect of EhPTEN1 on the molecular level that differentiate these processes (Trogo-/phago-cytosis, macropinocytosis, growth, and migration). Taken together, these findings emphasize the importance of EhPTEN1 in modulating

a plethora of functions in *E. histolytica*. Exploring PTEN functions in *E. histolytica* will hopefully increase our knowledge on the regulation of cellular processes related to actin remodeling through the PtdInsPs signaling pathway. Also, it will inform the rational design of novel therapies against eukaryotic pathogens.

ACKNOWLEDGMENT

My sincere gratitude to my academic supervisor and adviser, Prof. Tomoyoshi Nozaki, for accepting me as a Ph.D. student in his laboratory, and for his constructive guidance, unending support, and reassuring advice during my research. My gratitude also to Dr. Kumiko Nakada-Tsukui, senior researcher from National Institute of Infectious Disease, Tokyo; for her constant guidance and insightful advice throughout the conduct of this research. I am also grateful to associate professor, Dr. Yoh-ichi Watanabe, assistant professors, Dr. Herbert J. Santos, and Ghulam Jeelani for the valuable help and advice for the improvement of this research.

I would like to express my appreciation to all members of Nozaki sensei lab (both current and former), namely Dr. Michio Yamashita, Dr. Yoshinari Shigeo, Dr. Koushik Das, Dr. Arif Nurkanto, Dr. Konomi Marumo, Dr. Tetsuro Kawano, Dr. Ratna Wahyuni, Dr. Natsuki Watanabe, Mihoko Imada, Kumiko Shibata, Emi Mazaki, Chizuko Koresawa,Yumiko Nagai, Haruka Ohno, Penny Kartikasari, Jiang Han, Farida Ifadotunnikmah, Dewi Wulansari, Yulia Rachmawati, Rivo Yudhinata, Ruofan Peng, Satoki Itsuji, Quỳnh Anh, Suguru Taniguchi, Defi Kartika, Misato Shimoyama, Yuka Uesugi, Seiji Fujimoto, Bandaru Rahmatari, and Yang Daibing, for fruitful discussion and exchanges of ideas in laboratory work and research. I also would like to acknowledge the Ministry of Education, Culture, Sports, Science and Technology (MEXT) for providing me with the scholarship for my Ph.D. education in Japan.

I would like to express my deepest gratitude and love to my family; my mother Amani Al-Abed, my father Yasser Kadri, my sister Amal Kadri, and my brothers Ammar Kadri and Mohammad Kadri; for their unconditional love, continuous support, and for giving me the strength to reach my dreams. I also thank every member of my family and my friends for all the warm acts of kindness and encouragement. Thank you so much.

REFERENCES

Allen, L. A. H, Allgood J. Aaron, Han Xuemei, and Wittine Lara M. "Phosphoinositide3-Kinase Regulates Actin Polymerization during Delayed Phagocytosis of *Helicobacter Pylori*." *Journal of Leukocyte Biology*, vol. 78, no. 1, pp. 220–30, 2005, doi:10.1189/jlb.0205091.

Arai, Yoshiyuki, Tatsuo Shibata, Satomi Matsuoka, Masayuki J. Sato, Toshio Yanagida, and Masahiro Ueda. "Self-Organization of the Phosphatidylinositol Lipids Signaling System for Random Cell Migration." *Proceedings of the National Academy of Sciences of the United States of America*, vol. 107, no. 27, pp. 12399–404, 2010, doi:10.1073/pnas.0908278107.

Arhets P, Olivo JC, Gounon P, Sansonetti P, and Guillén N. ''Virulence and functions of myosin II are inhibited by overexpression of light meromyosin in *Entamoeba histolytica*.'' *Molecular Biology of the Cell*, 9(6):1537–47, 1998.

Balla T. "Phosphoinositides: Tiny lipids with giant impact on cell regulation." *Physiological Reviews*, vol. 93, pp. 1019-137, 2013.

Bharadwaj, Ravi, Ranjana Arya, M. Shahid mansuri, Sudha Bhattacharya, and Alok Bhattacharya. "EhRho1 Regulates Plasma Membrane Blebbing through PI3 Kinase in *Entamoeba Histolytica*." *Cellular Microbiology*, Vol. 19 (10), pp. 1–18, 2017.

Bharadwaj, Ravi, Shalini Sharma, Ranjana Arya, Janhawi, Sudha Bhattacharya, and Alok Bhattacharya. "EhRho1 Regulates Phagocytosis by Modulating Actin Dynamics through EhFormin1 and EhProfilin1 in *Entamoeba Histolytica*." *Cellular Microbiology*, Vol. 20 (9), pp. 1–20, 2018.

Bohdanowicz Michal and Grinstein Sergio. “ROLE OF PHOSPHOLIPIDS IN ENDOCYTOSIS, PHAGOCYTOSIS, AND MACROPINOCYTOSIS.” *American Physiological Society*, vol. 93, pp. 69–106, 2013, doi:10.1152/physrev.00002.2012.

Bracha, Rivka, Yael Nuchamowitz, Michael Anbar, and David Mirelman. “Transcriptional Silencing of Multiple Genes in Trophozoites of *Entamoeba Histolytica*.” *PLoS Pathogens*, vol. 2, no. 5, pp. 431–41, 2006, doi:10.1371/journal.ppat.0020048.

Byekova, Yevgeniya A., Rhonda R. Powell, Brenda H. Welter, and Lesly A. Temesvari. “Localization of Phosphatidylinositol (3,4,5)-Trisphosphate to Phagosomes in *Entamoeba Histolytica* Achieved Using Glutathione S-Transferase- and Green Fluorescent Protein-Tagged Lipid Biosensors.” *Infection and Immunity*, vol. 78, no. 1, pp. 125–37, 2010, doi:10.1128/IAI.00719-09.

Cao, Xianhua, Guo Wei, Huiqing Fang, Jianping Guo, Michael Weinstein, Clay B. Marsh, Michael C. Ostrowski, and Susheela Tridandapani. “The Inositol 3-Phosphatase PTEN Negatively Regulates Fcγ Receptor Signaling but Supports Toll-Like Receptor 4 Signaling in Murine Peritoneal Macrophages.” *The Journal of Immunology*, vol. 172, no. 8, pp. 4851–57, 2004, doi:10.4049/jimmunol.172.8.4851.

Chalhoub N, Baker SJ. ‘‘PTEN and the PI3-Kinase Pathway in Cancer.’’ *Annual Review of Pathology: Mechanisms of Disease*, 1;4(1):127–50, 2009.

Choorapoikayil, Suma, Raoul V. Kuiper, Alain De Bruin, and Jeroen Den Hertog. “Haploinsufficiency of the Genes Encoding the Tumor Suppressor Pten Predisposes

Zebrafish to Hemangiosarcoma." *DMM Disease Models and Mechanisms*, vol. 5, no. 2, pp. 241–47, 2012, doi:10.1242/dmm.008326.

Chung, Ji Hyun, and Charis Eng. "Nuclear-Cytoplasmic Partitioning of Phosphatase and Tensin Homologue Deleted on Chromosome 10 (PTEN) Differentially Regulates the Cell Cycle and Apoptosis." *Cancer Research*, vol. 65, no. 18, pp. 8096–100, 2005, doi:10.1158/0008-5472.CAN-05-1888.

Commisso C, Davidson SM, Soydaner-Azeloglu RG, Parker SJ, Kamphorst JJ, Hackett S, Grabocka E, Nofal M, Drebin JA, Thompson CB, Rabinowitz JD, Metallo CM, Vander Heiden MG, and Bar-Sagi D. ''Macropinocytosis of protein is an amino acid supply route in Ras-transformed cells.'' *Nature*, 30;497(7451):633-7, 2013, doi: 10.1038/nature12138.

Cristofano, Antonio Di, Barbara Pesce, Carlos Cordon-Cardo, and Pier Paolo Pandolfi. "Pten Is Essential for Embryonic Development and Tumour Suppression." *Nature Genetics*, vol. 19, no. 4, pp. 348–55, 1998, doi:10.1038/1235.

Das K, Watanabe N, Nozaki T. "Two StAR-related lipid transfer proteins play specific roles in endocytosis, exocytosis, and motility in the parasitic protist *Entamoeba histolytica*.'' *PLoS Pathog*, 17:1–27, 2021.

Das, S., J E Dixon, and W Cho. "Membrane-Binding and Activation Mechanism of PTEN." *Proceedings of the National Academy of Sciences*, vol. 100, no. 13, pp. 7491–96, 2003, doi:10.1073/pnas.0932835100.

Denning, G., B. Jean-Joseph, C. Prince, D. L. Durden, and P. K. Vogt. “A Short N-Terminal Sequence of PTEN Controls Cytoplasmic Localization and Is Required for Suppression of Cell Growth.” *Oncogene*, vol. 26, no. 27, pp. 3930–40, 2007, doi:10.1038/sj.onc.1210175.

Di Paolo, Gilbert, and Pietro De Camilli. “Phosphoinositides in Cell Regulation and Membrane Dynamics.” *Nature*, vol. 443, no. 7112, pp. 651–57, 2006, doi:10.1038/nature05185.

Diamond, Louis S., Dan R. Harlow, and Carol C. Cunnick. “A New Medium for the Axenic Cultivation of *Entamoeba Histolytica* and Other *Entamoeba*.” *Transactions of the Royal Society of Tropical Medicine and Hygiene*, vol. 72, no. 4, pp. 431–32, 1978, doi:10.1016/0035-9203(78)90144-X.

Diamond, L. S., Mattern, C. F., & Bartgis, I. L. “Viruses of *Entamoeba histolytica*. I. Identification of transmissible virus-like agents.’’ *Journal of virology*, 9(2), 326–341, 1972.

Fang, Min, Zhirong Shen, Song Huang, Liping Zhao, She Chen, Tak W. Mak, and Xiaodong Wang. “The ER UDPase ENTPD5 Promotes Protein N-Glycosylation, the Warburg Effect, and Proliferation in the PTEN Pathway.” *Cell*, vol. 143, no. 5, pp. 711–24, 2010, doi:10.1016/j.cell.2010.10.010.

Faucherre, A., G. S. Taylor, J. Overvoorde, J. E. Dixon, and J. Den Hertog. “Zebrafish Pten Genes Have Overlapping and Non-Redundant Functions in Tumorigenesis and Embryonic Development.” *Oncogene*, vol. 27, no. 8, pp. 1079–86, 2008, doi:10.1038/sj.onc.1210730.

Faust, Daniela M., and Nancy Guillen. "Virulence and Virulence Factors in *Entamoeba Histolytica*, the Agent of Human Amoebiasis." *Microbes and Infection*, vol. 14, no. 15, Elsevier Masson SAS, 2012, pp. 1428–41, doi:10.1016/j.micinf.2012.05.013.

Fujii M, Kawai K, Egami Y, Araki N. "Dissecting the roles of Rac1 activation and deactivation in macropinocytosis using microscopic photo-manipulation.'' *Scientific Reports*, 3:1–10, 2013.

Fukuyama, Masamitsu, Ann E. Rougvie, and Joel H. Rothman. "C. Elegans DAF-18/PTEN Mediates Nutrient-Dependent Arrest of Cell Cycle and Growth in the Germline." *Current Biology*, vol. 16, no. 8, pp. 773–79, 2006, doi:10.1016/j.cub.2006.02.073.

Furukawa, Atsushi, Kumiko Nakada-Tsukui, and Tomoyoshi Nozaki. "Novel Transmembrane Receptor Involved in Phagosome Transport of Lysozymes and β-Hexosaminidase in the Enteric Protozoan *Entamoeba Histolytica*." *PLoS Pathogens*, vol. 8, no. 2, 2012, doi:10.1371/journal.ppat.1002539.

Galicia, Vivian A., Lina He, Hien Dang, Gary Kanel, Christopher Vendryes, Barbara A. French, Ni Zeng, Jennifer–Ann Bayan, Wei Ding, Kasper S. Wang, Samuel French, Morris J. Birnbaum, Bart Rountree, and Bangyan L. Stiles. "Expansion of Hepatic Tumor Progenitor Cells in Pten-Null Mice Requires Liver Injury and Is Reversed by Loss of AKT2." *Gastroenterology*, vol. 139, no. 6, pp. 2170–82, 2010, doi:10.1053/j.gastro.2010.09.002.

Garcia-Cao, Isabel, Min Sup Song, Robin M. Hobbs, Gaelle Laurent, Carlotta Giorgi, Vincent C.J. De Boer, Dimitrios Anastasiou, Keisuke Ito, Atsuo T. Sasaki, Lucia Rameh, Arkaitz Carracedo, Matthew G. Vander Heiden, Lewis C. Cantley, Paolo Pinton, Marcia C. Haigis, and Pier Paolo Pandolfi. "Systemic Elevation of PTEN Induces a Tumor-Suppressive

Metabolic State." *Cell*, vol. 149, no. 1, Elsevier Inc., pp. 49–62, 2012, doi:10.1016/j.cell.2012.02.030.

Georgescu, Maria Magdalena, Kathrin H. Kirsch, Paul Kaloudis, Haijuan Yang, Nikola P. Pavletich, and Hidesaburo Hanafusa. "Stabilization and Productive Positioning Roles of the C2 Domain of PTEN Tumor Suppressor." *Cancer Research*, vol. 60, no. 24, pp. 7033–38, 2000.

Ghosh, Sudip K., and John Samuelson. "Involvement of P21(RacA), Phosphoinositide 3-Kinase, and Vacuolar ATPase in Phagocytosis of Bacteria and Erythrocytes by *Entamoeba Histolytica*: Suggestive Evidence for Coincidental Evolution of Amebic Invasiveness." *Infection and Immunity*, vol. 65, no. 10, pp. 4243–49, 1997.

Gil, E. B., Malone Link, E., Liu, L. X., Johnson, C. D., & Lees, J. A. "Regulation of the insulin-like developmental pathway of Caenorhabditis elegans by a homolog of the PTEN tumor suppressor gene.'' *Proceedings of the National Academy of Sciences of the United States of America*, 96(6), 2925–2930, 1999.

Gupta, Rajeev, Julie T.L. Ting, Lubomir N. Sokolov, Sheila A. Johnson, and Sheng Luan. "A Tumor Suppressor Homolog, AtPTEN1, Is Essential for Pollen Development in Arabidopsis." *Plant Cell*, vol. 14, no. 10, pp. 2495–507, 2002, doi:10.1105/tpc.005702.

Hacker, U., Albrecht, R., & Maniak, M. "Fluid-phase uptake by macropinocytosis in *Dictyostelium*.'' *Journal of cell science*, 110 (Pt 2), 105–112, 1997.

Haque, R., Huston, C. D., Hughes, M., Houpt, E., & Petri, W. A., Jr. "Amebiasis.'' *The New England journal of medicine*, 348(16), 1565–1573, 2003.

Heit, Bryan, Stephen M. Robbins, Charlene M. Downey, Zhiwen Guan, Pina Colarusso, Joan B. Miller, Frank R. Jirik, and Paul Kubes. "PTEN Functions to 'prioritize' Chemotactic Cues and Prevent 'Distraction' in Migrating Neutrophils." *Nature Immunology*, vol. 9, no. 7, pp. 743–52, 2008, doi:10.1038/ni.1623.

Horie, Yasuo, Akira Suzuki, Ei Kataoka, Takehiko Sasaki, Koichi Hamada, Junko Sasaki, Katsunori Mizuno, Go Hasegawa, Hiroyuki Kishimoto, Masahiro Iizuka, Makoto Naito, Katsuhiko Enomoto, Sumio Watanabe, Tak Wah Mak, and Toru Nakano. "Hepatocyte-Specific Pten Deficiency Results in Steatohepatitis and Hepatocellular Carcinomas." *Journal of Clinical Investigation*, vol. 113, no. 12, pp. 1774–83, 2004, doi:10.1172/JCI20513.

Hubbard, Leah L. N., Carol A. Wilke, Eric S. White, and Bethany B. Moore. "PTEN Limits Alveolar Macrophage Function against *Pseudomonas Aeruginosa* after Bone Marrow Transplantation." *American Journal of Respiratory Cell and Molecular Biology*, vol. 45, no. 5, pp. 1050–58, 2011, doi:10.1165/rcmb.2011-0079OC.

Iijima, Miho, and Peter Devreotes. "Tumor Suppressor PTEN Mediates Sensing of Chemoattractant Gradients." *Cell*, vol. 109, pp. 599–610, 2002.

Iijima, Miho, Yi Elaine Huang, Hongbo R. Luo, Francisca Vazquez, and Peter N. Devreotes. "Novel Mechanism of PTEN Regulation by Its Phosphatidylinositol 4,5-Bisphosphate Binding Motif Is Critical for Chemotaxis." *Journal of Biological Chemistry*, vol. 279, no. 16, 2004, doi:10.1074/jbc.M312098200.

Janetopoulos C, Borleis J, Vazquez F, Iijima M, Devreotes P. “Temporal and spatial regulation of phosphoinositide signaling mediates cytokinesis.’’ *Developmental Cell*. 8(4):467–77. 2005.

Kim, Jong Suk, Xiaodong Peng, Pradip K. De, Robert L. Geahlen, and Donald L. Durden. “PTEN Controls Immunoreceptor (Immunoreceptor Tyrosine-Based Activation Motif) Signaling and the Activation of Rac.” *Blood*, vol. 99, no. 2, pp. 694–97, 2002, doi:10.1182/blood.V99.2.694.

Kölsch, Verena, Pascale G. Charest, and Richard A. Firtel. “The Regulation of Cell Motility and Chemotaxis by Phospholipid Signaling.” *Journal of Cell Science*, vol. 121, no. 5, pp. 551–59, 2008, doi:10.1242/jcs.023333.

Koushik, Amrita B., Rhonda R. Powell, and Lesly A. Temesvari. “Localization of Phosphatidylinositol 4,5-Bisphosphate to Lipid Rafts and Uroids in the Human Protozoan Parasite *Entamoeba Histolytica*.” *Infection and Immunity*, vol. 81, no. 6, pp. 2145–55, 2013, doi:10.1128/IAI.00040-13.

Kumar, Nitesh, Somlata, Mohit Mazumder, Priyanka Dutta, Sankar Maiti, Samudrala Gourinath. “EhCoactosin Stabilizes Actin Filaments in the Protist Parasite Entamoeba Histolytica.” *PLoS Pathogens*, vol. 10, no. 9, 2014, doi:10.1371/journal.ppat.1004362.

Labruyère E, and Guillén N. “Host tissue invasion by *Entamoeba histolytica* is powered by motility and phagocytosis.’’ *Archives of Medical Research*, 37(2):252–7, 2006.

Lachlan, Katherine L., A. M. Lucassen, D. Bunyan, and I. K. Temple. “Cowden Syndrome and Bannayan-Riley-Ruvalcaba Syndrome Represent One Condition with Variable Expression

and Age-Related Penetrance: Results of a Clinical Study of PTEN Mutation Carriers." *Journal of Medical Genetics*, vol. 44, no. 9, pp. 579–85, 2007, doi:10.1136/jmg.2007.049981.

Laughlin RC, McGugan GC, Powell RR, Welter BH, and Temesvari LA. "Involvement of raft-like plasma membrane domains of *Entamoeba histolytica* in pinocytosis and adhesion.'' *Infection and Immunity*, 72:5349–5357, 2004.

Lee, Jie Oh, Haijuan Yang, Maria Magdalena Georgescu, Antonio Di Cristofano, Tomohiko Maehama, Yigong Shi, Jack E. Dixon, Pier Pandolfi, and Nikola P. Pavletich. "Crystal Structure of the PTEN Tumor Suppressor: Implications for Its Phosphoinositide Phosphatase Activity and Membrane Association." *Cell*, vol. 99, no. 3, pp. 323–34, 1999, doi:10.1016/S0092-8674(00)81663-3.

Lee, Yu Ru, Ming Chen, and Pier Paolo Pandolfi. "The Functions and Regulation of the PTEN Tumour Suppressor: New Modes and Prospects." *Nature Reviews Molecular Cell Biology*, vol. 19, no. 9, Springer US, pp. 547–62, 2018, doi:10.1038/s41580-018-0015-0.

Leslie, N. R., I. H. Batty, H. Maccario, L. Davidson, and C. P. Downes. "Understanding PTEN Regulation: PIP_2, Polarity and Protein Stability." *Oncogene*, vol. 27, no. 41, pp. 5464–76, 2008, doi:10.1038/onc.2008.243.

Li, Jing, Clifford Yen, Danny Liaw, Katrina Podsypanina, Shikha Bose, Steven I. Wang, Janusz Puc, Christa Miliaresis, Linda Rodgers, Richard McCombie, Sandra H. Bigner, Beppino C. Giovanella, Michael Ittmann, Ben Tycko, Hanina Hibshoosh, Michael H. Wigler, Ramon Parsons. "PTEN, a Putative Protein Tyrosine Phosphatase Gene Mutated in Human Brain,

Breast, and Prostate Cancer." *Science*, vol. 275, no. 5308, pp. 1943–47, 1997, doi:10.1126/science.275.5308.1943.

Li, Yitang, Amit Prasad, Yonghui Jia, Saurabh Ghosh Roy, Fabien Loison, Subhanjan Mondal, Paulina Kocjan, Leslie E. Silberstein, Sheng Ding, and Hongbo R. Luo. "Pretreatment with Phosphatase and Tensin Homolog Deleted on Chromosome 10 (PTEN) Inhibitor SF1670 Augments the Efficacy of Granulocyte Transfusion in a Clinically Relevant Mouse Model." *Blood*, vol. 117, no. 24, pp. 6702–13, 2011, doi:10.1182/blood-2010-09-309864.

Liliental, Joanna, Sun Young Moon, Ralf Lesche, Ramanaiah Mamillapalli, Daming Li, Yi Zheng, Hong Sun, and Hong Wu. "Genetic Deletion of the Pten Tumor Suppressor Gene Promotes Cell Motility by Activation of Rac1 and Cdc42 GTPases." *Current Biology*, vol. 10, no. 7, pp. 401–04, 2000, doi:10.1016/S0960-9822(00)00417-6.

López-Soto F, León-Sicairos N, Reyes-López M, Serrano-Luna J, Ordaz-Pichardo C, Piña-Vázquez C, Estrada G, Garza M. "Use and endocytosis of iron-containing proteins by *Entamoeba histolytica* trophozoites.'' *Infect Genet Evol*, 9(6):1038–50, 2009.

Lusche, Daniel F., Wessels, Deborah, Richardson, Nicole A., Russell, Kanoe B., Hanson, Brett M., Soll, Benjamin A., Lin, Benjamin H., Soll, David R. "PTEN Redundancy: Overexpressing Lpten, a Homolog of *Dictyostelium Discoideum* PtenA, the Ortholog of Human PTEN, Rescues All Behavioral Defects of the Mutant PtenA-." *PLoS ONE*, vol. 9, no. 9, 2014, doi:10.1371/journal.pone.0108495.

Maehama, Tomohiko, and Jack E. Dixon. “The Tumor Suppressor, PTEN/MMAC1, Dephosphorylates the Lipid Second Messenger, Phosphatidylinositol 3,4,5-Trisphosphate.” *Journal of Biological Chemistry*, vol. 273, no. 22, 1998, doi:10.1074/jbc.273.22.13375.

Maehama, Tomohiko, Gregory S Taylor, and Jack E Dixon. “PTEN AND M YOTUBULARIN : Novel Phosphoinositide Phosphatases.” *Annual Review of Biochemistry*, 70:247–79, 2001.

Mak, Lok Hang, and Rudiger Woscholski. “Targeting PTEN Using Small Molecule Inhibitors.” *Methods*, vol. 77, pp. 63–68, 2015, doi:10.1016/j.ymeth.2015.02.007.

Manich M, Hernandez-Cuevas N, Ospina-Villa JD, Syan S, Marchat LA, Olivo-Marin JC, Guillén N. “Morphodynamics of the actin-rich cytoskeleton in *Entamoeba histolytica*.’’ *Frontiers in Cellular and Infection Microbiology*, 8(MAY):1–16, 2018.

Manning, Brendan D., and Lewis C. Cantley. “AKT/PKB Signaling: Navigating Downstream.” *Cell*, vol. 129, no. 7, pp. 1261–74, 2007, doi:10.1016/j.cell.2007.06.009.

Marie, Chelsea, and William A. Petri. “Regulation of Virulence of *Entamoeba Histolytica*.” *Annual Review of Microbiology*, vol. 68, pp. 493–520, 2014, doi:10.1146/annurev-micro-091313-103550.

Martin-Belmonte, F., Gassama, A., Datta, A., Yu, W., Rescher, U., Gerke, V., & Mostov, K. “PTEN-mediated apical segregation of phosphoinositides controls epithelial morphogenesis through Cdc42.’’ Cell, 128(2), 383–397, 2007.

Masse, I., Molin, L., Billaud, M., & Solari, F. “Lifespan and dauer regulation by tissue-specific activities of *Caenorhabditis elegans* DAF-18.’’ *Developmental biology*, 286(1), 91–101, 2005.

Masson, Glenn R., and Roger L. Williams. “Structural Mechanisms of PTEN Regulation.” *Cold Spring Harbor Perspectives in Medicine*, vol. 10, no. 3, 2020, doi:10.1101/cshperspect.a036152.

Mi-ichi, Fumika, Takashi Makiuchi, Atsushi Furukawa, Dan Sato, and Tomoyoshi Nozaki. “Sulfate Activation in Mitosomes Plays an Important Role in the Proliferation of *Entamoeba Histolytica*.” *PLoS Neglected Tropical Diseases*, vol. 5, no. 8, pp. 1–7, 2011, doi:10.1371/journal.pntd.0001263.

Mihaylova Valia T., Christina Z. Borland, Laura Manjarrez, Michael J. Stern, Hong Sun. “The PTEN tumor suppressor homolog in *Caenorhabditis elegans* regulates longevity and dauer formation in an insulin receptor-like signaling pathway.’’ *Proceedings of the National Academy of Sciences*, 96 (13) 7427-7432; 1999, doi: 10.1073/pnas.96.13.7427.

Mirelman, David, Michael Anbar, and Rivka Bracha. “Epigenetic Transcriptional Gene Silencing in *Entamoeba Histolytica*.” *IUBMB Life*, vol. 60, no. 9, pp. 598–604, 2008, doi:10.1002/iub.96.

Mondal, Subhanjan, Saurabh Ghosh-Roy, Fabien Loison, Yitang Li, Yonghui Jia, Chad Harris, David A. Williams, and Hongbo R. Luo. “PTEN Negatively Regulates Engulfment of Apoptotic Cells by Modulating Activation of Rac GTPase.” *The Journal of Immunology*, vol. 187, no. 11, pp. 5783–94, 2011, doi:10.4049/jimmunol.1100484.

Muñoz-Muñoz, P., Mares-Alejandre, R. E., Meléndez-López, S. G., & Ramos-Ibarra, M. A. "Bioinformatic Analysis of Two TOR (Target of Rapamycin)-Like Proteins Encoded by *Entamoeba histolytica* Revealed Structural Similarities with Functional Homologs.'' *Genes*, 12(8), 1139, 2021.

Naguib, Adam, Gyula Bencze, Hyejin Cho, Wu Zheng, Ante Tocilj, Elad Elkayam, Christopher R. Faehnle, Nadia Jaber, Christopher P. Pratt, Muhan Chen, Wei-Xing Zong, Michael S. Marks, Leemor Joshua-Tor, Darryl J. Pappin, and Lloyd C. Trotman. "PTEN Functions by Recruitment to Cytoplasmic Vesicles." *Molecular Cell*, vol. 58, no. 2, Elsevier Inc., pp. 255–68, 2015, doi:10.1016/j.molcel.2015.03.011.

Nakada-Tsukui, Kumiko, and Tomoyoshi Nozaki. "Immune Response of Amebiasis and Immune Evasion by *Entamoeba Histolytica*." *Frontiers in Immunology*, vol. 7, no. MAY, pp. 1–13, 2016, doi:10.3389/fimmu.2016.00175.

Nakada-Tsukui, Kumiko, Hiroyuki Okada, Biswa Nath Mitra, and Tomoyoshi Nozaki. "Phosphatidylinositol-Phosphates Mediate Cytoskeletal Reorganization during Phagocytosis via a Unique Modular Protein Consisting of RhoGEF/DH and FYVE Domains in the Parasitic Protozoon *Entamoeba Histolytica*." *Cellular Microbiology*, vol. 11, no. 10, pp. 1471–91, 2009, doi:10.1111/j.1462-5822.2009.01341.x.

Nakada-Tsukui, Kumiko, Kumiko Tsuboi, Atsushi Furukawa, Yoko Yamada, and Tomoyoshi Nozaki. "A Novel Class of Cysteine Protease Receptors That Mediate Lysosomal Transport." *Cellular Microbiology*, vol. 14, no. 8, pp. 1299–317, 2012, doi:10.1111/j.1462-5822.2012.01800.x.

Nakada-Tsukui, Kumiko, Natsuki Watanabe, Tomohiko Maehama, and Tomoyoshi Nozaki. "Phosphatidylinositol Kinases and Phosphatases in *Entamoeba Histolytica*." *Frontiers in Cellular and Infection Microbiology*, vol. 9, pp. 1–36, 2019, doi:10.3389/fcimb.2019.00150.

Nozaki, Tomoyoshi, Takashi Asai, Seiki Kobayashi, Fumio Ikegami, Masaaki Noji, Kazuki Saito, and Tsutomu Takeuchi. "Molecular Cloning and Characterization of the Genes Encoding Two Isoforms of Cysteine Synthase in the Enteric Protozoan Parasite *Entamoeba Histolytica*." *Molecular and Biochemical Parasitology*, vol. 97 (1–2), pp. 33–44, 1998.

Nozaki, Tomoyoshi, Takashi Asai, Lidya B. Sanchez, Seiki Kobayashi, Miki Nakazawa, and Tsutomu Takeuchi. "Characterization of the Gene Encoding Serine Acetyltransferase, a Regulated Enzyme of Cysteine Biosynthesis Protist Parasites *Entamoeba Histolytica* and *Entamoeba Dispar*. Regulation and Possible Function of the Cysteine Biosynthetic Pathway in *Entamoeba*." *Journal of Biological Chemistry*, vol. 274, no. 45, 1999, doi:10.1074/jbc.274.45.32445.

Ogg, Scott, and Gary Ruvkun. "The *C. elegans* PTEN Homolog, DAF-18, Acts in the Insulin Receptor-like Metabolic Signaling Pathway." Molecular Cell, vol. 2, pp. 887–893, 1998.

Ortega-Molina, Ana, Alejo Efeyan, Elena Lopez-Guadamillas, Maribel Muñoz-Martin, Gonzalo Gómez-López, Marta Cañamero, Francisca Mulero, Joaquin Pastor, Sonia Martinez, Eduardo Romanos, M. Mar Gonzalez-Barroso, Eduardo Rial, Angela M. Valverde, James R. Bischoff, and Manuel Serrano. "Pten Positively Regulates Brown Adipose Function, Energy Expenditure, and Longevity." *Cell Metabolism*, vol. 15, no. 3, pp. 382–94, 2012, doi:10.1016/j.cmet.2012.02.001.

Pagliarini, David J., Carolyn A. Worby, and Jack E. Dixon. “A PTEN-like Phosphatase with a Novel Substrate Specificity.” *Journal of Biological Chemistry*, vol. 279, no. 37, pp. 38590–96, 2004, doi:10.1074/jbc.M404959200.

Pal, Aparna, Thomas M. Barber, Martijn Van de Bunt, Simon A. Rudge, Qifeng Zhang, Katherine L. Lachlan, Nicola S. Cooper, Helen Linden, Jonathan C. Levy, Michael J.O. Wakelam, Lisa Walker, Fredrik Karpe, and Anna L. Gloyn. “PTEN Mutations as a Cause of Constitutive Insulin Sensitivity and Obesity .” *New England Journal of Medicine*, vol. 367, no. 11, pp. 1002–11, 2012, doi:10.1056/nejmoa1113966.

Penuliar, Gil M., Kumiko Nakada-Tsukui, and Tomoyoshi Nozaki. “Phenotypic and Transcriptional Profiling in *Entamoeba Histolytica* Reveal Costs to Fitness and Adaptive Responses Associated with Metronidazole Resistance.” *Frontiers in Microbiology*, vol. 6, no. MAY, pp. 1–17, 2015, doi:10.3389/fmicb.2015.00354.

Peyrou, Marion, Sophie Clément, Christiane Maier, Lucie Bourgoin, Emilie Branche, Stéphanie Conzelmann, Vincent Kaddai, Michelangelo Foti, and Francesco Negro. “PTEN Protein Phosphatase Activity Regulates Hepatitis C Virus Secretion through Modulation of Cholesterol Metabolism.” *Journal of Hepatology*, vol. 59, no. 3, pp. 420–26, 2013,doi:10.1016/j.jhep.2013.04.012.

Powell, R. R., B. H. Welter, R. Hwu, B. Bowersox, C. Attaway, and L. A. Temesvari. “*Entamoeba Histolytica*: FYVE-Finger Domains, Phosphatidylinositol 3-Phosphate Biosensors, Associate with Phagosomes but Not Fluid Filled Endosomes.” *Experimental Parasitology*, vol. 112, no. 4, pp. 221–31, 2006, doi:10.1016/j.exppara.2005.11.013.

Pramanik MK, Iijima M, Iwadate Y, Yumura S. “PTEN is a mechanosensing signal transducer for myosin II localization in *Dictyostelium* cells.’’ *Genes to Cells*, 14(7):821–34, 2009.

Pribat, Anne, Rodnay Sormani, Mathieu Rousseau-Gueutin, Magdalena M. Julkowska, Christa Testerink, Jerôme Joubès, Michel Castroviejo, Michel Laguerre, Christian Meyer, Ve´ronique Germain, and Christophe Rothan. “A Novel Class of PTEN Protein in Arabidopsis Displays Unusual Phosphoinositide Phosphatase Activity and Efficiently Binds Phosphatidic Acid.” *Biochemical Journal*, vol. 441, no. 1, pp. 161–71, 2012, doi:10.1042/BJ20110776.

Ralston KS, Michael DS, Nicole M. MacKey-Lawrence, Somlata, Alok Bhattacharya, and William A. Petri. “Trogocytosis by *Entamoeba Histolytica* Contributes to Cell Killing and Tissue Invasion.” *Nature*, vol. 508, no. 7497, Nature Publishing Group, pp. 526–30, 2014, doi:10.1038/nature13242.

Ralston KS, and Petri WA Jr. “Tissue destruction and invasion by *Entamoeba histolytica*.’’ Trends in parasitology, 27(6):254-263, 2011, doi:10.1016/j.pt.2011.02.006

Reyes-López M, Magda, Rosa María Bermúdez-Cruz, Eva E. Avila, and Mireya De La Garza. “Acetaldehyde/Alcohol Dehydrogenase-2 (EhADH2) and Clathrin Are Involved in Internalization of Human Transferrin by *Entamoeba Histolytica*.” *Microbiology*, 157 (1): 209–19, 2011.

Reyes-López M, Piña-Vázquez C, Pérez-Salazar E, de la Garza M. “Endocytosis, Signal Transduction and Proteolytic Cleaving of Human Holotransferrin in *Entamoeba Histolytica*.” *International Journal for Parasitology*, vol. 50, no. 12, pp. 959–67, 2020, doi:10.1016/j.ijpara.2020.05.013.

Reyes-López M, Piña-Vázquez C, and Serrano-Luna J. “Transferrin: Endocytosis and Cell Signaling in Parasitic Protozoa.” BioMed Research International, vol. 2015, 2015, doi:10.1155/2015/641392.

Rosselli-Murai, Luciana K., Joel A. Yates, Sei Yoshida, Julia Bourg, Kenneth K. Y. Ho, Megan White, Julia Prisby, Xinyu Tan, Megan Altemus, Liwei Bao, Zhi-Fen Wu, Sarah L. Veatch, Joel A. Swanson, Sofia D. Merajver, and Allen P. Liu. “Loss of PTEN Promotes Formation of Signaling-Capable Clathrin-Coated Pits.” *Journal of Cell Science*, vol. 131, no. 8, 2018, doi:10.1242/jcs.208926.

Saavedra, Laura, Rita Catarino, Tobias Heinz, Ingo Heilmann, Magdalena Bezanilla, and Rui Malho. “Phosphatase and Tensin Homolog Is a Growth Repressor of Both Rhizoid and Gametophore Development in the Moss *Physcomitrella Patens*.” *Plant Physiology*, vol. 169, no. 4, pp. 2572–86, 2015, doi:10.1104/pp.15.01197.

Saito-Nakano, Yumiko, Ratna Wahyuni, Kumiko Nakada-Tsukui, Kentaro Tomii, Tomoyoshi Nozaki. “Rab7D Small GTPase Is Involved in Phago-, Trogocytosis and Cytoskeletal Reorganization in the Enteric Protozoan *Entamoeba Histolytica*.” *Cellular Microbiology*, vol. 23, no. 1, 2021, pp. 1–15, doi:10.1111/cmi.13267.

Sasaki, Takehiko, Shunsuke Takasuga, Junko Sasaki, Satoshi Kofuji, Satoshi Eguchi, Masakazu Yamazaki, and Akira Suzuki. “Mammalian Phosphoinositide Kinases and Phosphatases.” *Progress in Lipid Research*, vol. 48, no. 6, Elsevier Ltd, pp. 307–43, 2009, doi:10.1016/j.plipres.2009.06.001.

Schabbauer, Gernot, Ulrich Matt, Philipp Günzl, Joanna Warszawska, Tanja Furtner, Eva Hainzl, Immanuel Elbau, Ildiko Mesteri, Bianca Doninger, Bernd R. Binder, and Sylvia Knapp. "Myeloid PTEN Promotes Inflammation but Impairs Bactericidal Activities during Murine Pneumococcal Pneumonia." *The Journal of Immunology*, vol. 185, no. 1, pp. 468–76, 2010, doi:10.4049/jimmunol.0902221.

Schink, K. O., Tan, K. W., & Stenmark, H. "Phosphoinositides in Control of Membrane Dynamics." *Annual review of cell and developmental biology*, vol. 32, pp. 143-171, 2016, doi:10.1146/annurev-cellbio-111315-125349.

Seastone DJ, Lee E, Bush J, Knecht D, Cardelli J. "Overexpression of a novel Rho family GTPase, RacC, induces unusual actin-based structures and positively affects phagocytosis in *Dictyostelium discoideum*.'' *Molecular Biology of the Cell*, 9(10):2891–904, 1998.

Seastone DJ, Zhang L, Buczynski G, Rebstein P, Weeks G, Spiegelman G, Cardelli J. "The small M(r) Ras-like GTPase Rap1 and the phospholipase C pathway act to regulate phagocytosis in *Dictyostelium discoideum*.'' *Molecular Biology of the Cell*, 10(2):393–406, 1999.

Serezani, C. Henrique, Steve Kane, Alexandra I. Medeiros, Ashley M. Cornett, Sang Hoon Kim, Mariana Morato Marques, Sang Pyo Lee, Casey Lewis, Emilie Bourdonnay, Megan N. Ballinger, Eric S. White, and Marc Peters-Golden. "Host-Pathogen Interactions: PTEN Directly Activates the Actin Depolymerization Factor Cofilin-1 during PGE2-Mediated Inhibition of Phagocytosis of Fungi." *Science Signaling*, vol. 5, no. 210, pp. 1–11, 2012, doi:10.1126/scisignal.2002448.

Sharma, Shalini, Shalini Agarwal, Ravi Bharadwaj, Somlata, Sudha Bhattacharya, and Alok Bhattacharya. “Novel Regulatory Roles of PtdIns(4,5)P_2 Generating Enzyme EhPIPKI in Actin Dynamics and Phagocytosis of *Entamoeba Histolytica*.” *Cellular Microbiology*, vol. 21, no. 10, 2019, doi:10.1111/cmi.13087.

Shinde, Swapnil Rohidas, and Subbareddy Maddika. “PTEN Modulates EGFR Late Endocytic Trafficking and Degradation by Dephosphorylating Rab7.” *Nature Communications*, vol. 7, Nature Publishing Group, 2016, doi:10.1038/ncomms10689.

Somlata, Kumiko Nakada-Tsukui, and Tomoyoshi Nozaki. “AGC Family Kinase 1 Participates in Trogocytosis but Not in Phagocytosis in *Entamoeba Histolytica*.” *Nature Communications*, vol. 8, no. 1, Springer US, pp. 1–12, 2017, doi:10.1038/s41467-017-00199-y.

Song, Min Sup, Leonardo Salmena, and Pier Paolo Pandolfi. “The Functions and Regulation of the PTEN Tumour Suppressor.” *Nature Reviews Molecular Cell Biology*, vol. 13, no. 5, Nature Publishing Group, pp. 283–96, 2012, doi:10.1038/nrm3330.

Song, Shaojuan, Yanan Zhang, Tingting Ding, Ning Ji, and Hang Zhao State. “The Dual Role of Macropinocytosis in Cancers: Promoting Growth and Inducing Methuosis to Participate in Anticancer Therapies as Targets.” *Frontiers in Oncology*, vol. 10, no. January, 2021, pp. 1–23, doi:10.3389/fonc.2020.570108.

Stanley Samuel L. “Amoebiasis” Lancet, Vol. 361, pp. 1025–34, 2003.

Stiles Bangyan, Ying Wang, Andreas Stahl, Sara Bassilian, W. Paul Lee, Yoon-Jung Kim, Robert Sherwin, Sherin Devaskar, Ralf Lesche, Mark A. Magnuson, Hong Wu. “Liver-specific

deletion of negative regulator Pten results in fatty liver and insulin hypersensitivity.'' *Proceedings of the National Academy of Sciences*, 101 (7) 2082-2087; 2004, doi: 10.1073/pnas.0308617100.

Stumpf, Miriam, Suma Choorapoikayil, and Jeroen den Hertog. "Pten Function in Zebrafish: Anything but a Fish Story." *Methods*, vol. 77, Elsevier Inc., pp. 191–96, 2015, doi:10.1016/j.ymeth.2014.11.002.

Suzuki, Akira, José Luis De La Pompa, Vuk Stambolic, Andrew J Elia, Takehiko Sasaki, Ivén Del Barco Barrantes, Alexandra Ho, Andrew Wakeham, Annick Itie, Wilson Khoo, Manabu Fukumoto, and Tak W. Mak. "High Cancer Susceptibility and Embryonic Lethality Associated with Mutation of the PTEN Tumor Suppressor Gene in Mice." *Current Biology*, vol. 8, no. 21, pp. 1169–78, 1998, doi:10.1016/S0960-9822(07)00488-5.

Suzuki, Yo, and Min Han. "Genetic Redundancy Masks Diverse Functions of the Tumor Suppressor Gene PTEN during *C. Elegans* Development." *Genes and Development*, vol. 20, no. 4, pp. 423–28, 2006, doi:10.1101/gad.1378906.

Swanson, Joel A. "Shaping Cups into Phagosomes and Macropinosomes." *Nature Reviews Molecular Cell Biology*, vol. 9, no. 8, pp. 639–49, 2008, doi:10.1038/nrm2447.

Tamura, Masahito, Jianguo Gu, Kazue Matsumoto, Shin Ichi Aota, Ramon Parsons, and Kenneth M. Yamada. "Inhibition of Cell Migration, Spreading, and Focal Adhesions by Tumor Suppressor PTEN." *Science*, vol. 280, no. 5369, pp. 1614–17, 1998, doi:10.1126/science.280.5369.1614.

Taylor, Gregory S., and Jack E. Dixon. " PTEN and Myotubularins: Families of Phosphoinositide Phosphatases." *Methods in Enzymology*, vol. 366, no. 1997, pp. 43–56, 2003, doi:10.1016/S0076-6879(03)66004-0.

Temesvari L, Zhang L, Fodera B, Janssen KP, Schleicher M, Cardelli JA. "Inactivation of lmpA, encoding a LIMPII-related endosomal protein, suppresses the internalization and endosomal trafficking defects in profilin- null mutants.'' *Molecular Biology of the Cell*, 11(6):2019–31, 2000.

Tenen, Claudia C, and Iva Greenwald. "Cell Non-autonomous Function of daf-18/PTEN in the Somatic Gonad Coordinates Somatic Gonad and Germline Development in *C. elegans* Dauer Larvae." *Current biology* : CB vol. 29, pp. 1064-1072, 2019. doi:10.1016/j.cub.2019.01.076

Thompson, Julie D., Desmond G. Higgins, and Toby J. Gibson. "CLUSTAL W: Improving the Sensitivity of Progressive Multiple Sequence Alignment through Sequence Weighting, Position-Specific Gap Penalties and Weight Matrix Choice." *Nucleic Acids Research*, vol. 22, no. 22, pp. 4673–80, 1994, doi:10.1093/nar/22.22.4673.

Tsujita, Kazuya, and Toshiki Itoh. "Phosphoinositides in the Regulation of Actin Cortex and Cell Migration." *Biochimica et Biophysica Acta - Molecular and Cell Biology of Lipids*, vol. 1851, no. 6, Elsevier B.V., pp. 824–31, 2015, doi:10.1016/j.bbalip.2014.10.011.

Vazquez, Francisca, Satomi Matsuoka, William R. Sellers, Toshio Yanagida, Masahiro Ueda, and Peter N. Devreotes. "Tumor Suppressor PTEN Acts through Dynamic Interaction with the Plasma Membrane." *Proceedings of the National Academy of Sciences of the United States of America*, vol. 103, no. 10, pp. 3633–38, 2006, doi:10.1073/pnas.0510570103.

Veltman DM, Williams TD, Bloomfield G, Chen BC, Betzig E, Insall RH, Kay RR. “A plasma membrane template for macropinocytic cups.’’ *Elife.*; 5(DECEMBER2016):24, 2016, doi:10.7554/eLife.20085.

Watanabe, Natsuki, Kumiko Nakada-Tsukui, and Tomoyoshi Nozaki. “Two Isotypes of Phosphatidylinositol 3-Phosphate-Binding Sorting Nexins Play Distinct Roles in Trogocytosis in *Entamoeba Histolytica*.” *Cellular Microbiology*, vol. 22, no. 3, pp. 1–16, 2020, doi:10.1111/cmi.13144.

Welter BH, Powell RR, Laughlin RC, McGugan GC, Bonner M, King A, Temesvari LA. “*Entamoeba histolytica*: Comparison of the role of receptors and filamentous actin among various endocytic processes.’’ *Experimental Parasitology*, 113(2):91–9, 2006.

Wessels, Deborah, Daniel F. Lusche, Spencer Kuhl, Paul Held, and David R. Soll. “PTEN Plays a Role in the Suppression of Lateral Pseudopod Formation during *Dictyostelium* Motility and Chemotaxis.” *Journal of Cell Science*, vol. 120, no. 15, pp. 2517–31, 2007, doi:10.1242/jcs.010876.

Wong, J. T., P. T.W. Kim, J. W. Peacock, T. Y. Yau, A. L.F. Mui, S. W. Chung, V. Sossi, D. Doudet, D. Green, T. J. Ruth, R. Parsons, C. B. Verchere, and C. J. Ong. “Pten (Phosphatase and Tensin Homologue Gene) Haploinsufficiency Promotes Insulin Hypersensitivity.” *Diabetologia*, vol. 50, no. 2, pp. 395–403, 2007, doi:10.1007/s00125-006-0531-x.

Ximénez, Cecilia, Patricia Morán, Liliana Rojas, Alicia Valadez, and Alejandro Gómez. “Reassessment of the Epidemiology of Amebiasis: State of the Art.” *Infection, Genetics and Evolution*, vol. 9, no. 6, pp. 1023–32, 2009, doi:10.1016/j.meegid.2009.06.008.

York, Randall D., Derek C. Molliver, Savraj S. Grewal, Paula E. Stenberg, Edwin W. Mccleskey, and Philip J. S. Stork. “Role of Phosphoinositide 3-Kinase and Endocytosis in Nerve Growth Factor-Induced Extracellular Signal-Regulated Kinase Activation via Ras and Rap1.” *Molecular and Cellular Biology*, vol. 20, no. 21, 2000, pp. 8069–83, doi:10.1128/mcb.20.21.8069-8083.2000.

Yoshioka, Daisuke, Seiya Fukushima, Hiroyasu Koteishi, Daichi Okuno, Toru Ide, Satomi Matsuoka, and Masahiro Ueda. “Single-Molecule Imaging of PI(4,5)P_2 and PTEN in Vitro Reveals a Positive Feedback Mechanism for PTEN Membrane Binding.” *Communications Biology*, vol. 3, no. 1, Springer US, pp. 1–14, 2020, doi:10.1038/s42003-020-0818-3.

Zhang, Yan, Sha Li, Liang Zi Zhou, Emily Fox, James Pao, Wei Sun, Chao Zhou, and Sheila McCormick. “Overexpression of Arabidopsis Thaliana PTEN Caused Accumulation of Autophagic Bodies in Pollen Tubes by Disrupting Phosphatidylinositol 3-Phosphate Dynamics.” *Plant Journal*, vol. 68, no. 6, pp. 1081–92, 2011, doi:10.1111/j.1365-313X.2011.04761.x.

TABLES

Table 1. Percentage of amino acid identity among *E. histolytica* PTEN isoforms and Human PTEN by Clustal W multiple sequence alignment score.

Identity %	Human PTEN	EhPTEN1	EhPTEN2	EhPTEN3	EhPTEN4	EhPTEN5	EhPTEN6
Human PTEN	100.0	39.0	37.8	30.5	28.7	28.5	27.3
EhPTEN1		100.0	48.8	28.4	22.3	22.5	23.4
EhPTEN2			100.0	30.3	23.4	24.5	23.1
EhPTEN3				100.0	27.4	29.1	27.9
EhPTEN4					100.0	41.5	57.3
EhPTEN5						100.0	41.4
EhPTEN6							100.0

Table 2. Kinetic parameters of EhPTEN1. Assay were perforemed as described in the materials and methods in the presence of MOPS, EhPTEN1, and PtdInsPs. Reaction were conducted at 37°C at pH 6.0. Mean ± SEM of duplicates are shown**.**

Substrate	**Km (µM)**	**Vmax (nmoles min^{-1} mg^{-1})**	**Kcat (min^{-1})**
$PI(3,4)P_2$	292 ± 18.8	6.02 ± 1.11	0.11 ± 0.02
$PI(3,5)P_2$	161 ± 20.12	8.40 ± 0.42	0.15 ± 0.01
$PI(3,4,5)P_3$	92.5 ± 4.72	16.9 ± 1.83	0.31 ± 0.03

FIGURES

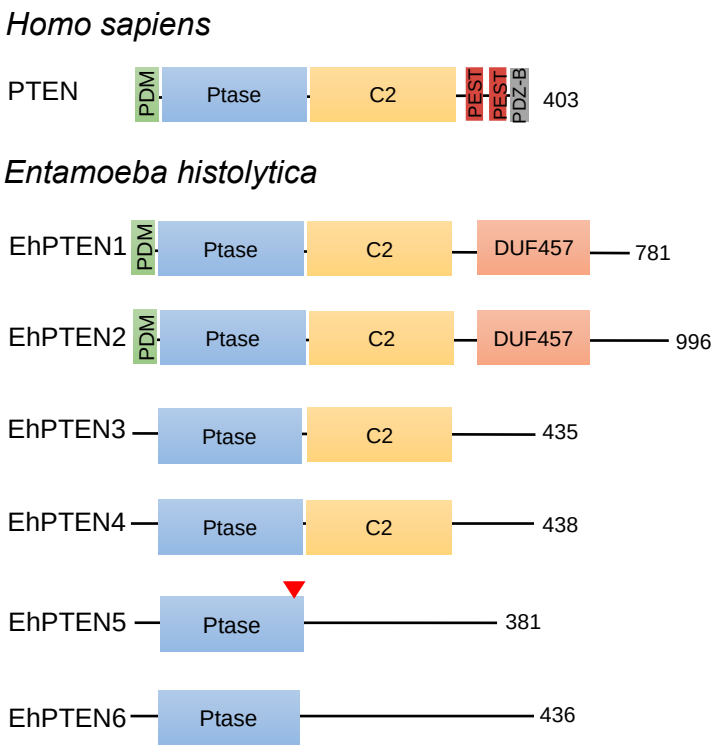

Figure 1. Domain organization of PTEN from human and *E. histolytica*. PDM [PtdIns(4,5)P_2-binding motif], Ptase (Phosphatase tensin-type domain), C2 (C2 tensin-type domain), DUF547 (Domain of unknown function), PEST (proline, glutamine, serine, threonine sequence), PDZ-BM (PDZ-binding motif), red triangle indicates the nuclear localization sequence.

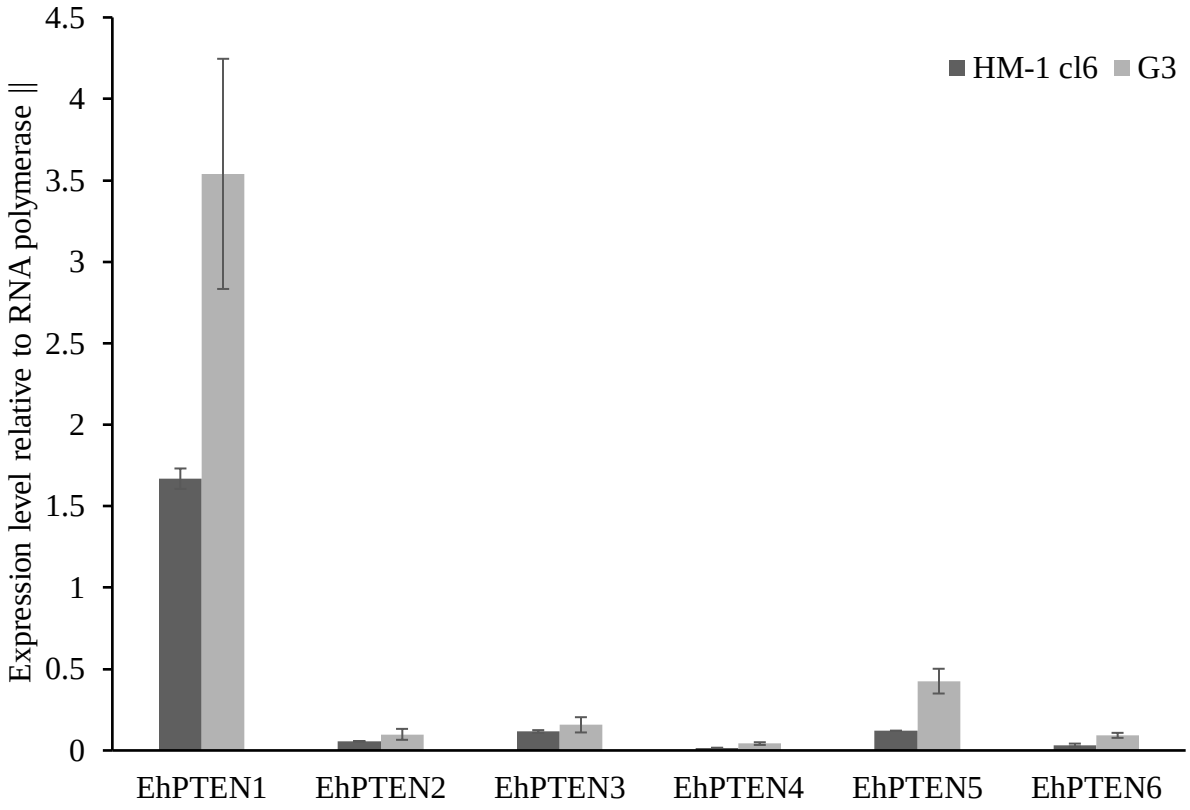

Figure 2. Relative mRNA expression of PTEN homologs in *E. histolytica* trophozoites HM1: IMSS cl6 and G3 strains. The expression profiles of PTEN homologs in *E. histolytica* were identified using the data provided from previous work (Penuliar et al., 2015; Nakada-Tsukui et al., 2012) where transcriptome of *E. histolytica* was analyzed using microarrays technology. Error bars indicate standard deviation for the biological replicates in each experiment.

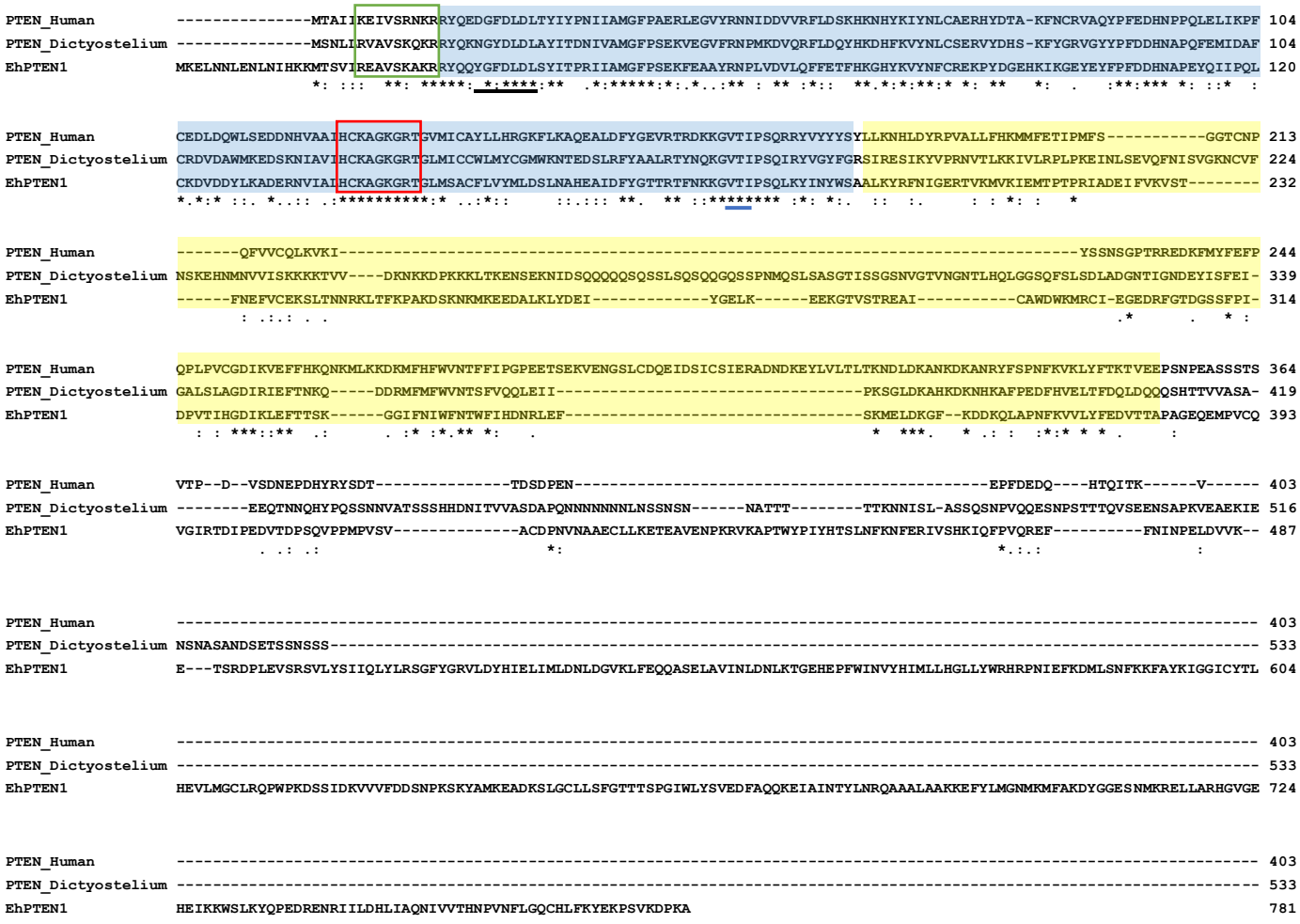

Figure 3. Alignment of EhPTEN1 with human PTEN and Dictyostelium PTEN. Multiple amino acid sequence alignment of Human PTEN (P60484), Dictyostelium PTEN (Q8T9S), and EhPTEN1 (XP_653141.2) was constructed by using Clustal W algorithm (http://clustalw.ddbj.nig.ac.jp). PTEN phosphatase domain and C2 domain are shown with blue and yellow backgrounds, respectively. The green rectangle corresponds to the PtdIns(4,5)P_2-binding motif. Amino acid residues implicated for PtdIns(3,4,5)P_3 catalysis are marked with a red rectangle. Cytosolic localization signal and residues important for TI loop formation are indicated in black and blue lines, respectively.

A

```
H. sapiens PTEN       HCKAGKGRTGVMICAYLLHRGK----FLKA-QEALD—FYGEVRTRDKKGVTIPSQ 171
M. musculus PTEN      HCKAGKGRTGVMICAYLLHRGK----FLKA-QEALD—FYGEVRTRDKKGVTIPSQ 171
X. tropicalis PTEN    HCKAGKGRTGVMICAYLLHRGK----FPRA-QEALD—FYGEVRTRDKKGVTIPSQ 170
C. elegans PTEN       HCKAGKGRTGVMICALLIYINF----YPSP-RQILD—YYSIIRTKNNKGVTIPSQ 216
D. melanogaster PTEN  HCKAGKGRTGTMICAYLVFSGI----KKSA-DEALA—WYDEKRTKDRKGVTIPSQ 179
S. cerevisiae PTEN    HCRMGKGRSGMITVAYLMKYLQ----CPL—GEARLIFMQARFKYGMTNGVTIPSQ 241
H. sapiens PTP        HCSAGIGRSGTFCLADTCLLLMDKRKDPSSVDIKKVLLEMRKFRMGLIQTA---- 191
H. sapiens DSP        HCREGYSRSPTLVIAYLMMRQK----MDV--KSALSIVRQNR-EIGPNDGF---- 166
                       **  * .*:  :  *                          .    .
```

B

```
Human PTEN            HCKAGKGRTGVMICAYLLHRGKFLKAQEALDFYGEVRTRDKKGVTIPSQ      171
EhPTEN1               HCKAGKGRTGLMSACFLVYMLDSLNAHEAIDFYGTTRTFNKKGVTIPSQ      187
EhPTEN2               HCKAGKGRTGLID---------CLHSYEAVDLYGNARTYDKKGVTIPSQ      184
EhPTEN3               HCLAGRGRTGTVITSFLQYIKLCATPQDALDHFASIRSMKNKGVSMPAQ      170
EhPTEN4               HCKAGRGRTGLVCSCVLLSLGKCGDAKKALELFARKRSKIMKGATSPPQ      167
EhPTEN5               HCRAGRGRTGIVVCSVLLALGKAKNTEESLYLFGERRSKKKRGVTAPCQ      167
EhPTEN6               HCKAGRGRTGLVCSCVLMGLGICSNAKEAMEFFAKRRSKINKGSTSPPQ      167
                      ** **:**** :              .::  :.  *:   :* : * *
```

Figure 4. Alignment of phosphatase signature motif. (A) Alignment of catalytic site sequences of multiple PTEN orthologs [human (*Homo sapiens*, P60484), mouse (*Mus musculus*, NP_032986), frog (*Xenopus tropicalis*, NP_001116943), worm (*Caenorhabditis elegans*, AAD21620), fruit fly (*Drosophila melanogaster*, NP_477423), and budding yeast (*Saccharomyces cerevisiae*, NP_014271)], protein tyrosine phosphatases (PTPs, NP_001265547), and dual specificity protein phosphatases (DSPs, NP_004081). (B) Alignment of catalytic site sequences of human PTEN and PTEN homologs in *E. histolytica*. The alignment was constructed by using Clustal W algorithm (http://clustalw.ddbj.nig.ac.jp). The active site sequences and conserved residues in TI loop are highlighted in yellow and red, respectively.

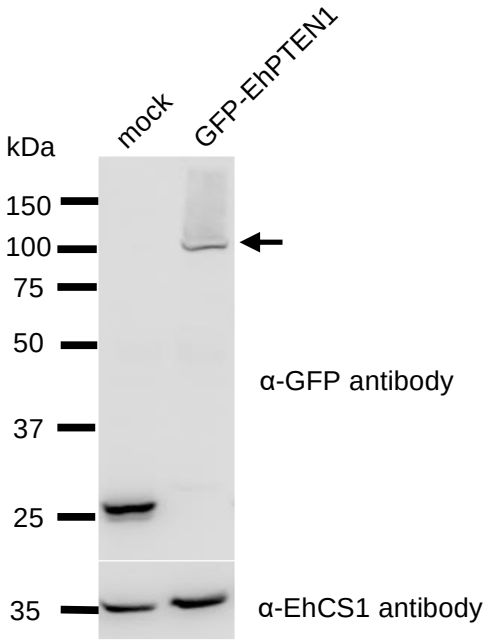

Figure 5. Expression of GFP-EhPTEN1 in motile trophozoites. Immunoblot of GFP-EhPTEN1 and mock control in *E. histolytica* transformants. Approximately 30 μg of total lysates from mock-transfected control (mock) and GFP-EhPTEN1-expressing transformant (GFP-EhPTEN1) were subjected to SDS-PAGE and immunoblot analysis using anti-GFP antibody and anti-CS1 antibody. Arrow indicates GFP-EhPTEN1.

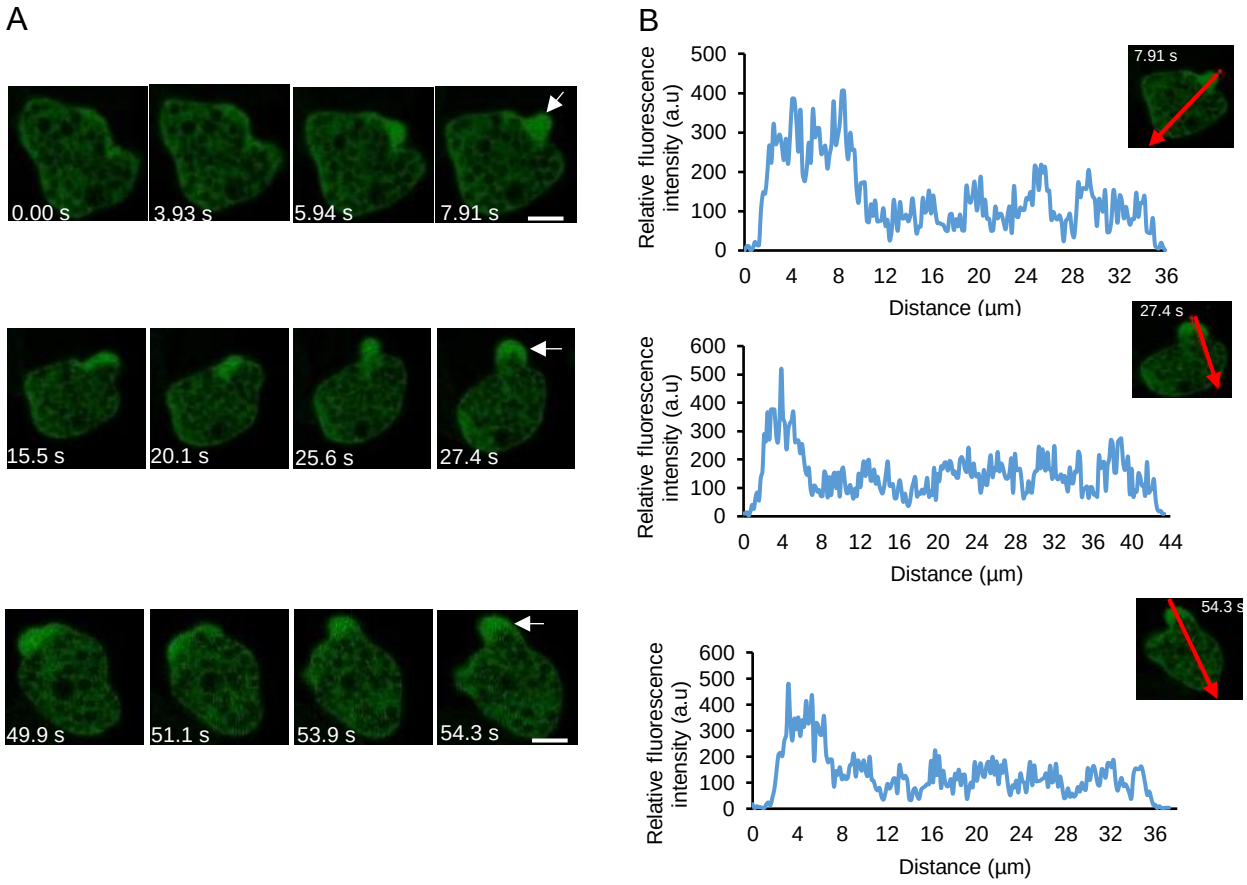

Figure 6. Live imaging montage showing a time series of motile trophozoites expressing GFP-EhPTEN1. (A) The pseudopodal localization of GFP-EhPTEN1 is indicated by white arrow. (B) The line intensity plot shows GFP-EhPTEN1 intensity in pseudopods vs. cytoplasm with the distance. (Scale bar, 10 µm).

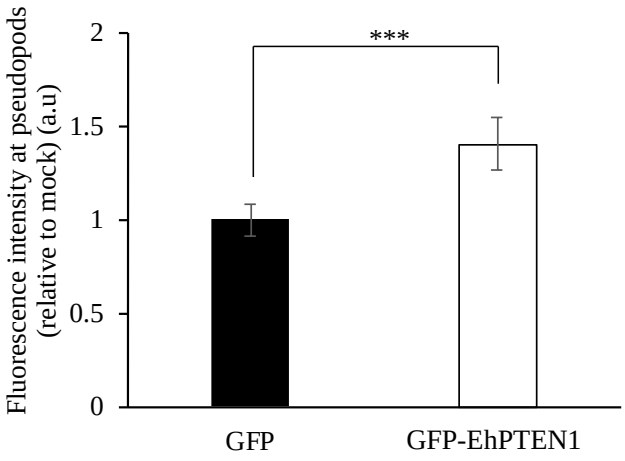

Figure 7. Relative fluorescence intensities were quantified in the pseudopod regions of GFP-EhPTEN1 and mock control expressing trophozoites then normalized to the fluorescence intensities in the total cells. Data points in the graph show the mean and error bars represent standard deviation for 30 cells. Statistical significance was examined with t-test (*** $P < 0.001$, p-value = 5.58×10^{-5}).

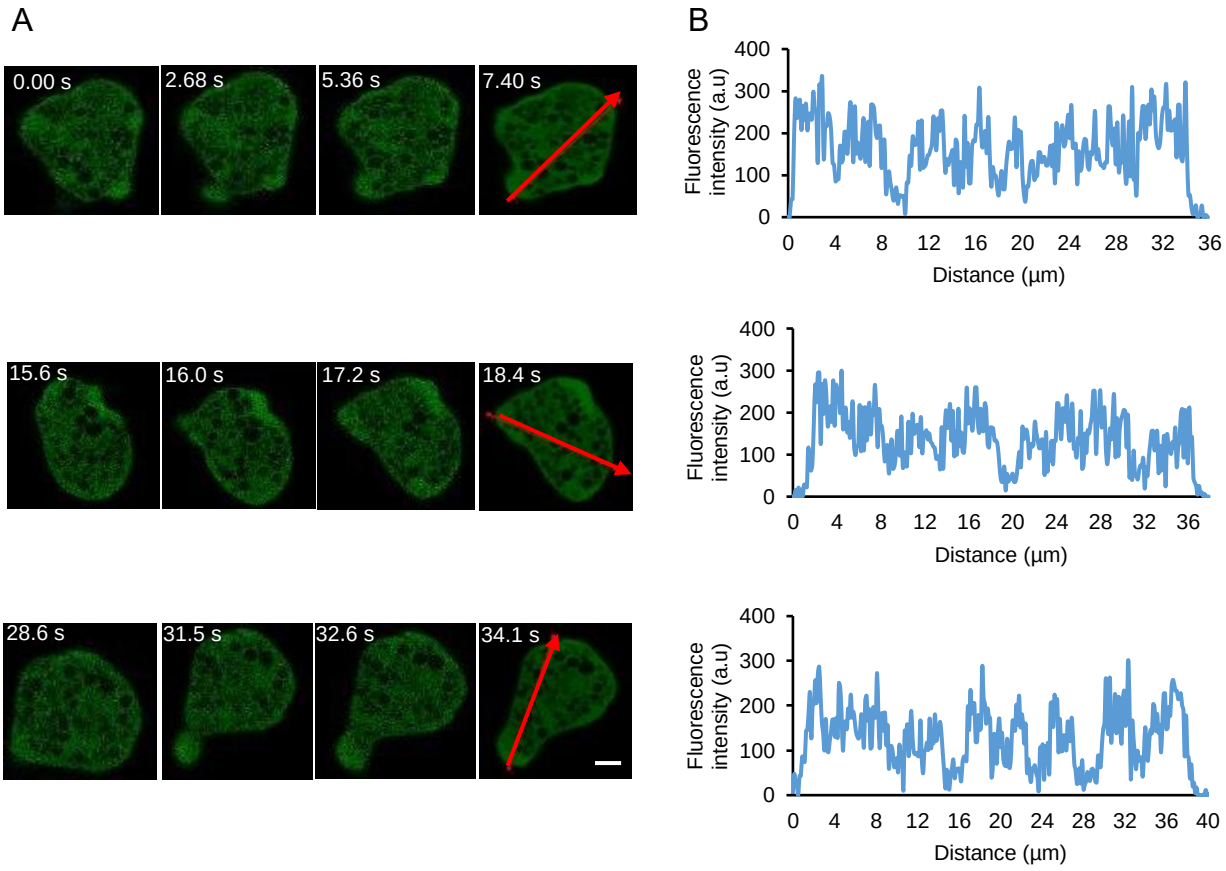

Figure 8. Live imaging montage showing localization of GFP mock in normal motile trophozoites. (A) Montage showing a time series of motile trophozoites expressing GFP in left panels. The pseudopods in different time frames have been analyzed for GFP intensity along the marked arrow line. (B) The line intensity plot shows the fluorescence intensity of GFP across the amoebic trophozoites. (Scale bar, 10 µm).

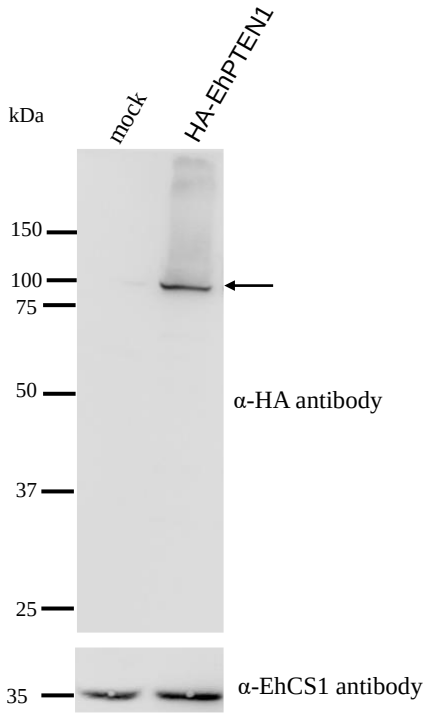

Figure 9. Expression of HA-EhPTEN1. Immunoblot analysis of HA-EhPTEN1 in *E. histolytica* transformants. Approximately 30 μg of total lysates from mock-transfected control (mock) and HA-EhPTEN1-expressing transformant (HA-EhPTEN1) were subjected to SDS-PAGE and immunoblot analysis using anti-HA antibody. EhCS1 (Cysteine synthase 1) was detected by anti-CS1 antiserum as a loading control. Arrow indicates HA-EhPTEN1.

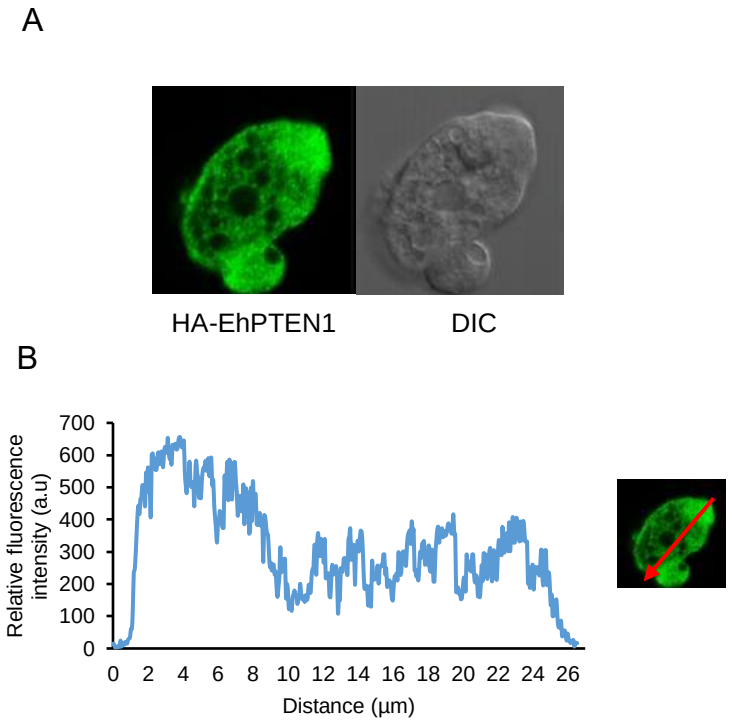

Figure 10. Localization of HA-EhPTEN1 in a quiescent state. (A) Immunofluorescence assay (IFA) micrographs of HA-EhPTEN1 expressing trophozoites stained with anti-HA antibody (green). (Scale bar, 5µm). (B) The line intensity plot shows HA-EhPTEN1 intensity in pseudopods vs. cytoplasm with the distance

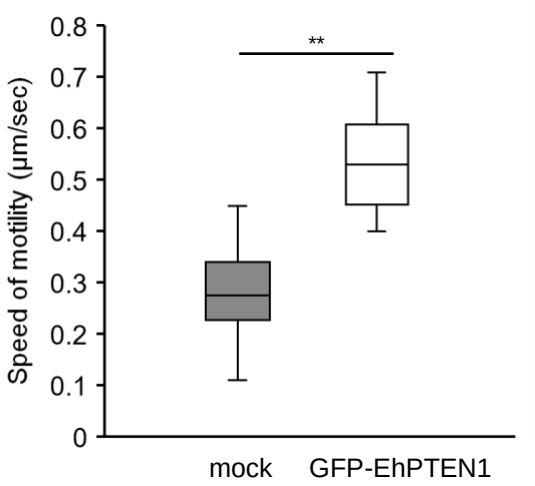

Figure 11. Cell motility of mock and GFP-EhPTEN1 transfected strains. Time-lapse images of the transformant trophozoites were collected every second for 5 minutes using CQ1 and 30 cells were selected randomly for analysis by CellPathfinder software. The experiments were performed three times independently. Statistical significance was examined with Dunnet test (**P < 0.05, p-value = 0.04).

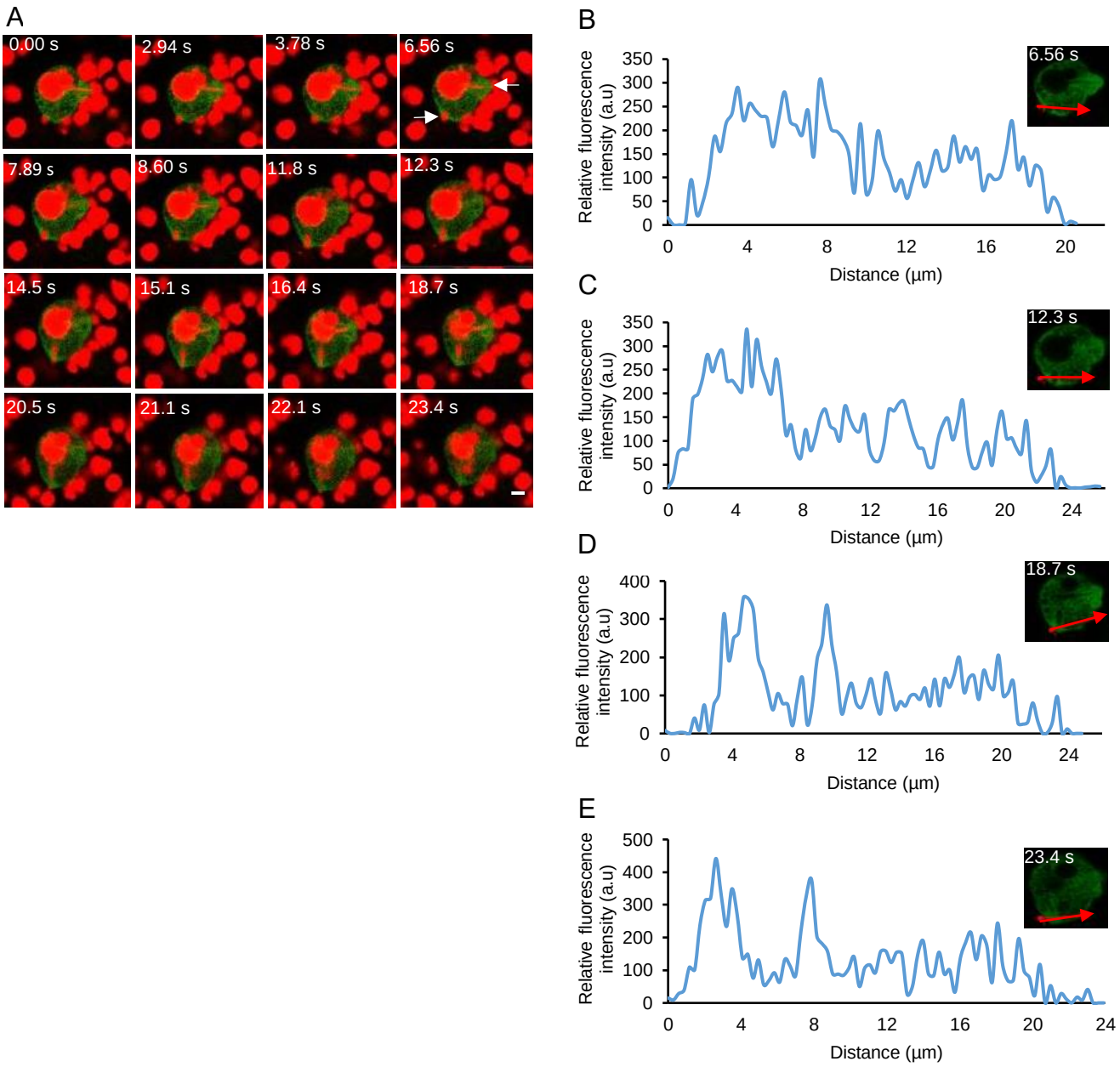

Figure 12. Localization of GFP-EhPTEN1 during trogocytosis. (A) Time series montage showing the localization of GFP-EhPTEN1 during trogocytosis of live CHO cells by amoebic trophozoites. The site of trogocytosis is marked with arrow. (Scale bar, 10 µm). (B) Analysis of GFP-EhPTEN1 intensity along the line drawn at the initial phase of CHO internalization soon after attachment. (C) The plot showing the intensity of GFP-EhPTEN1 along the line drawn reveals its enrichment in the tunnel formed during amoebic trogocytosis. (D) The graph shows the intensity of GFP-EhPTEN1 at the late phase of trogocytosis soon after closure of the trogocytic cup (E) The graph shows the intensity of GFP-EhPTEN1 after the closure of the trogocytic cup.

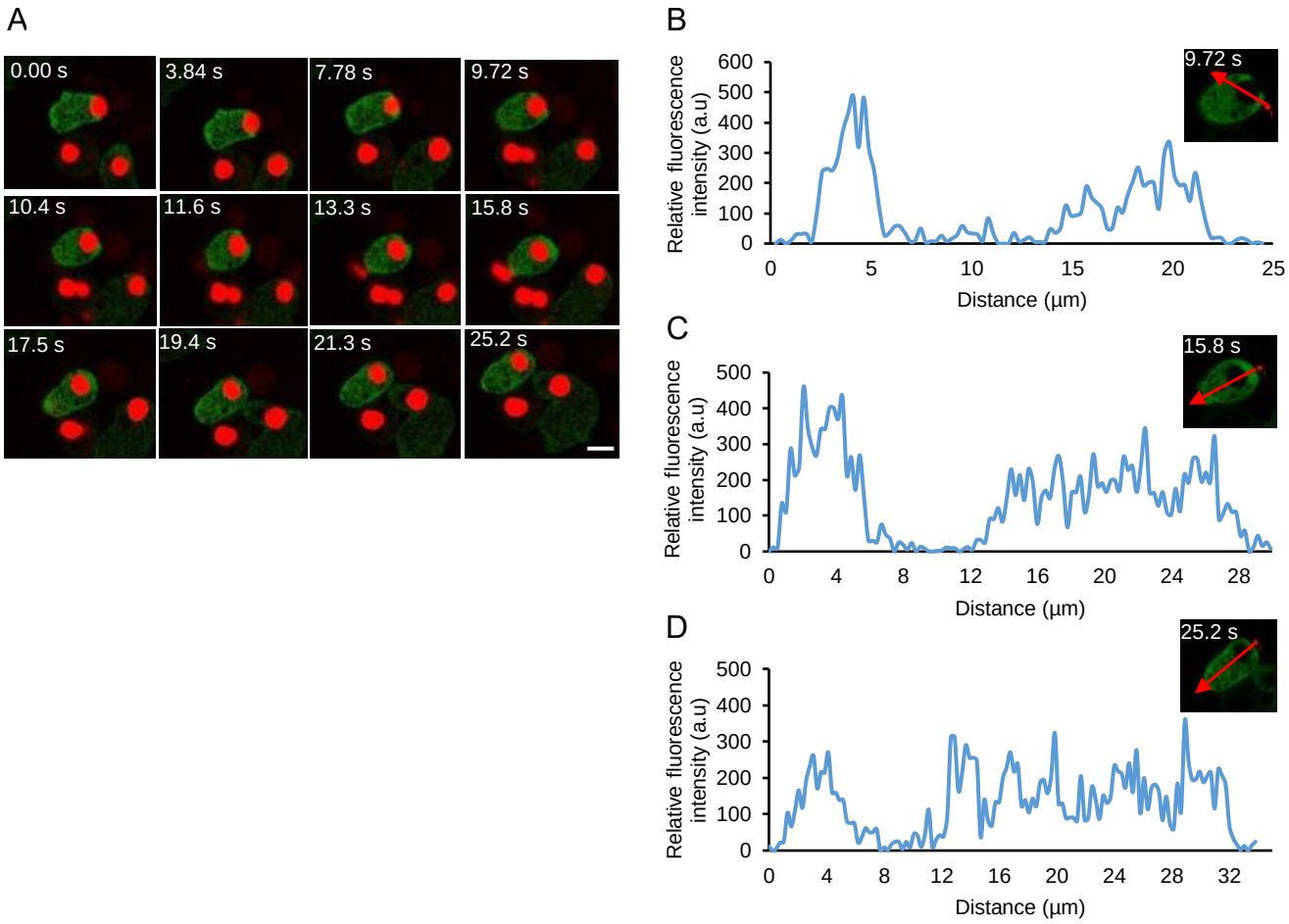

Figure 13. Localization of GFP-EhPTEN1 phagocytosis of pre-killed CHO cells. (A) Montage of live trophozoite expressing GFP-EhPTEN1 ingesting pre-killed CHO cells by phagocytosis. (Scale bar, 10 µm). (B) Analysis of intensity of GFP-EhPTEN1 across the phagocytic cup along the line drawn. (C) The plot showing the intensity of GFP-EhPTEN-1 along the line drawn across the newly formed phagosome. (D) The graph shows the intensity of GFP-EhPTEN1 after phagosome maturation.

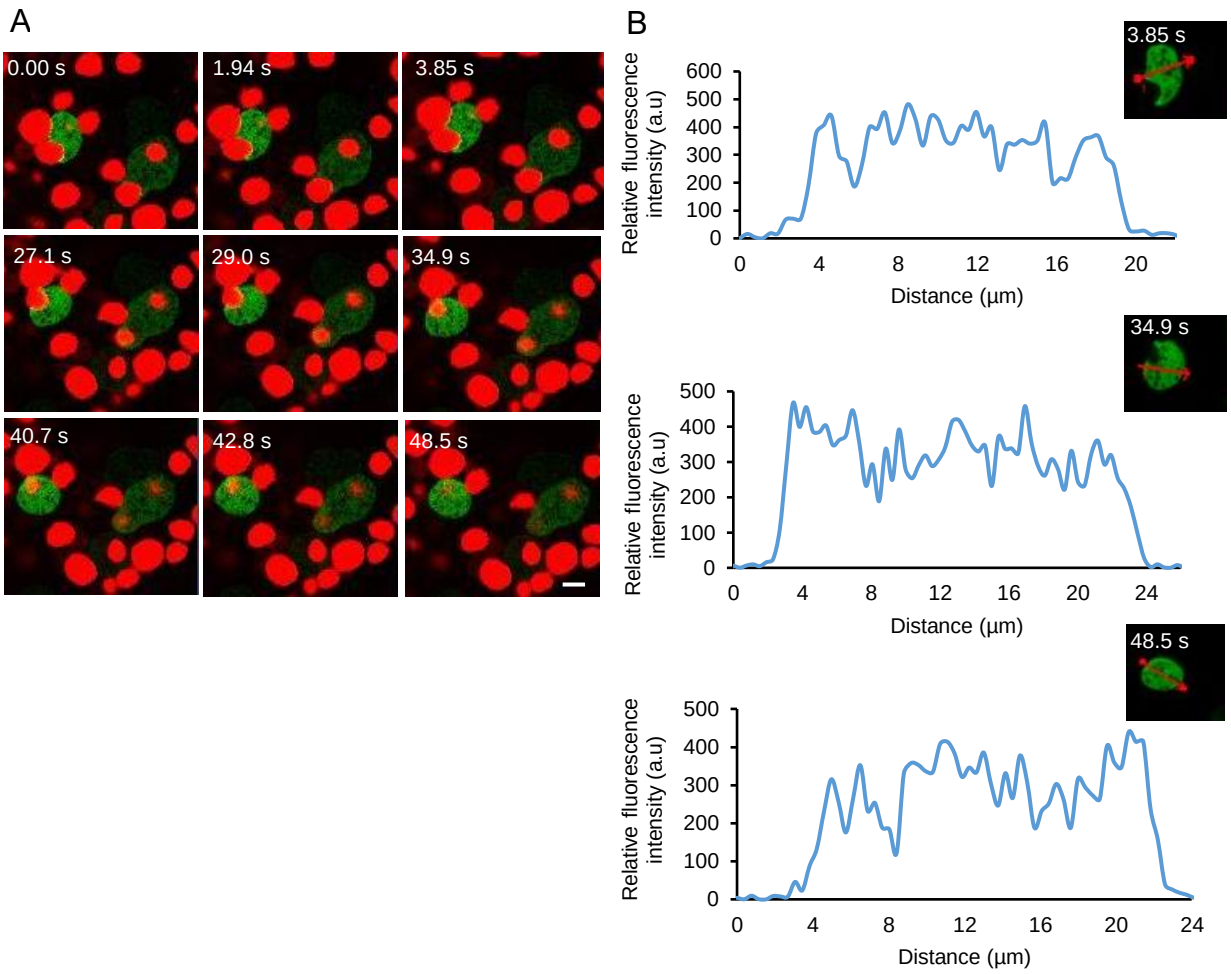

Figure 14. Localization of GFP mock during phagocytosis. (A) Montage of live trophozoite expressing GFP ingesting pre-killed CHO cells by phagocytosis. (Scale bar, 10 µm). (B) Analysis of intensity of GFP across the phagocytic cup along the line drawn.

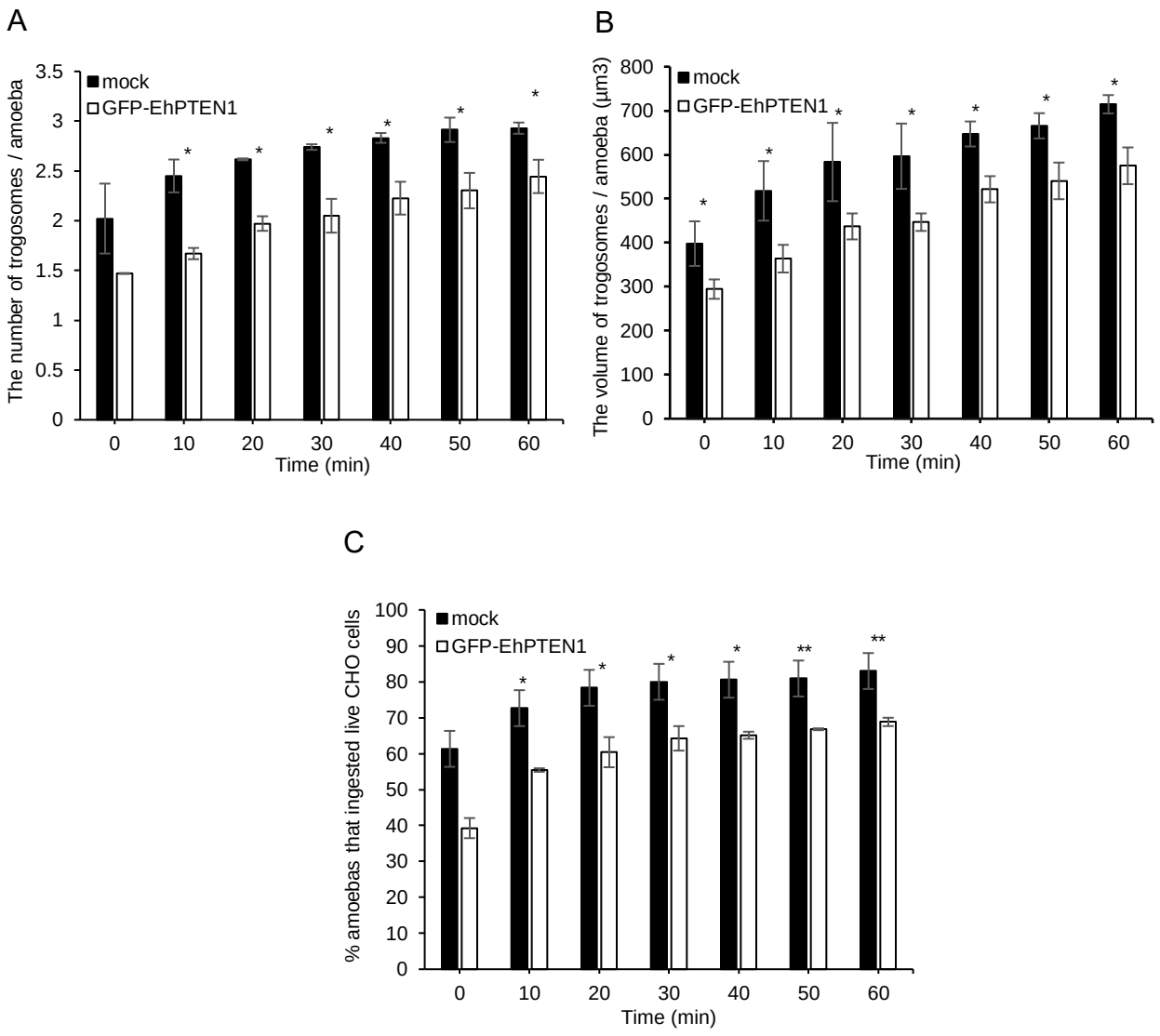

Figure 15. Effect of GFP-EhPTEN1 expression on trogocytosis. (A) Trophozoites of mock transfected and GFP-EhPTEN1 expressing strains were incubated with live CHO cells that have been stained with CellTracker Orange to evaluate trogocytosis. The images were taken on CQ1 as described in the materials and methods and analyzed to calculate the average numbers of CHO cell-containing trogosomes per amoeba. (B) The volume of the ingested CHO cells was calculated using three-dimensionally reconstituted data. (C) The percentage of amoeba trophozoites that ingested live CHO cells. Experiments were conducted three times independently in triplicates and a representative data set is shown. Statistical significance was examined with t-test (* $P < 0.05$, ** $P < 0.01$). Error bars indicating standard deviation.

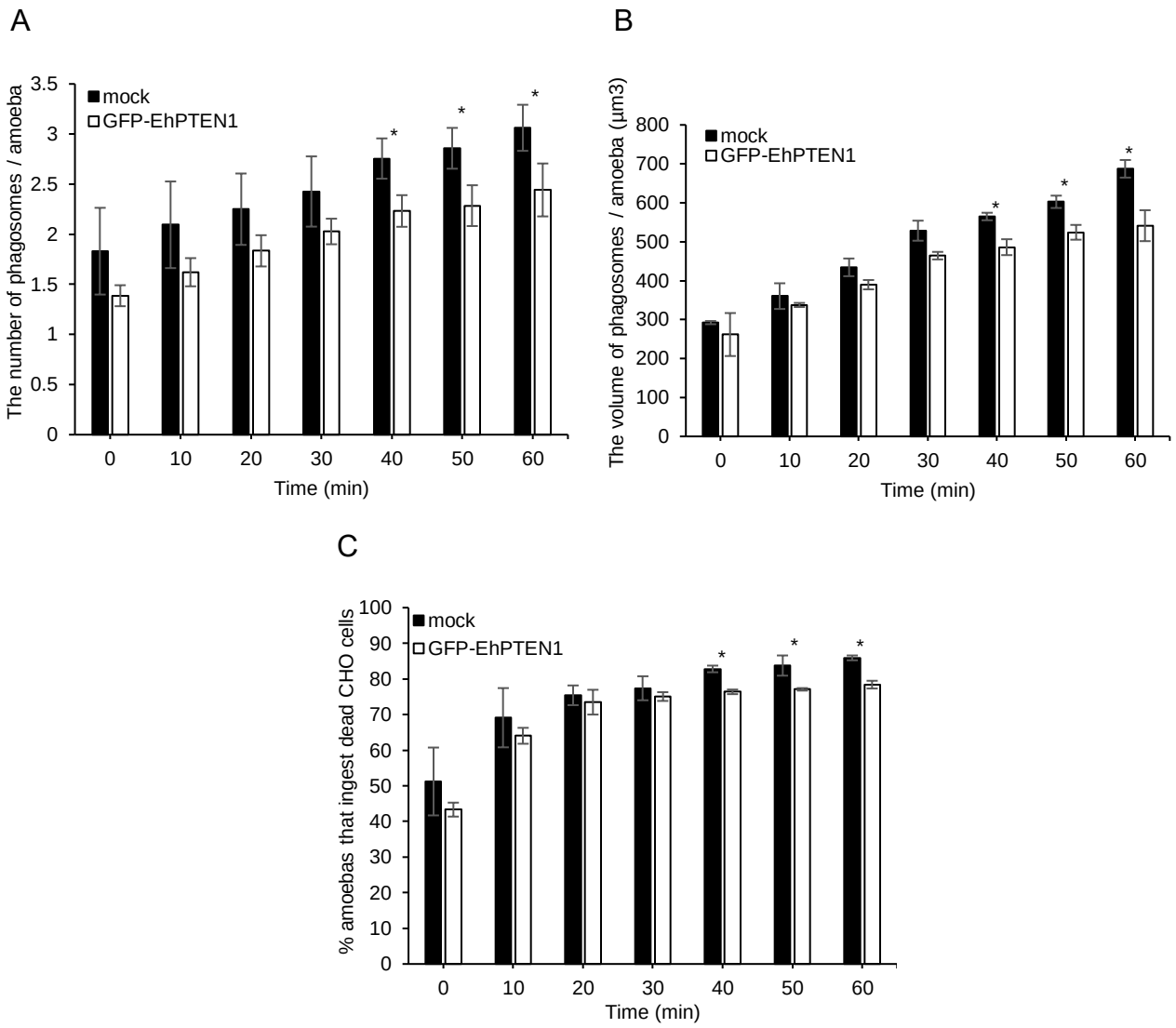

Figure 16. Effect of GFP-EhPTEN1 expression on phagocytosis. (A) Trophozoites of mock transfected and GFP-EhPTEN1 expressing strains were incubated with heat killed CHO cells that have been stained with CellTracker Orange to evaluate phagocytosis. The images were taken on CQ1 as described in the materials and methods and analyzed to calculate the average numbers of CHO cell-containing phagosomes per amoeba. (B) The volume of the ingested CHO cells was calculated using three-dimensionally reconstituted data. (C) The percentage of amoeba trophozoites that ingested pre-killed CHO cells. Experiments were conducted three times independently in triplicates and a representative data set is shown. Statistical significance was examined with t-test (*P < 0.05). Error bars indicating standard deviation.

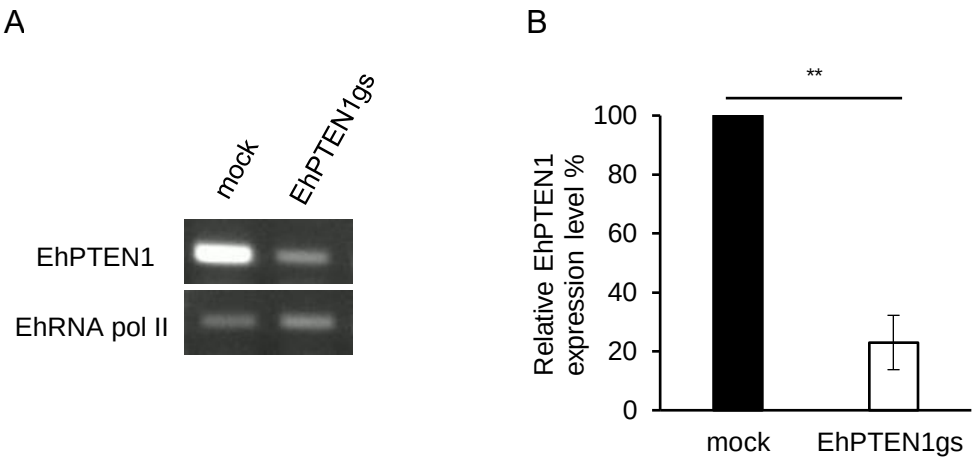

Figure 17. Establishment of *EhPTEN1* gene silenced strain. (A) Confirmation of gene silencing by RT-PCR analysis of mock transfected and *EhPTEN1* gene silenced strain (gs) strain. Transcripts of *EhPTEN1* and *RNA polymerase II* genes were amplified by RT-PCR from cDNA isolated from the transformants and examined by agarose gel electrophoresis. (B) Relative levels of *EhPTEN1* transcripts by qRT-PCR analysis in EhPTEN1gs and mock strains. The transcript levels were normalized against RNA polymerase II and are shown in percentage relative to the transcript level in mock control strain. Data shown are the means ± standard deviations of two biological replicates. Statistical comparison is made by t-test (** $P < 0.01$).

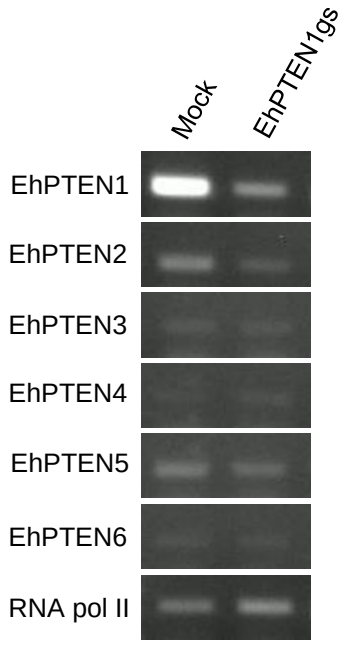

Figure 18. Evaluation of gene expression by RT-PCR analysis of *EhPTEN1* gene silenced transformant. The steady-state levels of transcripts of *E. histolytica* PTEN isoforms and *EhRNA pol II* genes were measured in mock and EhPTEN1gs transformants trophozoites. cDNA from the generated cell lines was subjected to 25 cycles of PCR. RNA polymerase II served as a control.

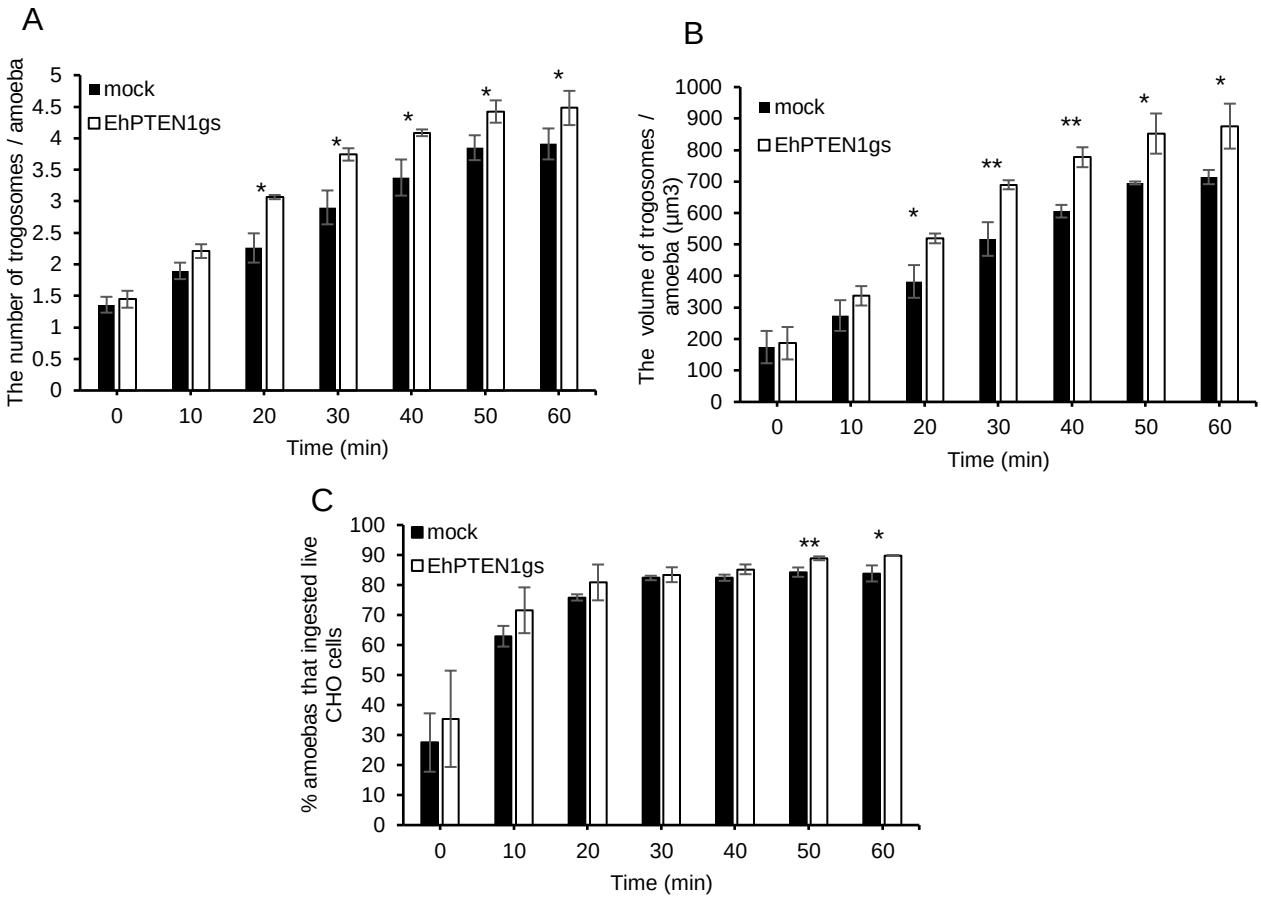

Figure 19. The effect of gene silencing of EhPTEN1 on trogocytosis. Trophozoites of mock and EhPTEN1gs strains were prestained with CellTracker Blue were incubated with live CHO cells that have been stained with CellTracker Orange to evaluate trogocytosis. The images were taken on CQ1 as described in the materials and methods. (A) The average numbers of CHO cell-containing trogosomes per amoeba. (B) The volume of the ingested CHO cells was calculated using three-dimensionally reconstituted data. (C) The percentage of amoeba trophozoites that ingested live CHO cells. Experiments were conducted three times independently in triplicates. Statistical significance was examined with t-test (* $P < 0.05$). Error bars indicating standard deviation.

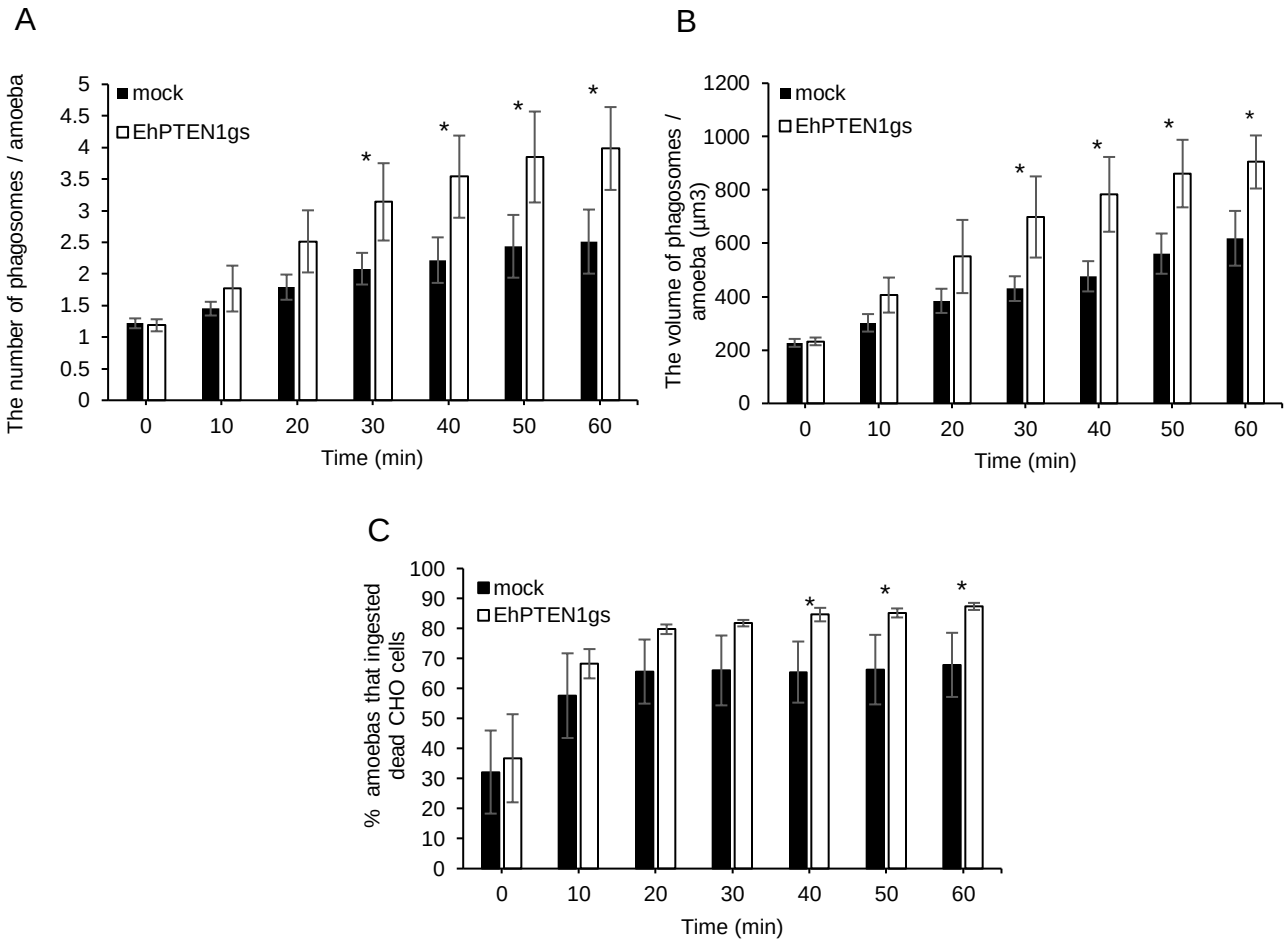

Figure 20. The effect of gene silencing of EhPTEN1 on phagocytosis. Trophozoites of mock and EhPTEN1gs strains were prestained with CellTracker Blue were incubated with heat killed CHO cells that have been stained with CellTracker Orange to evaluate phagocytosis. The images were taken on CQ1 as described in the materials and methods. (A) The average numbers of CHO cell-containing phagosomes per amoeba. (B) The volume of the ingested CHO cells was calculated using three-dimensionally reconstituted data. (C) The percentage of amoeba trophozoites that ingested pre-killed CHO cells. Experiments were conducted three times independently in triplicates. Statistical significance was examined with t-test (* $P < 0.05$). Error bars indicating standard deviation.

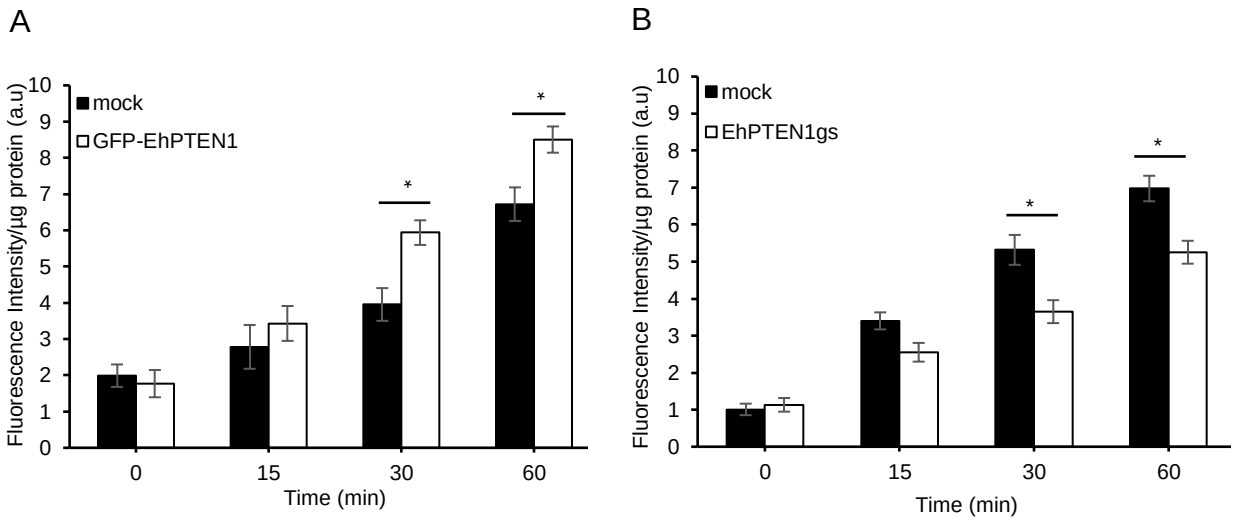

Figure 21. Effect of EhPTEN1 on pinocytosis. (A) The effect of GFP-EhPTEN1 expression on pinocytosis. Trophozoites of mock transfected and GFP-EhPTEN1 expressing strains were assayed for RITC-dextran uptake in a time-dependent manner. (B) The effect of pinocytosis upon EhPTEN1 silencing in comparison to mock control. Trophozoites of mock and EhPTEN1gs strains were incubated in BI-S-33 medium containing RITC-dextran and assayed for its uptake for indicated time points. Experiments were conducted three times independently and statistical significance was examined with t-test (* $P < 0.05$). Error bars indicating standard errors.

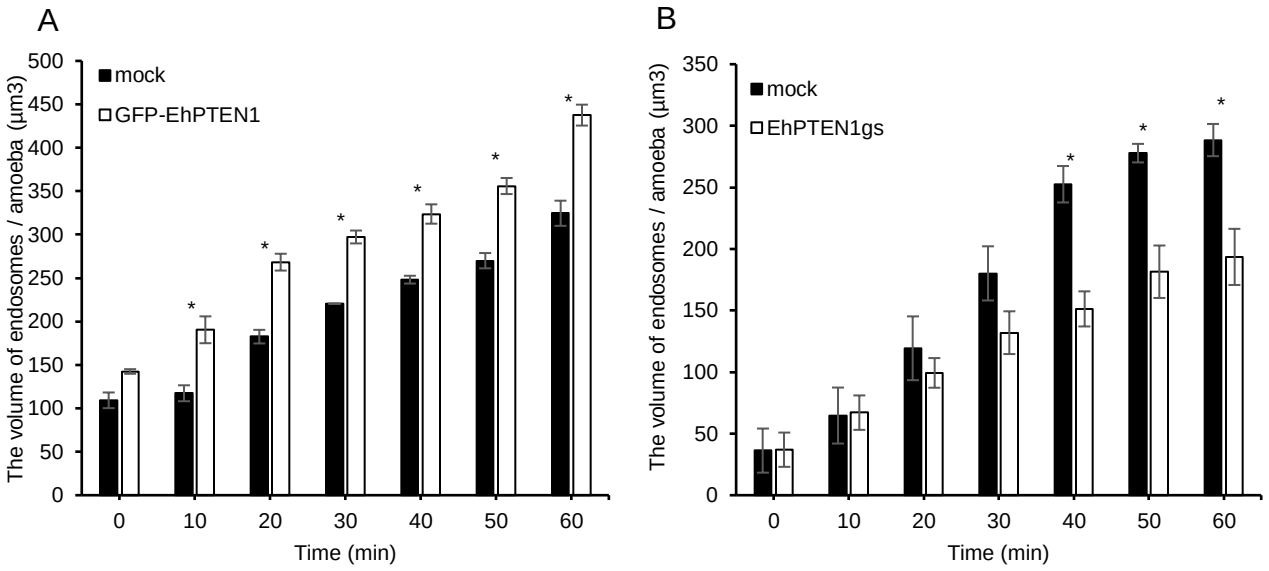

Figure 22. Effect of EhPTEN1 on endocytosis. (A) The effect of GFP-EhPTEN-1 expression on endocytosis. Trophozoites of mock transfected and GFP-EhPTEN-1 expressing strains were incubated in BI-S-33 medium containing transferrin and images were taken every 10 minutes for 1 hour by CQ1 as described in the materials and methods. The volume of endosomes was calculated using three-dimensionally reconstituted data. (B) The effect of *EhPTEN1 gene* silencing on endocytosis. Images of mock and EhPTEN1gs transformant trophozoites that have been co-cultivated with transferrin were taken every 10 minutes for 1 hour by CQ1 as described in the materials and methods. The volume of endosomes was calculated using three-dimensionally reconstituted data. All experiments were conducted three times independently and statistical significance was examined with t-test (* $P < 0.05$). Error bars indicating standard errors.

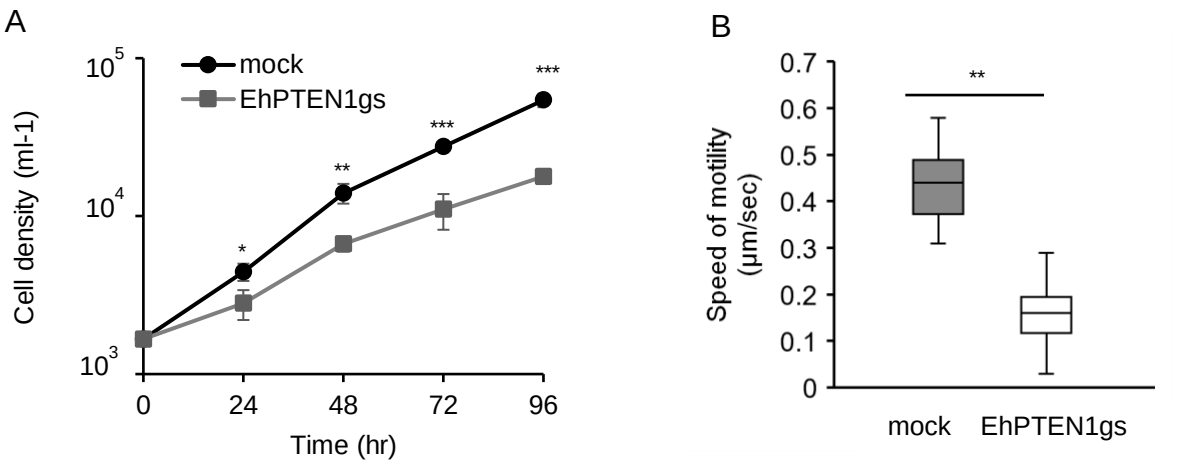

Figure 23. Phenotypes of *EhPTEN1* gene silenced strain. (A) Growth kinetics of mock and EhPTEN1gs transformants s during 96 h incubation in BI-S-33 medium. Data shown are the means ± standard deviations of three biological replicates. Statistical comparison is made by t-test (* $P < 0.05$, ** $P < 0.01$, *** $P < 0.001$). (B) Cell motility of mock transfected and *EhPTEN1* gene silenced strains. The indicated transformant trophozoites were pre-stained with CellTracker green and time-lapse images were collected every second for 2 minutes using CQ1 and 30 cells were selected randomly for analysis by CellPathfinder software. The experiments were performed three times independently. Statistical significance was examined with Dunnet test (**$P < 0.05$, p-value = 0.04).

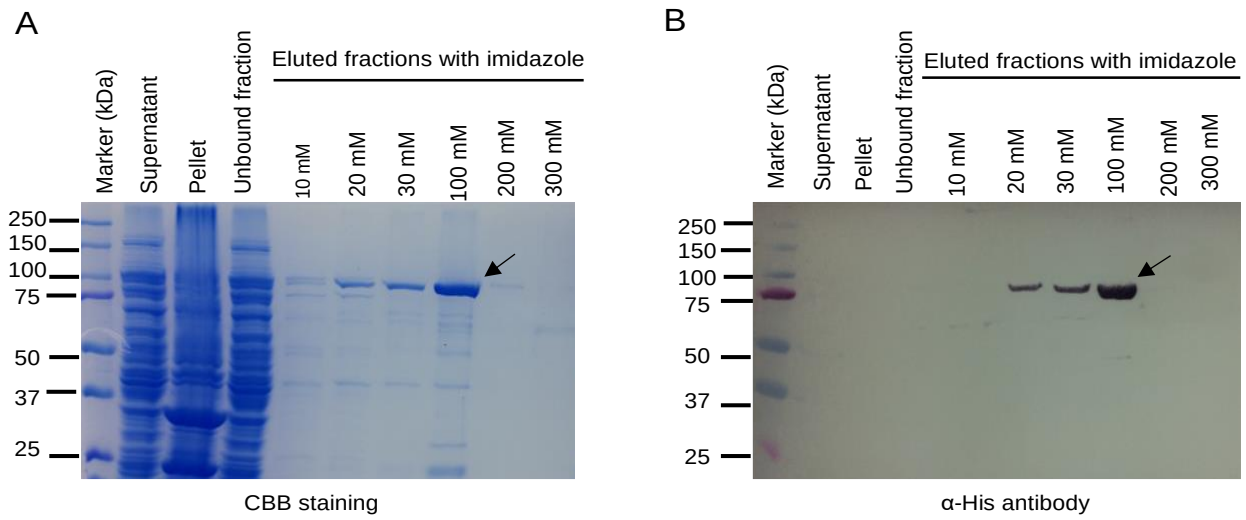

Figure 24 Expression and purification of EhPTEN1 in *E. coli*. (A) Expression of and purification of recombinant EhPTEN1. Protein samples at each step of purification were subjected to 10% SDS-PAGE and the gel was stained with Coomassie Brilliant Blue. (B) Immunoblot analysis of purified recombinant EhPTEN1 using anti-His-tag antibody. The recombinant EhPTEN1 in the supernatant was visualized after longer exposure.

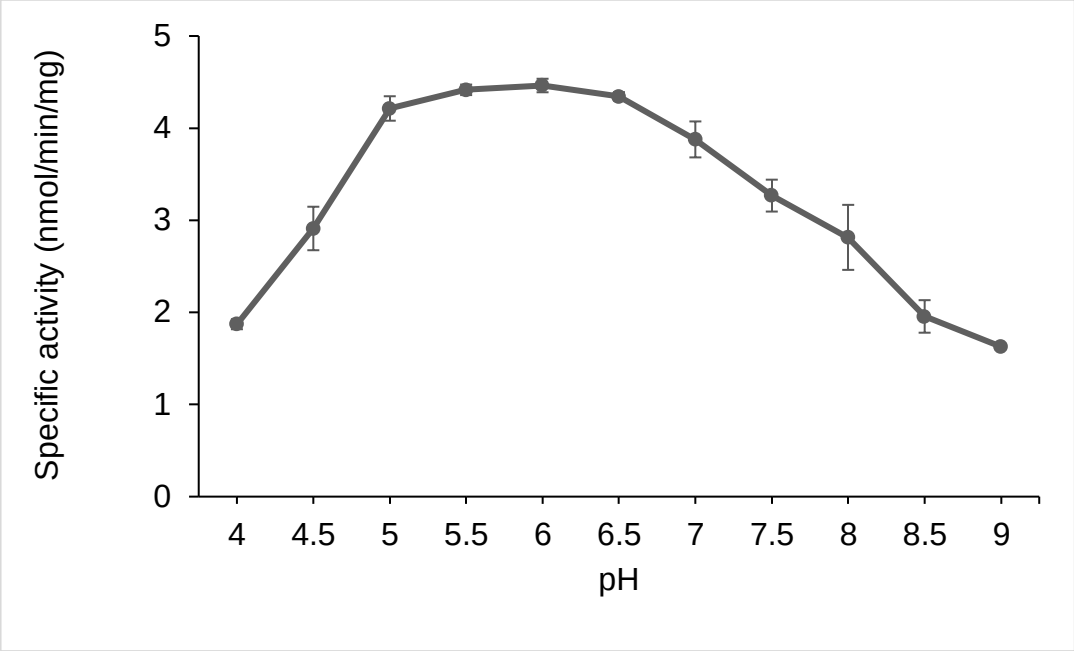

Figure 25. Optimum pH of EhPTEN1. Enzyme specific activity of recombinant EhPTEN1 was measured at various pHs indicated in the figure. The means ± standard error of three independent experiments is shown.

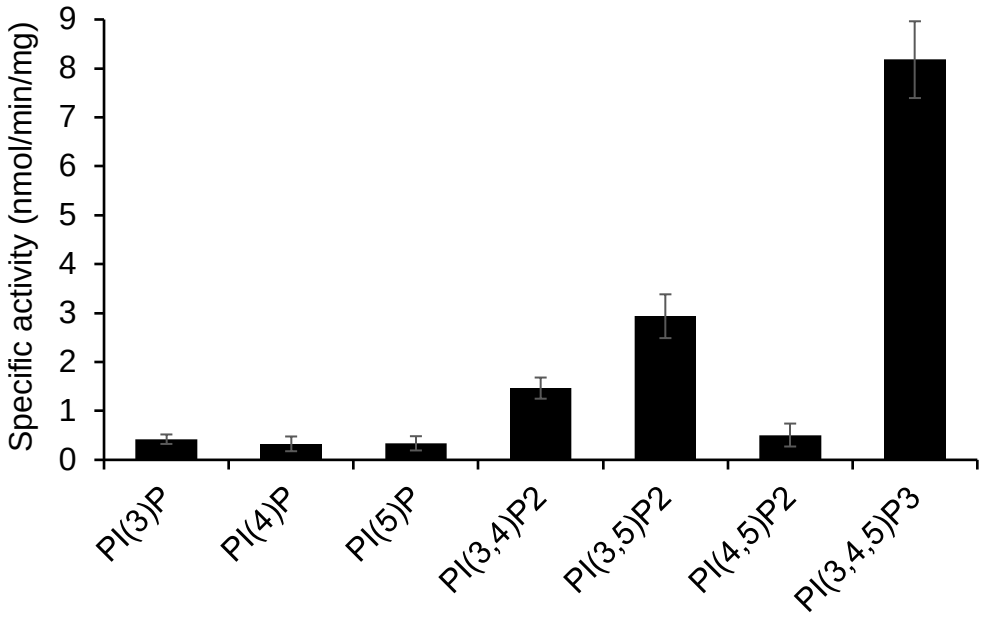

Figure 26. Substrate specificity and enzymatic activity of EhPTEN1. Determination of Eh-PTEN1 Specific Activity. The specific activity of bacterial recombinant Eh-PTEN1 fusion protein toward a panel of synthetic di-C8-phosphoinositide substrates was determined using a malachite green-based assay for inorganic phosphate. Reactions were carried out in a volume of 25 µl for 40 minutes at 37 ○ C, then terminated by the addition of 50 µl of malachite green reagent as described in the Materials and methods. The absorbance at 630 nm was measured and phosphate released was quantified by comparison to a standard curve of inorganic phosphate. The means ± standard deviations of three independent experiments performed in duplicates are shown.

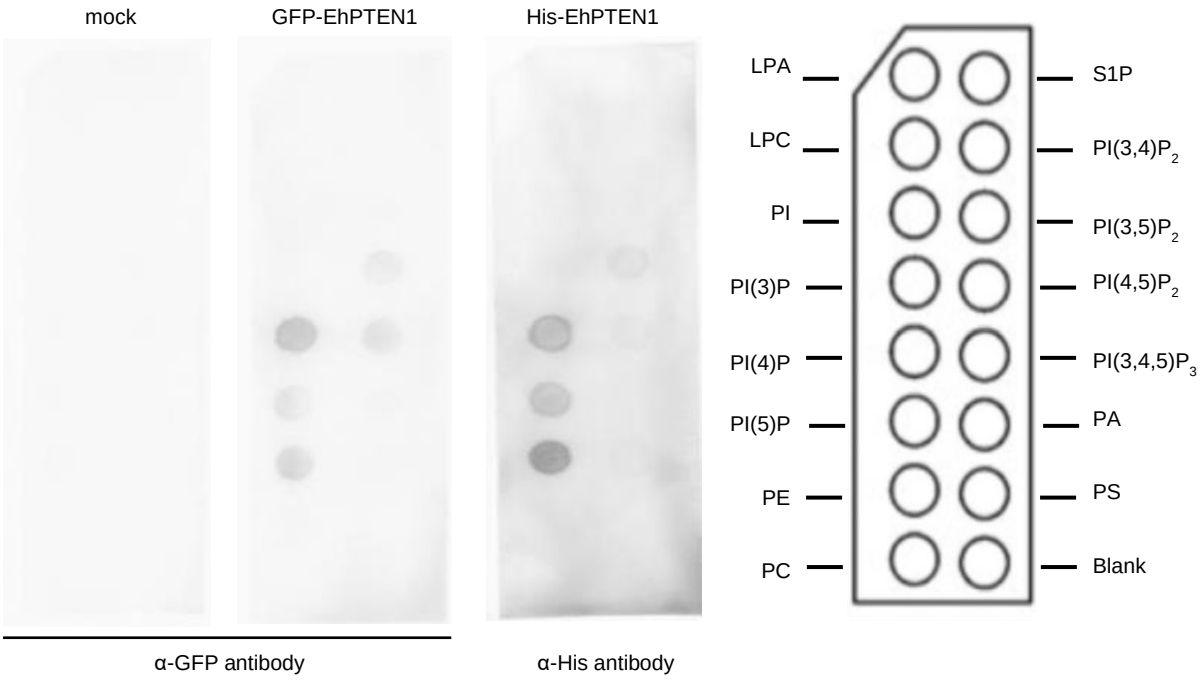

Figure 27. Lipid binding specificty of EhPTEN1. Lipid binding specificity of EhPTEN1 observed by lipid ovelay assay. A panel of PIPs and phospholipid spotted in nitocellulose membrane was incubated with total lysates from GFP-EhPTEN1 and mock expressing transformants, and recombinant His-EhPTEN1. LPA, lysophosphatidic acid; LPC, lysophosphocholine; PE phosphatidylethanolamine; PC, phosphatidylcholine; S1P, sphingosine-1-phosphate, PA, phosphatidic acid; PS, phosphatidylserine.